Charles University in Prague

Faculty of Mathematics and Physics

DIPLOMA THESIS

Tomáš Špringer

Surface-Enhanced Photophysical Processes of Organic Molecules in Metal Nanoparticles

Supervisor: RNDr. Marek Procházka, Dr.
Assistant supervisor: RNDr. Jiří Pfleger, CSc.

Study program: Physics
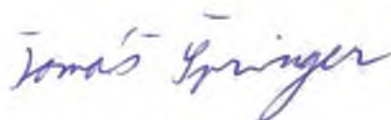
Specialization: Biophysics

Prague 2006

It would like to express my thanks to RNDr. Marek Procházka, Dr. for his patient guidance my Thesis, valuable discussions and passion that he passed onto me. I would like to thank RNDr.Jiří Pfleger, CSc., for valuable advices and careful editing of my Thesis and Mgr. Natália Hajduková for her help during measurements and acquisition of AFM images of gold substrates.

I am grateful to my parents the most for their help and their permanent support, and to my great brothers.

I declare I wrote my Msc. Thesis single-handed and only with using of the quoted sources. I agree with lending of my Msc. Thesis.

In Prague, 21.4.2006

Tomáš Špringer

Contents

Abstrakt

Název práce:	Povrchově zesílené fotofyzikální jevy v organických molekulách na kovových nanočásticích
Autor:	Tomáš Špringer
Ústav:	Fyzikální ústav UK
Vedoucí diplomové práce:	RNDr. Marek Procházka, Dr.
e-mail vedoucího:	prochaz@karlov.mff.cuni.cz
Konzultant:	RNDr. Jiří Pfleger, CSc.

Abstrakt:

Hlavním cílem diplomové práce bylo studium fotoaktivních molekul (zinkové a měděné ftalocyaniny a 5-[4-(4-Octyloxy-phenylazo)-phenoxy]-pentane-1-thiol) a jejich chování na kovových nanočásticích pomocí povrchem zesíleného Ramanova rozptylu (SERS) a UV-vis absorpční spektroskopie. Stabilní a reprodukovatelné SERS aktivní povrchy, citrátem redukované zlaté koloidní částice imobilizované na silanem modifikovaných skleněných sklíčkách, byly připravovány a úspěšně použity k tomuto studiu. Všechny studované molekuly byly úspěšně adsorbovány na zlaté povrchy a byla získána jejich SERS spektra. Závislosti na době ponoření a na koncentraci studovaných molekul v roztoku nám umožnilo porovnat adsorpční proces pro každou molekulu. Získané výsledky pomohou vybrat vhodné systémy pro studium zesílených fotofyzikálních jevů v organických molekulách na kovových nanosubstrátech.

Klíčová slova: SERS, fotoaktivní molekuly, ftalocyaniny, zlaté imobilizované nanočástice

Abstract

Title:	Surface-enhanced photophysical processes of organic molecules in metal nanoparticles
Author:	Tomáš Špringer
Department:	Institute of Physics, Charles University
Supervisor:	RNDr. Marek Procházka, Dr.
Supervisor's e-mail address:	prochaz@karlov.mff.cuni.cz
Assistant supervisor:	RNDr. Jiří Pfleger, CSc.

Abstract:

Main goal of this MSc. Thesis was study of photoactive molecules (zinc and copper phthalocyanines and 5-[4-(4-Octyloxy-phenylazo)-phenoxy]-pentane-1-thiol) and their behavior onto gold metal nanoparticles using surface-enhanced Raman scattering (SERS) and UV-vis absorption spectroscopy. Stable and reproducible SERS-active substrates, citrate-reduced gold nanoparticles immobilized on silane-modified glass slides, were prepared and successfully used in this study. All studied molecules were successfully adsorbed on the gold substrates and their SERS spectra were obtained. Dependences on soaking time and on concentration of studied molecule in solution enabled us to compare adsorption processes for each molecule. Obtained results can help us to select suitable systems for study of enhanced photophysical phenomena of organic molecules on gold nanosubstrates.

Keywords: SERS, photoactive molecules, phthalocyanines, gold immobilized nanoparticles

Chapter I

Objectives

Main goal of this study is the investigation of photoactive organic molecules, namely zinc and copper phthalocyanines, and azobenzene derivates. These molecules demonstrate interesting photoinduced phenomena, like generation of free charge carriers, singlet oxygen generation upon photon absorption or photoinduced conformational changes. Such phenomena can be exploited in practical applications as photoelectrical conversion or photodynamic therapy as it is in the case of phthalocyanines, or in photochromic optical memories, as in azobenzene dyes.

Surface-enhanced Raman scattering (SERS) spectroscopy, based on the interaction of an incident electromagnetic wave and molecules, located in a vicinity of a nanostructured noble metal surface, with quasi-free electrons collective excitations in metal (surface plasmons) was used as a very sensitive method to measure the Raman spectra of molecules at an extremely low concentration. It was also used as a suitable tool for studying an interaction of active molecules with a nanostructured surface of noble metals or with noble metals nanoparticles. On the other hand, SERS is not the only possible exploitation of surface plasmon electromagnetic field enhancement. One could also expect that the electromagnetic enhancement, originated in an resonance interaction of an incident electromagnetic wave with electrons in metal, i.e. surface plasmons, could also enhance other photoinduced photophysical phenomena, like photoinduced charge transfer or photochromic conversion, with possible applications in solar energy conversion and in the data recording and processing. Better understanding of these phenomena can help us to produce solar cells with better conversion efficiency or data medium with greater storage capacity.

In this work, SERS-active substrates formed by citrate-reduced gold nanoparticles immobilized onto silanized glass plates were employed. These substrates are stable, reproducible and suitable for detection of studied molecules. Affinity of all molecules to the gold substrates, efficiency of adsorption process and possibility to obtain their SERS spectra was a main goal of this work. Dependences on soaking time and on concentration of studied molecules in solution enabled us to compare adsorption processes for each molecule. These results can help us to select suitable systems for study of enhanced photophysical phenomena of phtalocyanines on gold nanosubstrates.

Chapter II

General introduction

1 Raman and Surface-enhanced Raman scattering

1.1 Optical spectroscopy

Optical spectroscopy is a very important tool for investigation of structures and functions of biomolecules. Non-invasive influence of studied molecules, wide region of received information and relatively easy manipulation are some examples of its advantages.

According to the light interaction with a molecule, the methods of optical spectroscopy can be classified into three categories: light absorption (IR, UV-Vis absorption spectroscopy), light absorption and emission (fluorescence and phosphorescence spectroscopy) and light scattering (Raman scattering spectroscopy).

1.2 Raman Scattering

Raman phenomenon was discovered by C.V.Raman 60 years ago. He irradiated a sample by high power monochromatic light and observed three peaks (see Figure 1.1). The middle peak is scattered light with the same energy as the incident light (Rayleigh scattering). The other two correspond to scattered light with a small change of energy with respect to the incident light (Raman scattering). The lower energy peak is called Stokes scattering and the higher one is Antistokes scattering. Changes in energy are not dependent on the wavelength of incident light but on the properties of irradiated molecules. The energy shifts are the same in both cases (Stokes and Antistokes scattering). Generally the

ratio between intensities of Rayleigh and Raman scattering is 10^9-10^{12}. Since the ratio of the intensities of Antistokes and Stokes peaks depends on the population of the respective vibrational states, given by the Boltzman distribution, Stokes scattering is 10^3 times stronger than Antistokes scattering in normal conditions.

RAMAN ANTISTOKES   RAYLEIGH   RAMAN STOKES
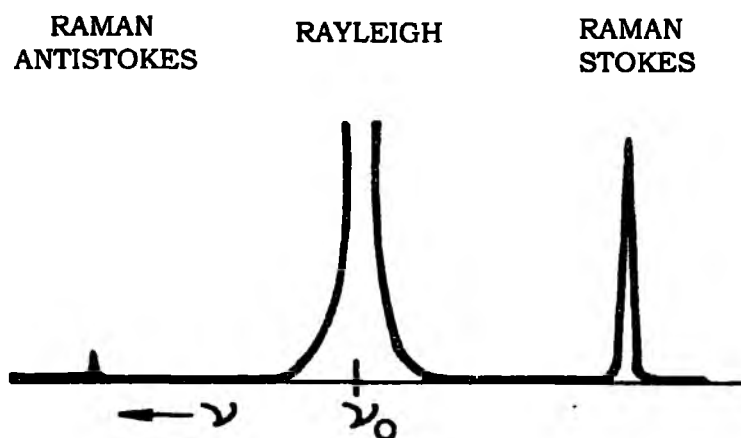
Figure 1.1. Peaks observed by C.V. Raman 60 years ago, ν_0 is the frequency of incident light (taken from [11]).

The physical nature of Raman scattering is a change of polarizability of the molecule due to interaction with incident light. A molecule interacts with incident photons whereby the molecule electron state is changed to the "virtual electron state" that does not correspond to the real electron state (see Figure 1.2). Immediately the photon with different energy is scattered and the molecule returns to the real electron state. The scattered photon energy is given as follows:

$$h \upsilon_R = h \nu_0 \pm \left(E_n - E_m \right) \tag{1.1}$$

The upper sign corresponds with Antistokes scattering (the electron transition from state n to state m) and the lower sign with Stokes scattering (the electron transition from state m to state n). A molecule is irradiated by the frequency ν_0. Since this effect involves transitions between vibrational energy levels of the same (ground) electron state of the molecule, thus it belongs to vibrational spectroscopy.
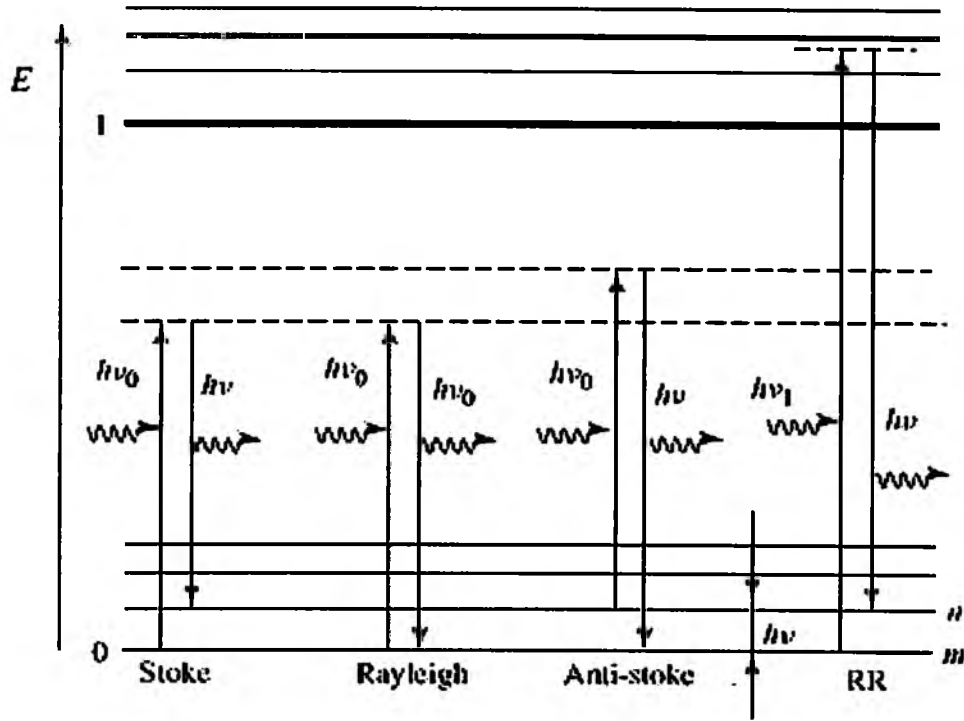
Figure 1.2. The principle of Raman scattering.

The incident electromagnetic field **E** induces in the interacting molecule a dipole moment **p**, proportional to its molecular polarizability α:

$$p = \alpha E \qquad (1.2)$$

In a quantum mechanical treatment, using a simplified second-order time-dependent theory, we obtain the probability of the molecular transition from electron state 1 to electron state 2 inducing the photon emission with polarization e^R into the spatial angle $d\Omega$:

$$\frac{dW_{12}^R}{d\Omega} = \left(\frac{2^4 \pi^4}{hc^4}\right)\left[e_i^R \left(\alpha_{12}^R\right)_{ij} e_j^0\right] F_{12}^R(v) v_R^3 I_0 \qquad (1.3)$$

where $\left(\alpha_{12}^R\right)_{ij}$ is:

$$\left(\alpha_{12}^R\right)_{ij} = \sum_{s \neq 1,2} \left(\frac{\langle\psi_2|D_i|\psi_s\rangle\langle\psi_s|D_j|\psi_1\rangle}{E_1 - E_s + hv_0} + \frac{\langle\psi_2|D_j|\psi_s\rangle\langle\psi_s|D_i|\psi_1\rangle}{E_2 - E_s - hv_0}\right) \qquad (1.4)$$

10

In the relations above $\hat{D}$ is the operator of the molecular dipole moment, e^R (e^0) is the normalized vector of the scattering radiation (or the incident radiation), F^R_{12} describes shapes of Raman peaks, I_0 corresponds with the intensity of incident light, ψ are wave functions of electron states and E_1 and E_2 are energies of electron states 1 and 2, respectively. The term α^R_{12} denotes the Raman tensor and ν_R and ν_0 are frequencies of the Raman scattered light and the incident light. The summation denotes summation over all states except states 1 and 2.

When the energy of incident photons approaches a real electron state, the first part of Raman tensor grows compared to the second part. This effect is called resonance Raman scattering (see also Figure 1.2). Since in this case the molecule crosses a virtual state located within its proper electron energy levels, the fluorescence may become a competitive process.

1.3 Surface-enhanced Raman scattering (SERS)

Surface-enhanced Raman scattering (SERS) was discovered by Fleischmann et al. in 1974 [1]. They studied Raman spectra of pyridine adsorbed on a silver electrode surface and were surprised how strong the signal was. The first explanation of this anomalous effect was that it was only a summation of signals from single molecules absorbed on a large surface area of the roughened electrode. Three years later two independent groups (Van Duyne, R.P.[2], Creighton, J.A. [3]) came with an experimental confirmation of this effect and also a theoretical explanation of the enhancement mechanism (e.g. Moskovits, M. [4], Creighton, J. A. [5]). Nowadays, SERS is understood as a very large enhancement of Raman scattering for molecules located in the proximity of roughened metal surfaces. Two mechanisms are considered to contribute to the overall SERS enhancement:

1) Electromagnetic (physical) mechanism
2) Molecular (chemical) mechanism

1.3.1 Electromagnetic (physical) mechanism

The electromagnetic mechanism is based on an intensity enhancement of the electromagnetic field **E** (1.2) in the proximity of a roughened metal surface(see Figure 1.3). The incident light with suitable frequency causes the surface plasmon (SP) excitation in metal. SPs are collective oscillations of electrons localized in surface nanostructures. Resonantly excited SPs produce a locally enhanced electromagnetic field that is Raman scattered by adsorbed molecules. Subsequently, scattered light is enhanced by the metal surface.
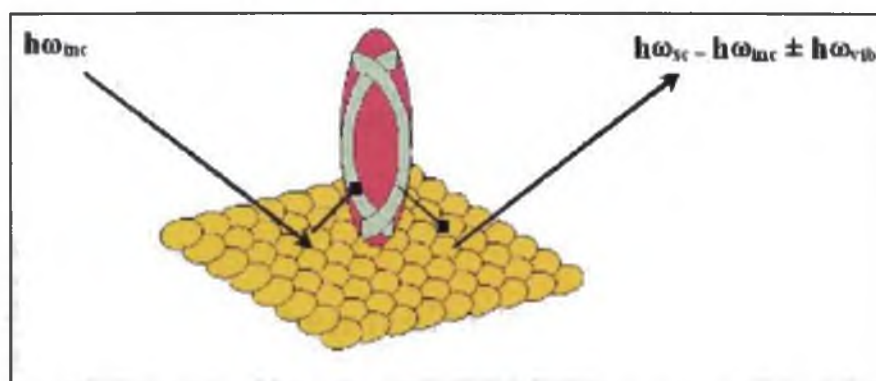
Figure 1.3. Principle of the electromagnetic mechanism in SERS.

Roughness of a metal surface in a scale of tens or hundreds of nm is essential for the electromagnetic mechanism. The highest enhancement occurs in the proximity of sharp edges and tips. Common enhancement by the electromagnetic mechanism is 10^6-10^7 times, but in some special conditions (adsorption of molecules at extremely enhancing structures such as "hotspots", dimers of nanoparticles or small fractal aggregates) can reach even 10^{14}-10^{15} [6] and thus detection on a single-molecular levels is possible.

Roughness of a surface can be approximated in the first approximation by spherical particles, the radius r is smaller than $0.05\lambda_L$ where λ_L is the wavelength of the incident light. A molecule is located in distance d away from the metal surface. The total electromagnetic field is a superposition of the incident field and the field induced in metal particles. The enhancement factor A(v) gives a ratio between the field at the position of the molecule and the incident field.

$$A(v) = \frac{E_M(v)}{E_0(v)} \sim \frac{\varepsilon - \varepsilon_0}{\varepsilon + 2\varepsilon_0}\left(\frac{r}{r+d}\right)^3 \qquad (1.5)$$

The highest enhancement is achieved when the real part of the permittivity $\varepsilon(v)$ is approaching $-2\varepsilon_0$ and the imaginary part is small. In the visible spectral region this condition can be fulfilled for gold, silver, copper and some alkali metals. The enhancement of Raman signal may be expressed by factor G_{em}:

$$G_{em}(v_S) = \left|A(v_L)\right|^2 \left|A(v_S)\right|^2 \sim \left|\frac{\varepsilon(v_L) - \varepsilon_0}{\varepsilon(v_L) + 2\varepsilon_0}\right|^2 \left|\frac{\varepsilon(v_S) - \varepsilon_0}{\varepsilon(v_0) + 2\varepsilon_0}\right|^2 \left(\frac{r}{r+d}\right)^{12} \qquad (1.6)$$

An absorbed molecule does not need to be in a direct interaction with a metal surface, however, with the increasing distance d the intensity of scattered light decreases very rapidly. This dependence is proportional to $\frac{1}{d^{12}}$.

1.3.2 Molecular (chemical) mechanism

The chemical (molecular) mechanism increases the polarizability α (1.2) of an absorbed molecule. It is a short-range effect that requires a strong interaction of absorbed molecules with a metal surface, even creation of a molecule/surface complex (chemisorption) allowing charge transfer (CT) between molecule and metal. One possible model of the CT mechanism is shown in Figure 1.4. An electron in a metal surface is excited into a higher electron state (a). Subsequently, the electron is transferred into an adsorbed molecule electron state with the same energy as in metal and, consequently, the polarizability of the absorbed molecule is changed (b). This process is called charge transfer (CT). The excited electron is relaxes within the adsorbed molecule and, subsequently, the electron returns back into metal (c) and light is radiated (d).

Surface roughness and the presence of localized SPs are not required for this enhancement mechanism as is demonstrated by SERS measurements on smooth metal surfaces [7]. The chemical mechanism is generally weaker than the electromagnetic one, and contributes to the total enhancement by a factor of 10-10^3.
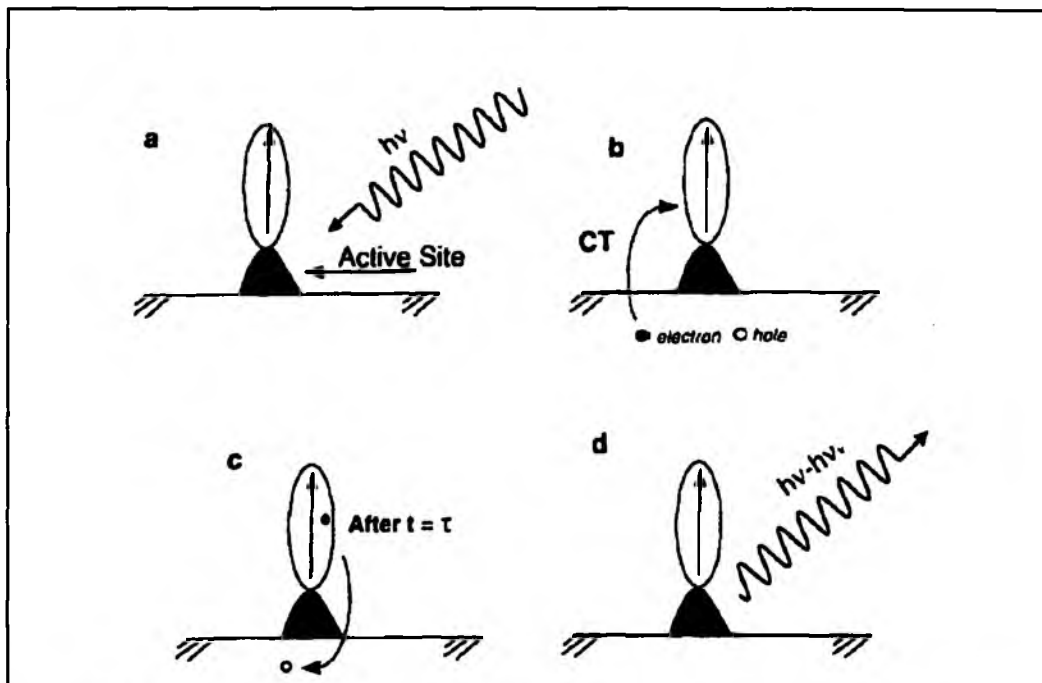
Figure 1.4. The molecular mechanism in a model of charge transfer (taken from [12])

1.3.3 Surface-enhanced resonance Raman scattering (SERRS)

Surface enhanced resonance Raman scattering (SERRS) is a special case of SERS when the energy of the incident light coincides simultaneously with the excitation energy of the SPs localized on the roughened surface and with the energy of the electron transition of the adsorbed molecule. Although in this case we can profit simultaneously from surface and enhancement mechanisms, these two enhancements are not simply additive.

In the case of excitation under molecular resonance, a metal surface supplies a quenching mechanism arising from possible non-radiative transfer of the energy from the molecule to the surface. This effect can lead to an efficient quenching of the absorbed molecule's fluorescence.

1.4 SERS-active surfaces

Although a lot of SERS-active surfaces are commonly used in SERS spectroscopy, there are three main types of metal surfaces: roughened electrodes, island films and nanoparticles in colloids.

1.4.1 Metal electrodes

Metal electrodes are prepared by repetitive oxidation-reduction cycles in the presence of electrolytes. In the first phase the electrode is oxidized and metal atoms are dissolved in the electrolyte. In the second, reduction part, of the cycle metal atoms are reversibly reconverted. During numerous oxidation-reduction cycles the rough surface structures are formed. The surface roughness is between 25-500 nm. The properties of the metal electrode depend on many preparation conditions such as number of oxidation-reduction cycles, composition of electrolytes and electrode potential.

1.4.2 Metal island films

Metal island films are typically prepared by vapor deposition of metal atoms on a heated glass or quartz substrate. The mobility of metal atoms increases on a hot substrate that causes them to form an island film. Metal atoms might be deposited on a cold substrate. In this case the island film is formed during a rapid decrease of metal atom mobility. The surface roughness varies between 150-600 nm. Roughness is closely dependent on temperature of substrates and metal and the speed of deposition. Metal island films are easily reproducible and stable, however, in the presence of atmosphere oxidation may contaminate the metal surface by an oxide layer.

1.4.3 Metal colloids

Colloids are water suspensions of metal nanoparticles whose shapes are mainly close to spheres. Colloids are most often prepared by reduction of metal salts with reducing agents (sodium borohydrate and sodium citrate are the most frequently used) [5, 8]. The

preparation is easy and routine, however, the purity of all chemicals and glass vessels used is crucial. The diameters of spherical particles vary between 10-100 nm and their size distribution is narrower than in the case of metal island films and metal electrodes.

Freshly chemically prepared colloidal nanoparticles are isolated due to coulombic repulsion barriers of negatively charged anions covering their surfaces. Such colloid is characterized by an SPE spectrum with a maximum at ~ 390 nm or ~440 nm in the case of silver borohydride- or citrate-reduced colloid, respectively, or 510-520 nm in the case of gold one (Figure 1.5). Addition of an adsorbate or of aggregate agents (e.g. salts) into colloids leads to an aggregation of nanoparticles. The aggregation can be seen by the SPE spectra via the appearance of a new extinction band at longer wavelength. The aggregation allows the fulfilling of conditions of SP excitation in the visible spectral region as well as obtaining higher surface enhancement. On the other hand, the aggregation process is very difficult to control and often causes irreproducibility of spectral measurements. Colloid aggregation depends on many factors such as added aggregate reagents and their concentrations, purity of original colloids, temperature, the colloid concentration itself, etc.
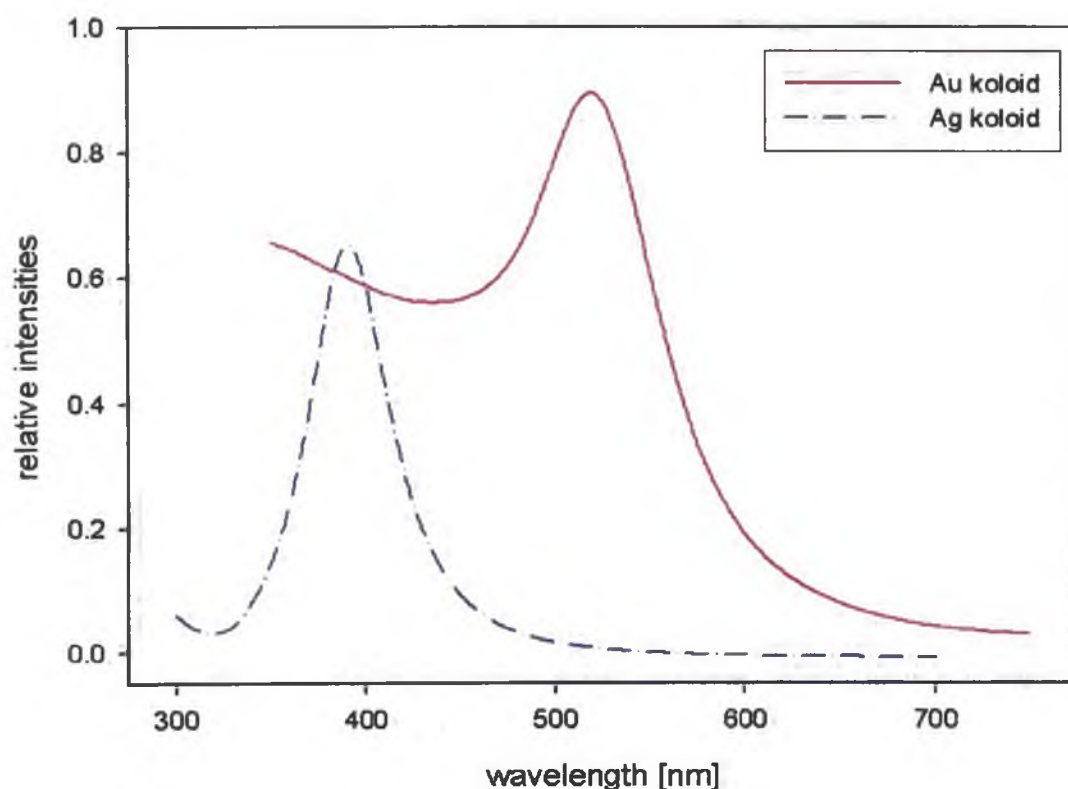

Figure 1.5. Extinction spectra of gold and silver colloids.

A different way of metal colloid preparation of metal colloids is a laser ablation where a metal foil is irradiated by short pulses of a powerful laser in ultrapure water [9,10, 20]. Sizes, shapes and the distribution of particles are primarily influenced by excitation wavelength (1064 nm, 532 nm), pulse duration (ps, ns) and laser power. The advantage of these colloids in comparison to chemically prepared ones is their chemical purity. On the other hand, colloids prepared in this way are less stable in some cases.

1.4.4 Colloidal particles immobilized on silane-modified glass slides

Although colloidal nanoparticles are the most frequently used SERS-active surfaces, their serious disadvantage is their low stability and the low reproducibility of spectral measurements. Thus, many efforts have been devoted to find a simple preparation method of stable and highly reproducible SERS-active surfaces. A promising way seems to be a combination of the optical and morphological properties of colloidal nanoparticles (narrow and sharp particle size distribution) and of the stability and reproducibility of solid surfaces.
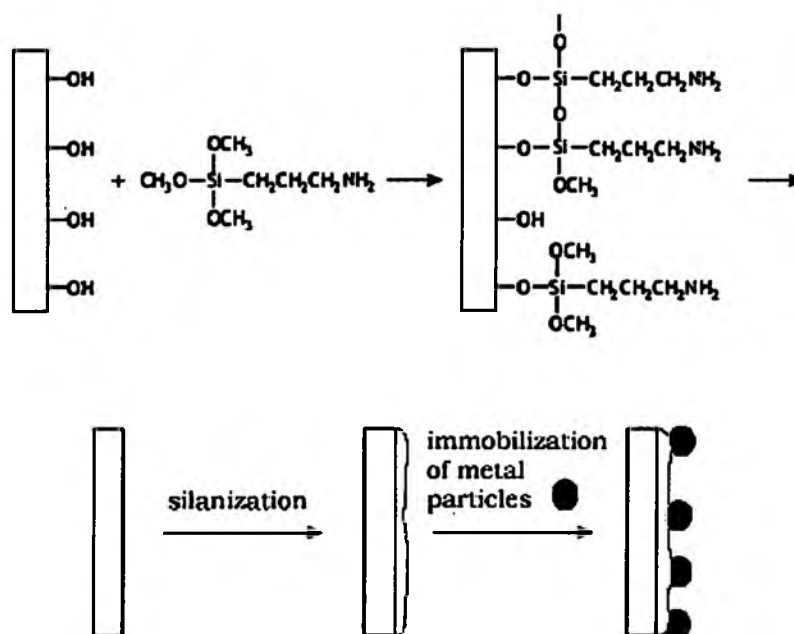

Figure 1.6. Substrate preparation (taken from [13]).

A well-developed and successfully employed technique is based on the immobilization of colloidal nanoparticles on silane-modified glass slides (substrates in the following text, [21, 22, 23]). Pure glass slides are first silanized in a solution of organosilane (having amino- or mercapto- functional group). Then, silanized glass plates are immersed into a solution of colloidal nanoparticles to bind them into a glass surface via organosilane functional groups (see Figure 1.6). The preparation is easy and reproducible. The purity during the whole preparation process is absolutely essential.

2 SERS study of biomolecules

Raman spectroscopy is a powerful tool in the research of biomolecules. This method is nondestructive and very fast. The resolution is much higher than in fluorescence or UV-Vis absorption spectroscopy. Raman peaks are so narrow that it makes fingerprint possible. A great disadvantage of Raman spectroscopy is its low sensibility. SERS is a promising way to overcome this problem.

The SERS enhancement effect allows to obtain Raman spectra of biomolecules at very low concentrations. Possibilities of single-molecular level measurement opened SERS spectroscopy for trace analytical detection as well as applications in biophysics and biomedicine [14, 15]. The large enhancement factor of SERS, in combination with the quenching of fluorescence, helps to measure spectra of chromophoric biomolecules with a powerful fluorescence signal that often overlaps a weak Raman signal. In the case of biological objects, (cells, microorganisms) strongly enhanced signal allows to use shorter collection times (1 second and lower using Raman microscope) providing the opportunity of Raman mapping on a time scale corresponding with chemical changes in a cell.

The limitations of SERS spectroscopy are attributed to the fact that studied molecules have to be adsorbed onto a "SERS-active surface". Possible irreproducibility and instability of SERS-active surfaces strongly influence SERS spectral measurement. Moreover, not all molecules can be easily adsorbed on a metal surface and if adsorbed, strong interaction with a metal surface can influence their properties. Conformation changes of adsorbed molecules, denaturation of nucleic acids or proteins, chemical changes (such as metalation of free-base porphyrins), etc. can be the results of interaction with a metal surface and should be considered in interpretations of results.

2.1 Photoactive biomolecules

Photoactive molecules are molecules that change their physical properties due to light irradiation. It is a large group of molecules with enormous practical use.

Phthalocyanine derivates belong to a wide group of photoactive molecules. The basic chemical structure of phthalocyanine (Pt) is shown in Figure 2.1, left. The majority of applications use the metal-substituted form of the molecule that has several peripheral groups or chains (see Figure 2.1, right).
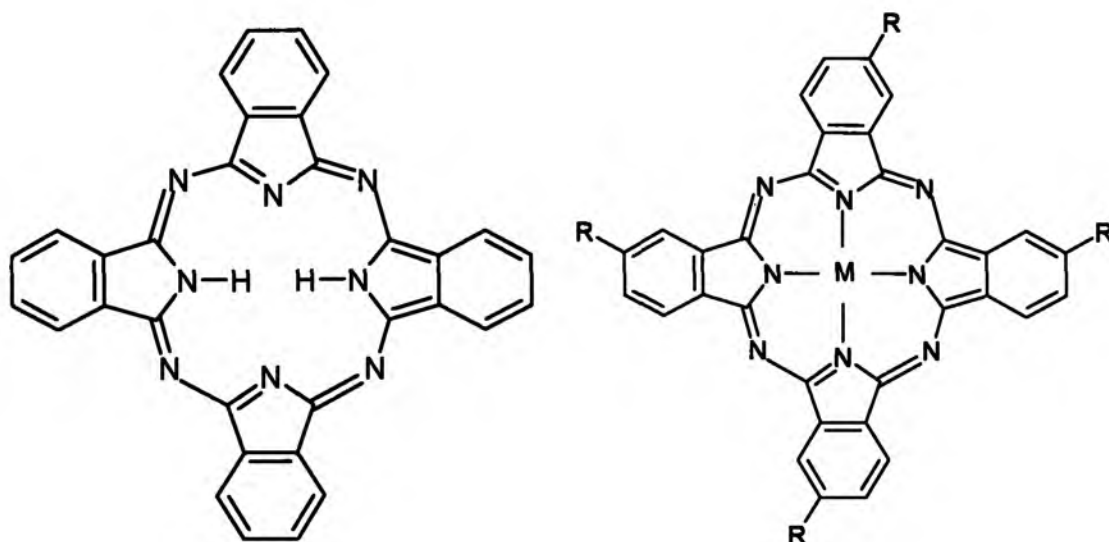
Figure 2.1. The chemical structure of basic phthalocyanine (left) and a metalophthalocyanine derivate with several peripheral R groups (right).

Since its discovery over seventy years ago, Pts and its derivatives have been extensively used as colorants (dyes or pigments). More recently they have been employed in several 'hi-tech' applications such as photoconducting materials in laser printers and light absorbing layers in recordable CDs. They are also used as photosensitisers in photodynamic cancer therapy.

SERS is not the only possible exploitation of SP electromagnetic field enhancement. Interesting application could be found also in some other photoinduced physical phenomena on organic molecules. For example, photochromic organic molecules have a broad application potential in the data recording and processing. The storage and/or operational density in the classical devices are physically limited by the interference phenomena to the range of the optical wavelength used, i.e. the scale of hundreds of nanometers. One possibility to achieve higher operational density is to limit the

photoinduced processes used for the data recording to the smaller scale by a localization of the photochromic process. This might be achieved by a confinement of the optical excitation into spatially localized strong electromagnetic fields in "hot spots". As the photoexcitation is the first step of any photochemical reaction, it is straightforward to assume that the fields in the vicinity of the metal nanostructure can substantially decrease the threshold intensity of the incident light necessary for the initialization of the photochemical changes. It may thus lead to very localized photoreactions. An example of such a process was published based on the study of the photochromic behavior of the polymer films molecularly doped by the organic photochromic molecules of azobenzene type [16]. The authors observed local photoinduced photochromic changes based on the cis-trans izomerization mechanism of azobenzene derivative in the vicinity of the tip of scanning AFM microscope. The change was easily detectable by measurements of the surface electric potential induced by a change of the dipole moment of a molecule during cis-trans izomerization. In the case of an exposure of such azobenzene doped polymer films to the coherent light the local mechanical deformation was observed with the period equal to the interference pattern leading to the creation of the relief optical grating [17]. The physical nature behind this phenomenon was ascribed to the opto-mechanical process. Local electric field in the vicinity of the AFM tip can localize the effect to the region smaller than the optical wavelength used and nanostructures can be thus created that can reach the space resolution far behind the limits accessible by usual photolithographic methods. There is a recent note in the literature about similar effects observed on organic molecules in the vicinity of Au nanoparticles [18]. It was found that the magnitude of photoinduced photochemical changes has a maximum at the distance ca 11 nm between the surface and the conductive tip, which is in agreement with the contradictory dependencies of the EM enhancement and the damping factor on the separation distance, respectively.

The EM enhancement mechanism is also mainly responsible for the interesting behavior of phthalocyanine in organic solar cells that was shown in studies of Rand P. R. et al. [19]. These solar cells consisted of the electron donor, copper phthalocyanine (CuPt), and clusters of small spherical silver particles with diameters approximately 5nm. In the presence of metal particles the efficiency of electron excitation increases rapidly, thus the total efficiency of solar cells is considerably higher.

Surface-enhanced Raman scattering is a promising tool for investigation of photophysical properties of molecules that combines high sensibility and measurement at very low concentrations close to natural environment.

21

Chapter III

Preparation of experiments

3 Chemical reactants and photoactive molecules

3.1 Chemical reactants

The following reagents were used during measurements and preparation of samples:

96% H_2SO_4, 30%H_2O_2, 35% HCl., 65% HNO_3, chloroform were manufactured by LaChema p.a.

Deionized water (18MΩ resistance) prepared in our laboratory.

$HAuCl_4$ and citrate sodium $C_6H_5O_7Na_3.2H_2O$ (all from Sigma Aldrich) were used for the preparation of gold citrate colloids.

99.8% methanol and 97% 3aminopropyltrimethoxysilane (all from Sigma Aldrich) for silanization.

3.2 Photoactive molecules

It is very interesting to study the behavior of new phthalocyanines in different conditions, as well as photophysical and photoconductive properties on metal surfaces. Surface-enhanced Raman scattering (SERS) is a technique suited to study basic properties of phtalocyanines, such as spectral characteristics and adsorption on suitable metal nonstructural substrates that can potentially enhance their photoconductive properties.

3.2.1 Derivates of phthalocyanines

Four different phthalocyanine derivates were studied during this Msc. Theses. Individual phtalocyanines differ in central atoms (zinc or copper) and have relatively well-defined adjacent chains. The central metal atom affects mainly the phthalocyanine macrocycle and protects a phtalocyanine against metalation by surface atoms. Phthalocyanines have been synthesized at VUOS (Výzkumný ústav organických syntéz, a.s., Pardubice, within project "TANDEM").

Zinc phthalocyanine (ZnPt) is shown in Figure 3.1. The material is a mixture of molecules with one or two -SO_3Na groups bound to the basic macrocycle. The ratio of molecules with one and two substituents is approximately 1:1. ZnPt is highly soluble in polar solvents including water. ZnPt has a neutral charge in powder, a negative charge at SO_3 dissociated groups in solution. Total negative charge depends on a degree of substitution.
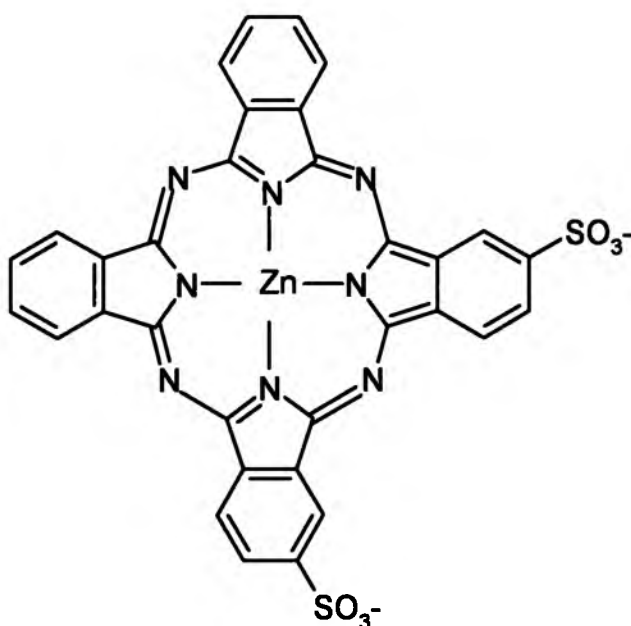

Figure 3.1. The chemical structure of ZnPt.

The other phthalocyanines are copper-metalated with various side groups. The chemical structure of copper phthalocyanine CuPt1 is shown in Figure 3.2. The degree of substitution is not well defined, it can reach from 1.5 to 2 alifatic chain containing substituents and from 0.5 to 1 -SO_3H substituents per copper phthalocyanine. CuPt1 is neutrally charged in solution and is soluble in non-polar solvents.
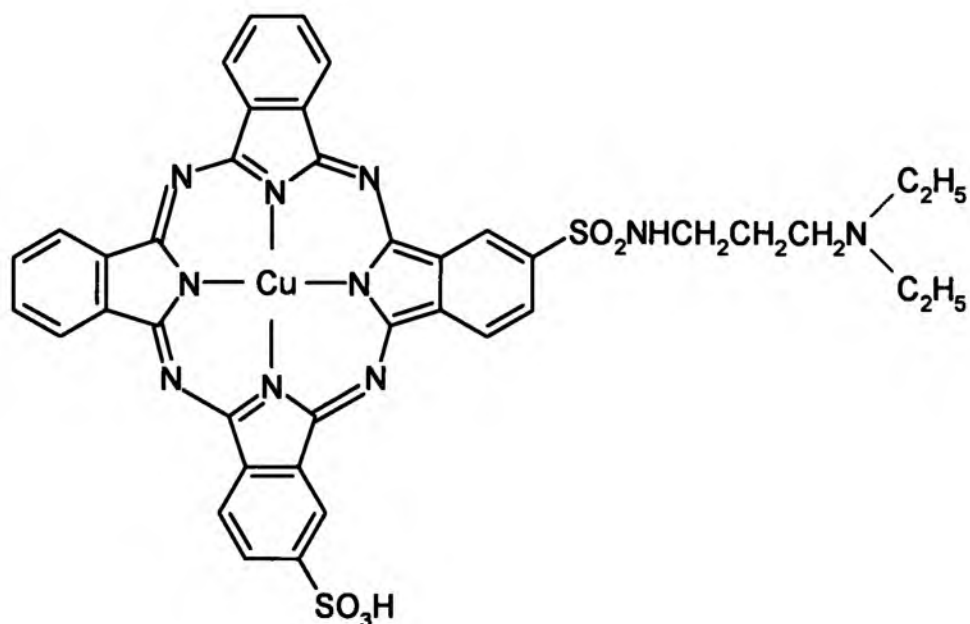
Figure 3.2. The chemical structure of CuPt1.

Chemical structure of the second copper phthalocyanine, CuPt2, is shown in Figure 3.3. As in the first case the substitution degree was not completely known, however, from the elemental analysis can be estimated 1.5-2 of alifatic chains containing substituent and 0,5-1 -SO$_3$H, per one copper phthalocyanine molecule. Compared to CuPt1, CuPt2 contains alifatic substutuents with two methyl instead of two ethyl groups. CuPt2 has a neutral charge and is soluble in non-polar solvents.
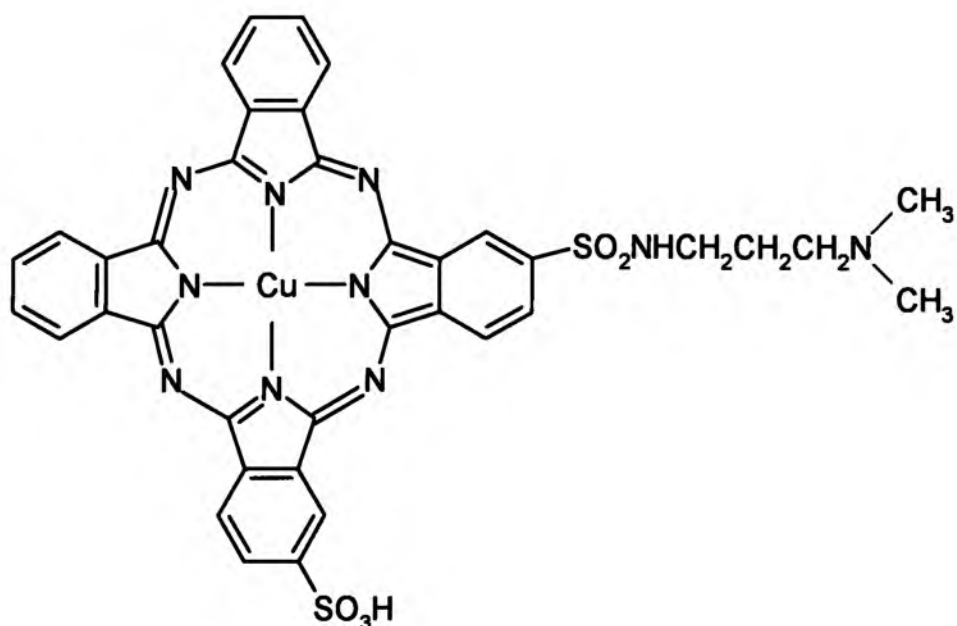

Figure 3.3. The chemical structure of CuPt2.

The last copper phtalocyanine, CuPt3, is a salt of sulphonated CuPt with a quaternary adduct containing with long aliphatic chains. It is a mixture having again 1-3 -SO₃H substituents per one copper phthalocyanine molecule. The number of CH_2 groups in the aliphatic chain is not well defined. The chemical structure of CuPt3 is shown in Figure 3.4. CuPt3 is soluble in non-polar solvents. Substituents of CuPt3 bear partial charges, SO₃ group is negatively charged and nitrogen positively.
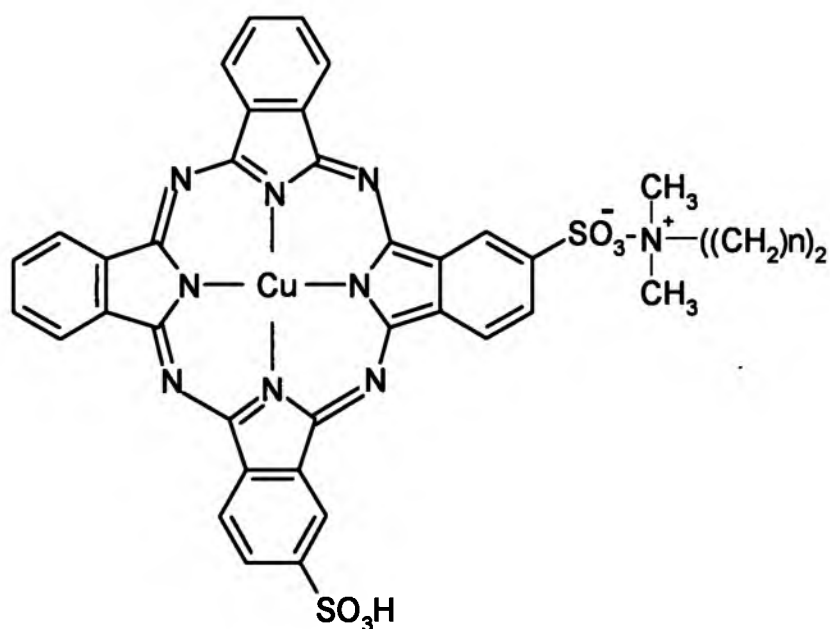

Figure 3.4. The chemical structure of CuPt3.

Extinction spectra in the region from 300 to 850 nm were measured for all phthalocyanines at 1×10^{-5}M concentration in aqueous solution (ZnPt) or in chloroform (CuPt1, CuPt2 and CuPt3). All spectra are shown in Figure 3.5. The samples were acquired in a 1cm quartz cuvette. The spectra have common features: Soret band at 340 nm and three Q-bands at 550-750 nm region. It is known that absorption band at 630 nm belongs to dimers of phtalocyanines (formed even for very low concentration, 0.1 μM for instance) and absorption band at 660 nm belongs to monomers. Spectra of all CuPts are very similar showing only different relative intensities of bands and a new band centered at 700 nm in the case of CuPt3. The spectrum of ZnPt significantly differs from the spectra of all CuPts. This difference can be explained by the effect of used solvents (water in the case of ZnPt and chloroform in the case of all CuPts). Amount of phtalocyanine dimers is higher in water than in chloroform.
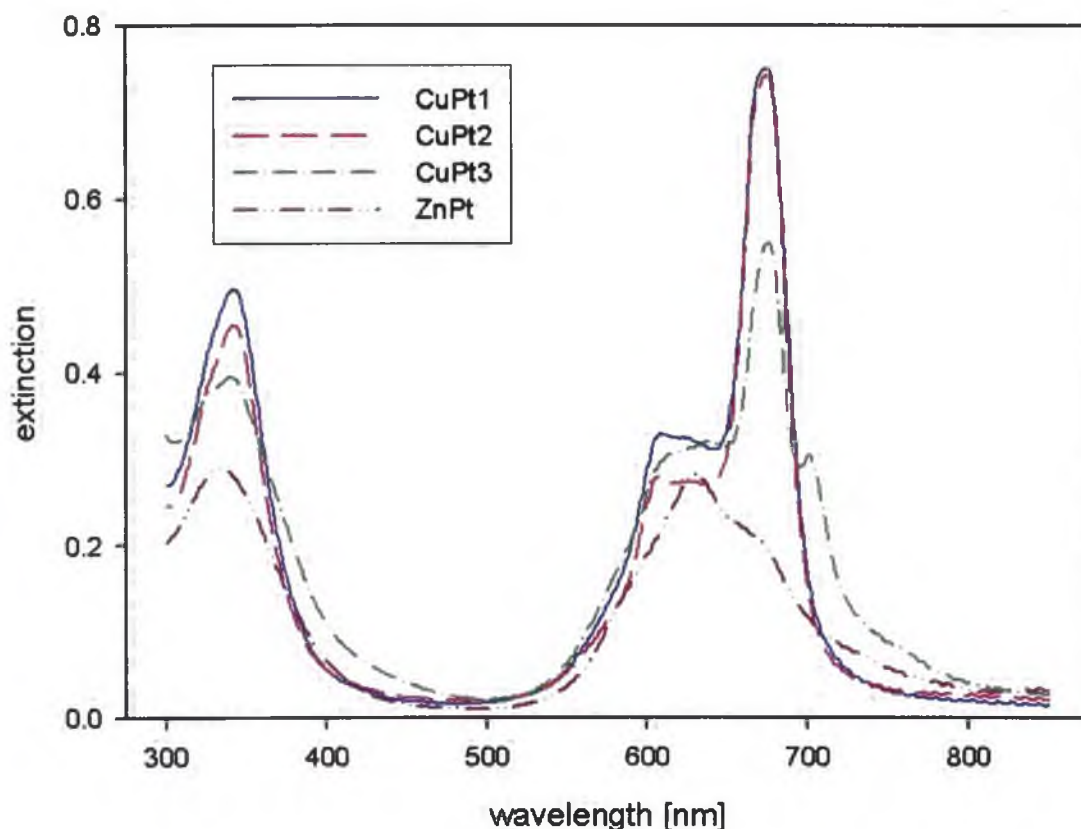
26

Figure 3.5. Extinction spectra of solutions of phthalocyanines in water, concentration 1×10^{-5}M (ZnPt), and in chloroform, concentration 1×10^{-5}M (CuPt1, CuPt2 and CuPt3).

3.2.2 "Azo" molecule

We also tested "azo" (5-[4-(4-Octyloxy-phenylazo)-phenoxy]-pentane-1-thiol; see Figure 3.6) but only first preliminary study was carried out. In the presence of metal nanoparticles many other interesting effects occur with higher efficiency, e.g photochromatic changes. After the photon absorption ($\lambda = 350$ nm) a trans conformation
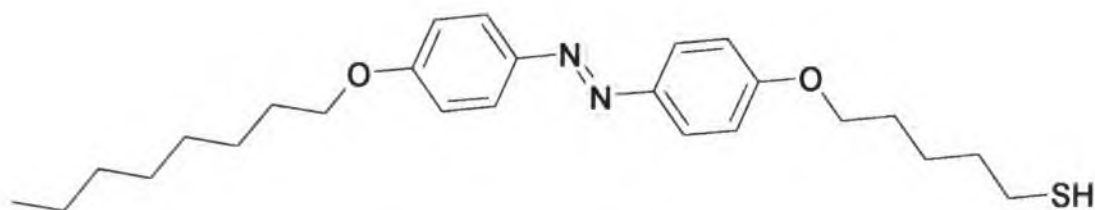

Figure 3.6. The chemical structure of "azo" molecule (5-[4-(4-Octyloxy-phenylazo)-phenoxy]-pentane-1-thiol).

is changed into a cis conformation with higher efficiency. The extinction spectrum is given in Figure 3.7 where only one maximum at 360nm was observed. A sample was measured in 1×10^{-4}M solution of chloroform using a 1 cm quartz cuvette.
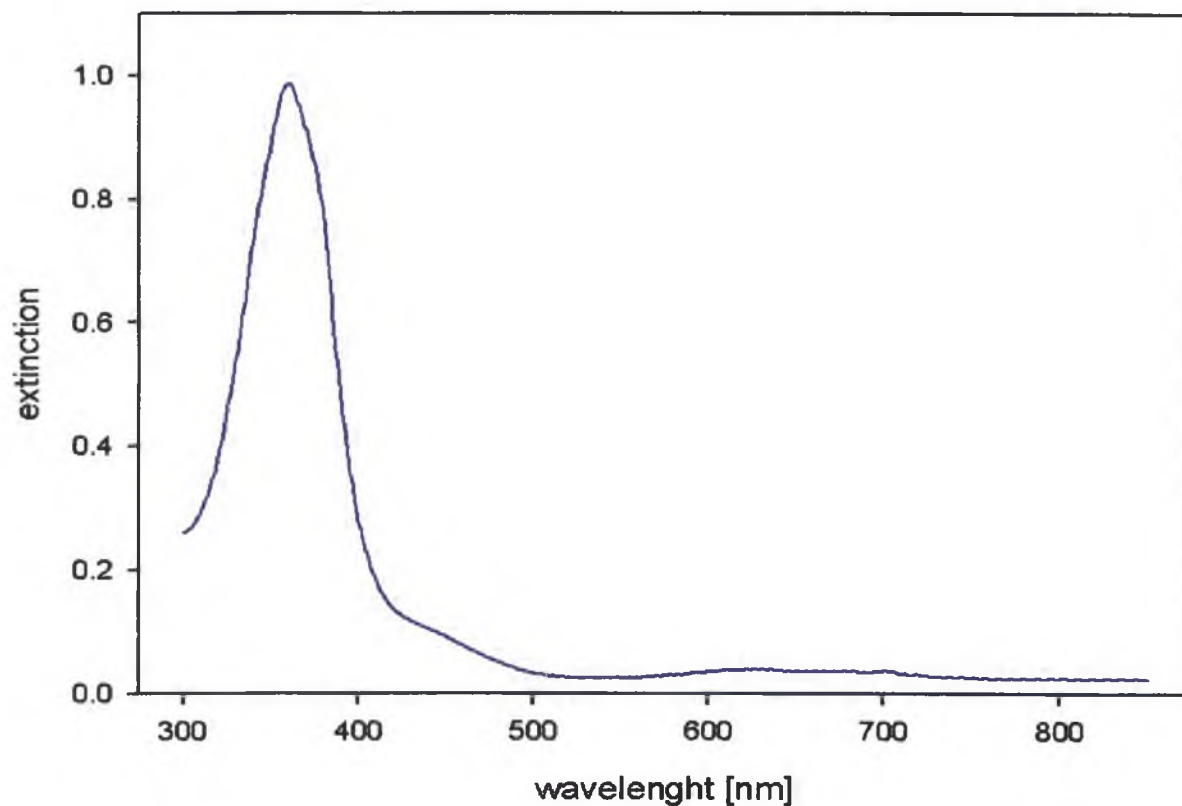

Figure 3.7. The extinction spectrum of the "azo" molecule, 1×10^{-4}M solution in chloroform.

4 Preparation of SERS-active surfaces

The purity of all reagents and glassware is crucial in the preparation of colloidal nanoparticles and their immobilization on silane-modified glass slides. All glassware as well as all glass slides were carefully cleaned using the "piranha" solution (4 parts of 96% H_2SO_4, 1 part of 30% H_2O_2) to remove organics and then the "aqua regia" (3 parts of 35% HCl, 1 part 65% HNO_3) to remove metals. Afterwards all glass vessels were rinsed several times in pure deionized water (resistance of 18 MΩ).

4.1 Citrate-reduced gold colloids

A citrate-reduced gold colloid was prepared in a reaction where $HAuCl_4$ was reduced by sodium citrate. 0.0978g $HAuCl_4$ were dissolved in 250 ml deionized water (18MΩ) and heated to the boiling point. Subsequently, the reducing agent 0.2853g sodium citrate in 25 ml deionized water was added into the boiling solution. During the chemical reduction an originally yellow color changed to the dark blue and finally to a dark purple. The solution was boiled for 25 minutes.

The extinction spectrum of a prepared gold citrate colloid is shown in Figure 4.1 where only one maximum at 519 nm is presented showing a very homogenous distribution of metal nanoparticles and no aggregation.
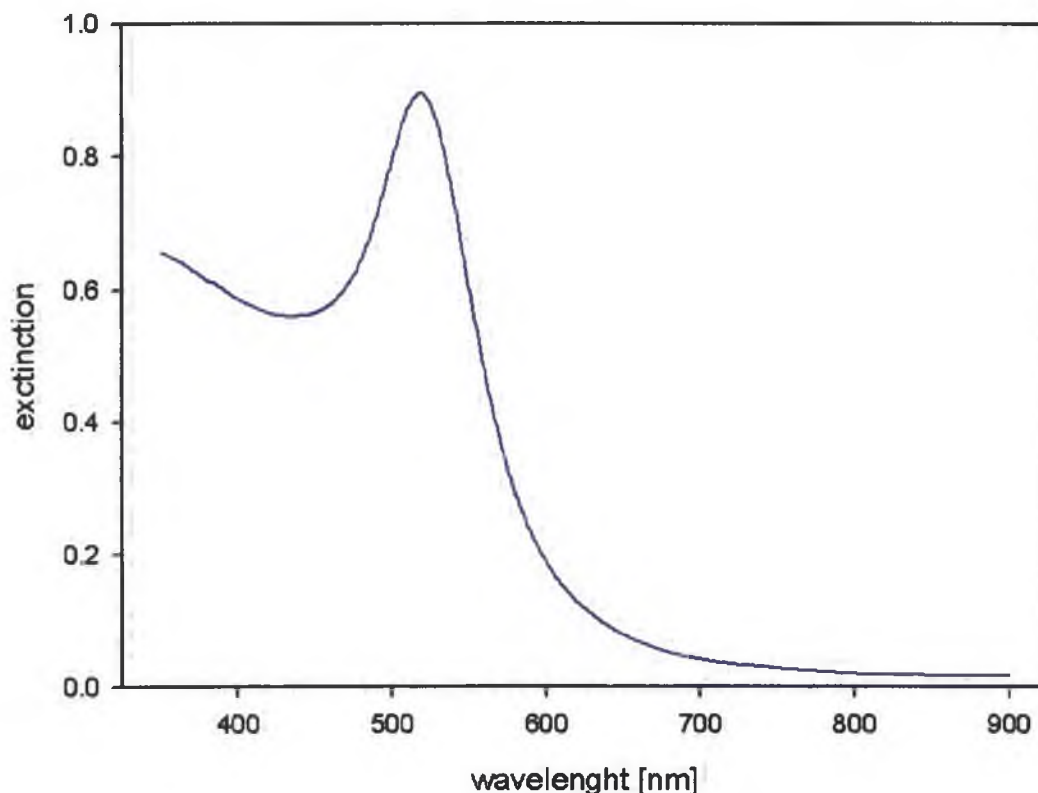
Figure 4.1. The extinction spectrum of a citrate-reduced gold colloid.

4.2 Colloidal nanoparticles immobilized on silane-modified glass slides ("substrates")

Gold SERS substrates were prepared onto 1cm x 2cm glass slides. Clean glass slides were put into a teflon holder and immersed into a solution of 90ml 99.8% methanol and 10ml 97% 3aminopropyltrimethoxysilane for 30 minutes. Silane-modified glasses were carefully rinsed with 99.8% methanol and deionized water to remove any physisorbed organosilane which could cause the aggregation of gold colloidal particles in the colloidal suspension during the next step. Each silanized glass plate was dipped vertically (thus a gold surface is formed on both sides of the glass slide) in a test-tube containing 1 ml of the colloidal suspension for 2-4 hours. Silane-modified glasses with immobilized gold particles were subsequently rinsed with deionized water and left to dry at 100°C for 20 minutes. The drying treatment subsequent to the immobilization of citrate-reduced nanoparticles stabilizes morphological properties of the surfaces and thus significantly improves the preparation procedure. High temperature increases the mobility of aminogroups in silane

chains; gold nanoparticles move closer together, which is seen by a second extinction band at 600-650 nm (Figure 4.2), typical for aggregates. The preparation of colloidal particles immobilized on silane-modified glass slides is described in detail in MSc. thesis of Natália Hajduková [23].
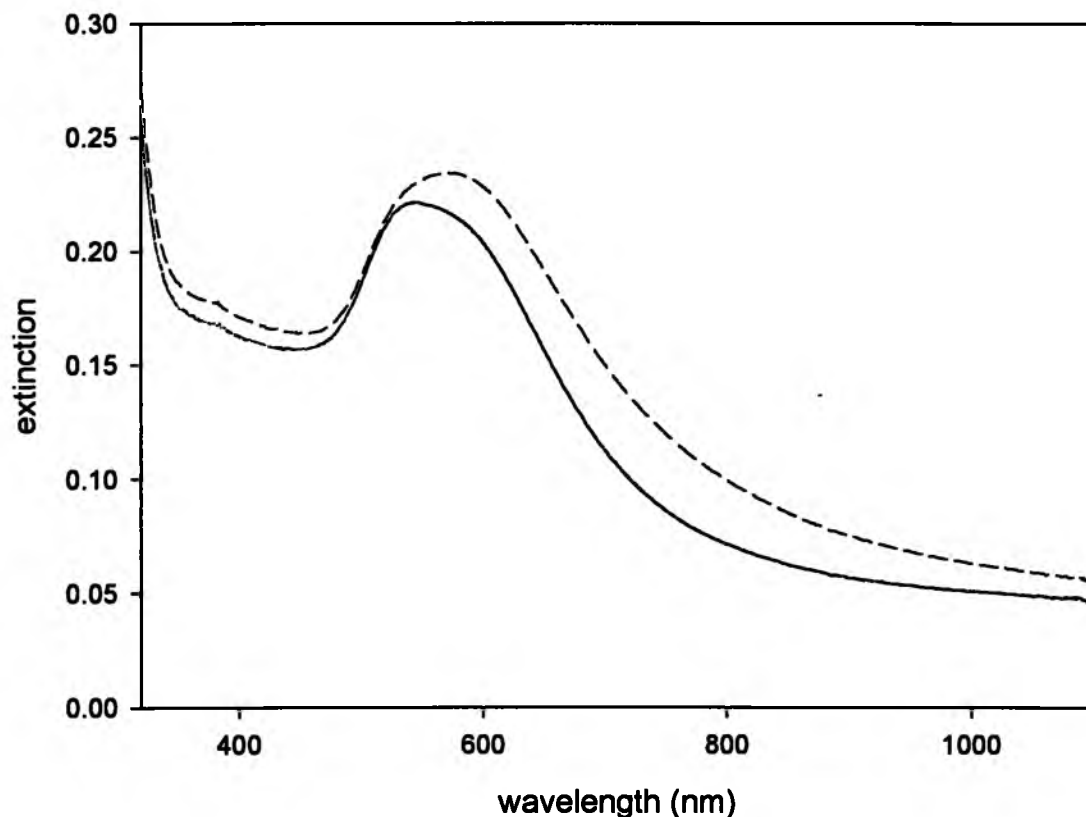

Figure 4.2. Extinction spectra of three gold substrates.

Surface roughness of gold citrate substrates is directly visible on AFM scans (see Figure 4.3). Two substrates were scanned in a tapping mode for three different resolutions. In both cases the surfaces consist of small aggregates of the size of a hundred nanometers and of isolated particles with diameters varying from ~ 30 to 100 nm, and some amount of small aggregates and/or of larger particles is also present. A multilayer probably forms the surface.
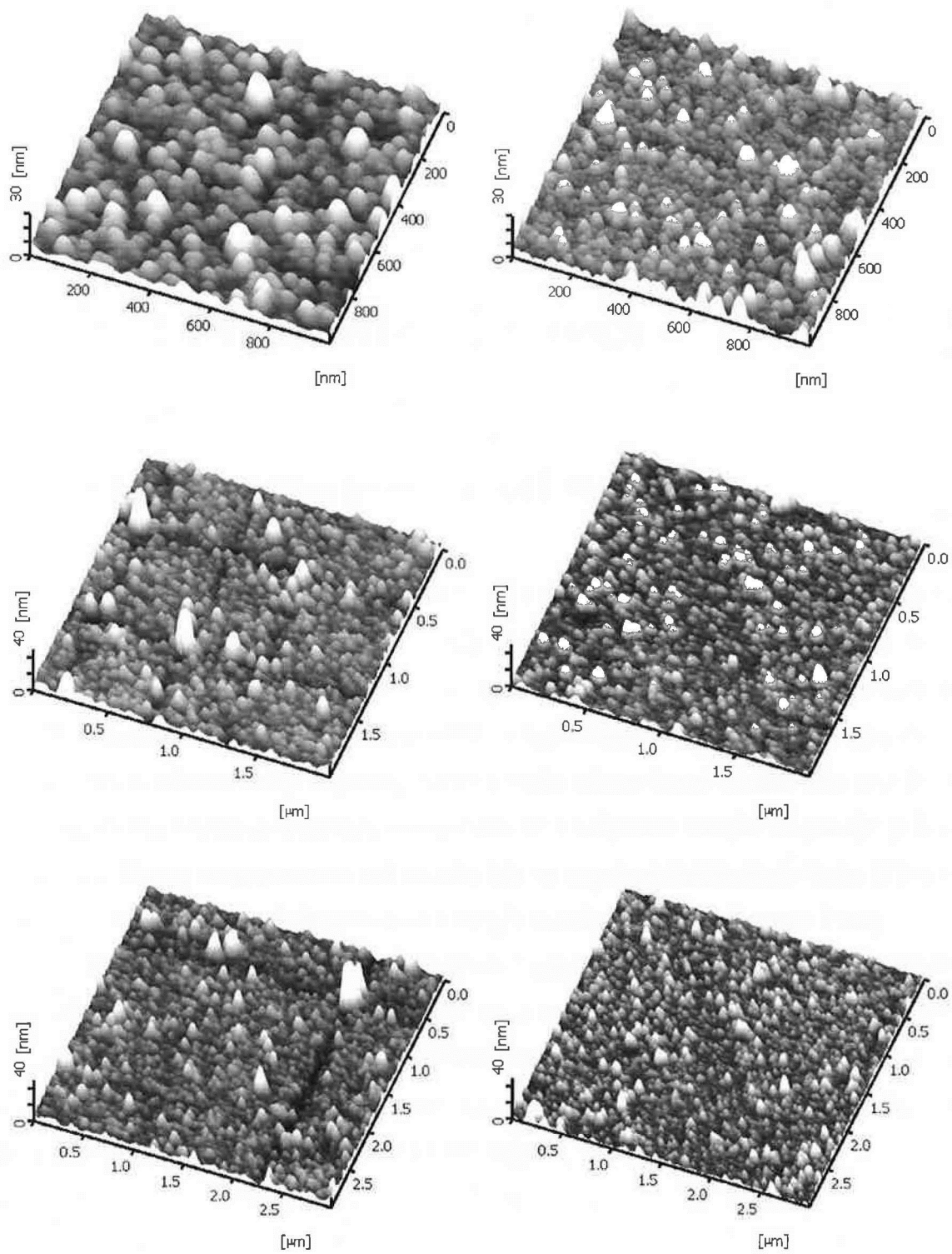
Figure 4.3. AFM images of two gold substrates prepared from citrate-reduced nanoparticles (substrate A left, substrate B right), three different AFM scans (length of the scan 1μm, 2μm and 3μm from the top, respectively).

5 Experimental devices

5.1 Optical absorption spectrometer

Optical absorption and extinction spectra were obtained using a double-beam absorption spectrometer UV-VIS Lambda 12 (Perkin Elmer). The schema of the spectrometer is shown in Figure 5.1. The spectrometer contains two different lamps, a visible halogen and an UV deuterium lamp. A light beam is generated in lamps and the wavelength is chosen using a grating. Subsequently a laser beam is split into two beams, one illuminates a measured sample and the second a reference sample. A change of lamps is possible during measurements and spectra can be acquired continuously from 190 nm to 1100 nm. The size of the light spot on the sample surface was about 9 mm x 1 mm.

Absorption spectra of studied molecules and extinction (extinction = absorption + scattering) spectra of initial gold colloids were measured in 1 cm cuvettes. Extinction spectra of gold substrates and gold substrate/molecule systems were measured in a vertical position to insure that whole light beam would illuminate the sample. All samples were measured from 300 nm to 1000 nm in a 1 nm step.
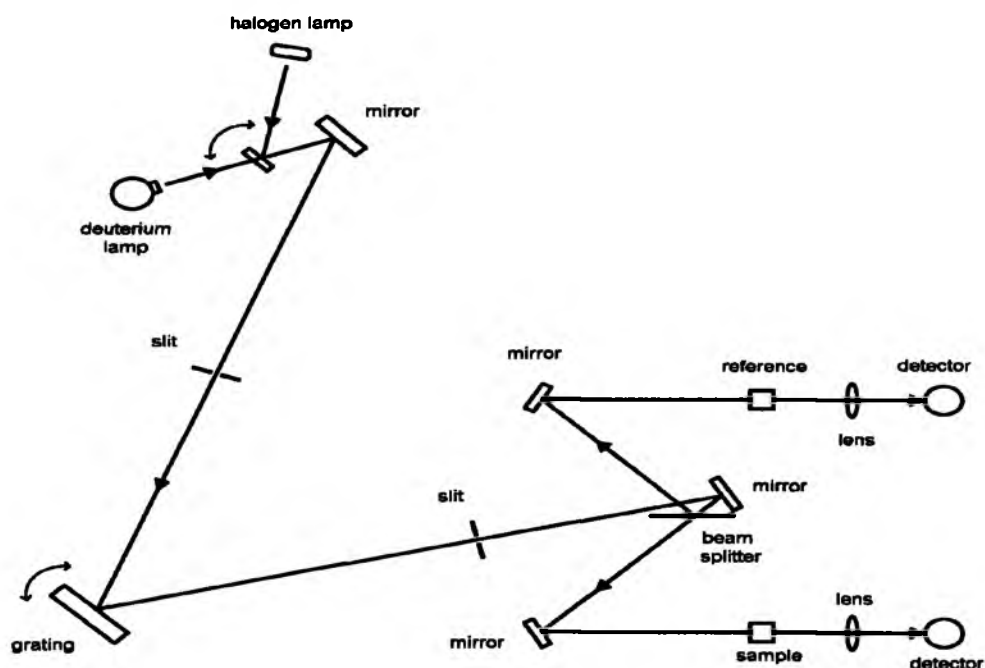
Figure 5.1. The schema of a double-beam absorption spectrometer UV-VIS Lambda 12 (Perkin Elmer).

5.2 Atomic force microscopy (AFM)

The atomic force microscopy (AFM) is a technique to determine surface morphology using a probe (tip) placed very close to a sample. AFM measures attractive or repulsion forces between a tip and a sample. AFM works usually in two modes. In the repulsive "contact" mode a tip is in close contact with the scanned surface. In the "tapping" mode a tip oscillates at its own frequency and thus, it touches the surface for a very short time.

AFM images of gold substrates were obtained on the SPA 400 apparatus, Seiko Instruments Inc. manufactured, at the National Institute for Materials Science in Japan with the great help of Mgr. Natália Hajduková.

5.3 Raman spectrometer

SERS spectra were obtained using a Raman spectrometer adapted to measurement of macroscopic samples in a 90° geometry (see the scheme in Figure 5.2). A laser beam is generated by the continuous-wave argon laser INNOVA 300 (Coherent). The laser beam

passes through an interference filter in order to suppress argon plasma lines. The use of grey filters can reduce the laser power. Glass lens was used to focus the beam (to a spot about 1mm x 1mm) on the sample where Raman scattering occurs. The scattering light is collected by an objective and focused into the monochromator through a holographic Notch-filter (Kaiser Optical Systems) that suppresses Rayleigh scattering. Light diffracted on a grating is detected by a nitrogen-cooled (–120°C) CCD detector. Since a new Raman spectrometer was build in our laboratory while this thesis was being compiled, two different spectrometers were used as a result: (i) the old one: with a monochromator (1200 gr/mm grating, Hilger&Watts), with a CCD detector (Princeton Instruments, 1024x1024 pixels), (ii) the new one: a monochromator (1600 gr/mm grating, Jobin Yvon-Spex 270M Instruments S.A., Inc.), with a CCD detector (100x1340 pixels, Princeton Instruments). New spectrometer provides higher sensitivity and broader detectable spectral region in comparison to old one.

514.5 nm line of an argon laser with the laser power on a sample about 150 mW was used. The entrance aperture width of the monochromator was adjusted to 48 μm. Raman spectra were accumulated for 300s that comprised of 30 accumulations for 10s. The spectrum of a neon lamp was measured for each Raman spectrum of a sample to calibrate the x-scale of the spectra using the NEOKAL program created by Doc. Jiří Bok. All necessary spectral treatment was done by the SPECTRACALC program (Galactic Industries Corp.).
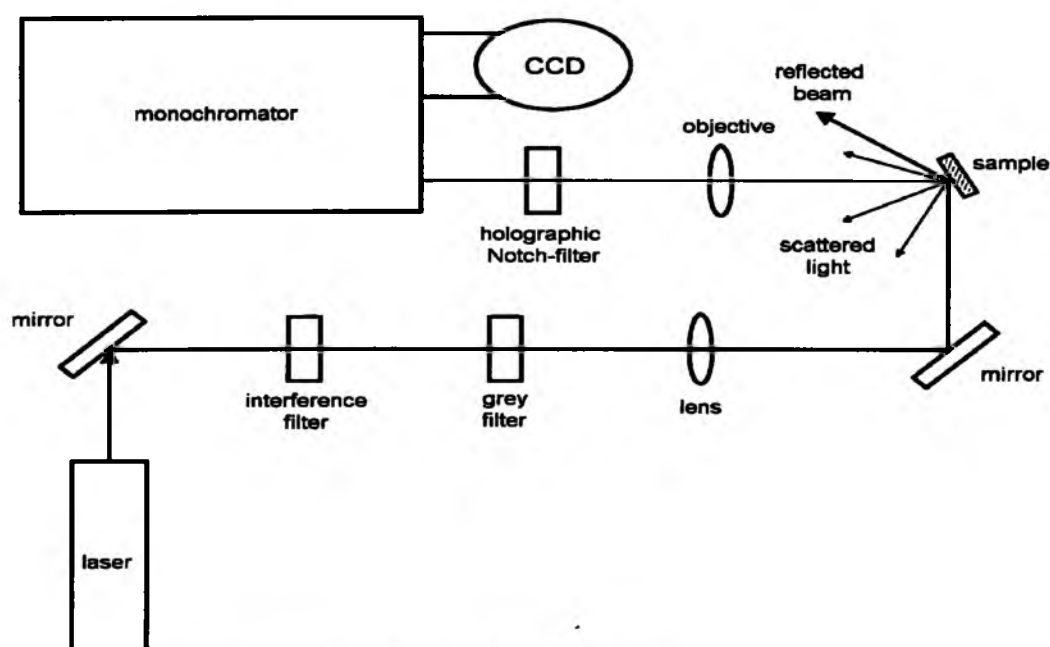

Figure 5.2. The schema of a Raman spectrometer.

6 Measurement

To study adsorption properties of different phthalocyanines on gold surfaces, time and concentration dependencies of their SERS spectra were studied. Time dependence measurements show us affinity of the studied phthalocyanines and kinetics of their adsorption to gold substrates and help us estimate the suitable soaking time to obtain their best SERS spectra. Concentration dependencies give us rough information about real concentration of adsorbed molecules on gold surfaces.

In case of the time dependence measurement a gold substrate was immersed into a solution of studied phthalocyanine with a particular concentration (mainly 10^{-4}M) for an appropriate period of time (soaking time). Then it was rinsed in deionised water or chloroform and SERS (and/or extinction) spectra were measured. The glass substrate was then placed again in the same phthalocyanine solution for a certain additional period of time, rinsed in deionised water (chloroform) and the next SERS (and/or extinction) spectra were measured. The soak-rinse-measure cycles were repeated gradually and the total time of soaking was counted. The time dependence measurements started from several minutes of soaking time and finished in 75 minutes.

The concentration dependence of SERS spectra was measured the same way, but the soaking time was fixed and phthalocyanine concentration was gradually increased. The soaking time was mostly 15 minutes. Concentration measurements varied from approximately 5×10^{-7}M to 10^{-4}M.

In a majority of cases, SERS spectra of studied molecules are overlapped by the background Raman spectrum of a glass substrate. On the other hand, the strong glass spectrum can be used as an internal intensity standard helping to reduce the effect of

possible variation of experimental conditions from sample to sample and consequently, making possible the quantitative comparison of SERS spectra of studied molecules measured from different samples. In Figure 6.1 a usual Raman spectrum (dominating by three strong bands at 556, 786 and 1096 cm^{-1}) of background glass substrate free of gold and adsorbed samples is presented. Firstly, spectra of adsorbed molecules were normalized on the intensity of the highest glass band at 1096 cm^{-1} and subsequently the spectrum measured from a pure glass substrate with a spectral background (fluorescence, Rayleigh scattering,...) was subtracted by the method of orthogonal difference. Several orthogonal multinominals together with the Raman spectrum of glass multiplied by appropriate coefficients fit the shape of a spectral background and the Raman spectrum of glass in this method. The method is described by D. Němeček [24] in detail.
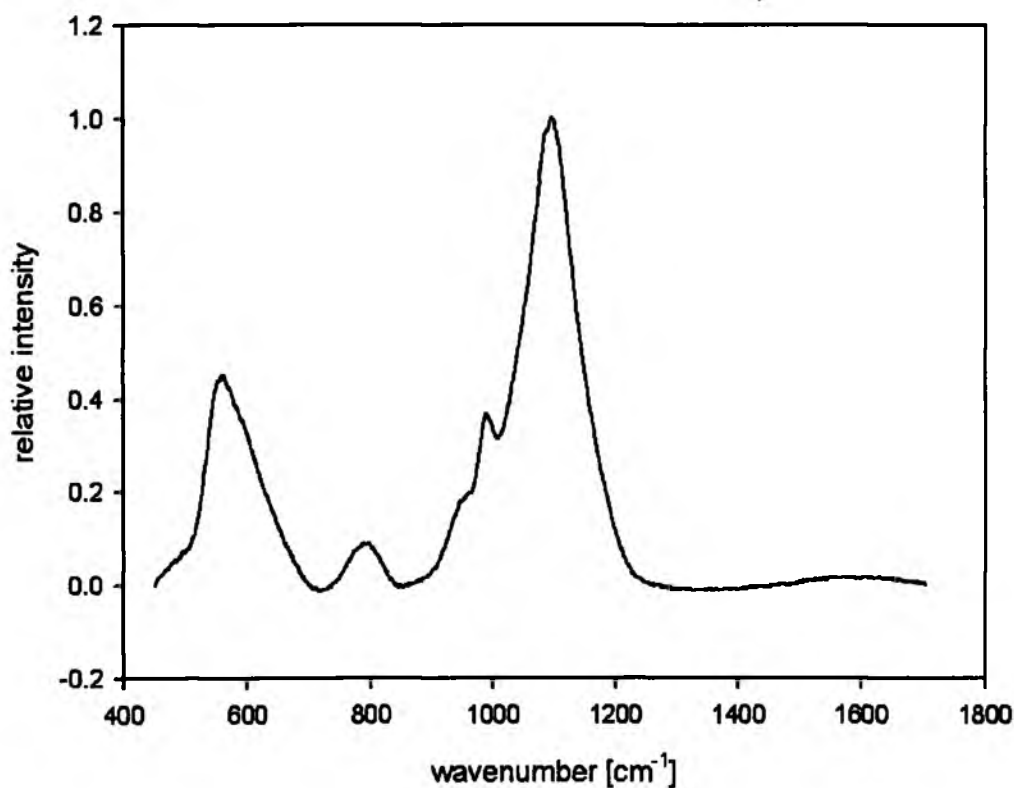

Figure 6.1. The Raman spectrum of an glass substrate with three dominant broad peaks of glass at 556, 786 and 1096 cm^{-1}.

Chapter IV

Results and discussion

7 Phthalocyanines

7.1 Comparison of Raman and SERS spectra

Before time and concentration dependencies Raman spectra of phthalocyanines were measured. Solution of phthalocyanine of desired concentration was dropped on a clean glass substrate. After drying of a drop, Raman spectra were measured using the new Raman spectrometer. A laser spot was focused to the edge of dried drop where the amount of phthalocyanine is the highest. Two concentrations 1×10^{-4}M and approximately 2×10^{-3}M were chosen for measurements.
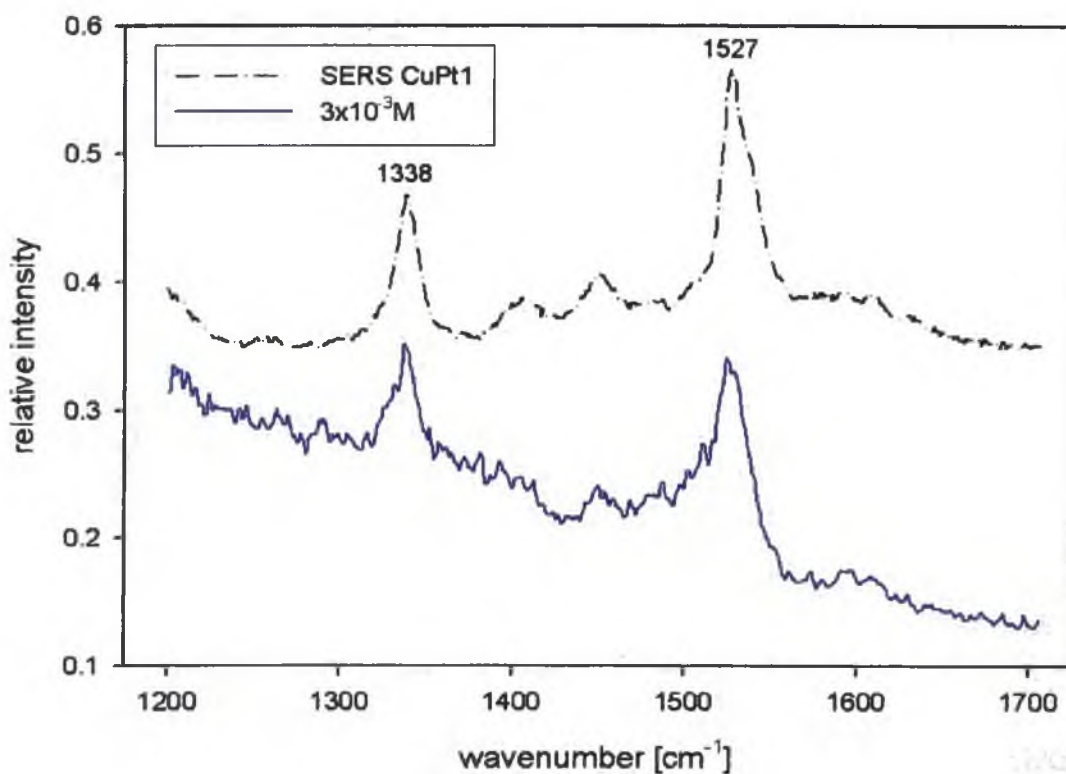
Figure 7.1 The Raman spectrum of CuPt1 for 3×10^{-3}M concentration. For comparison the SERS spectrum of CuPt1 (concentration 1.10^{-4}M for 75 min of soaking time) was added.

39
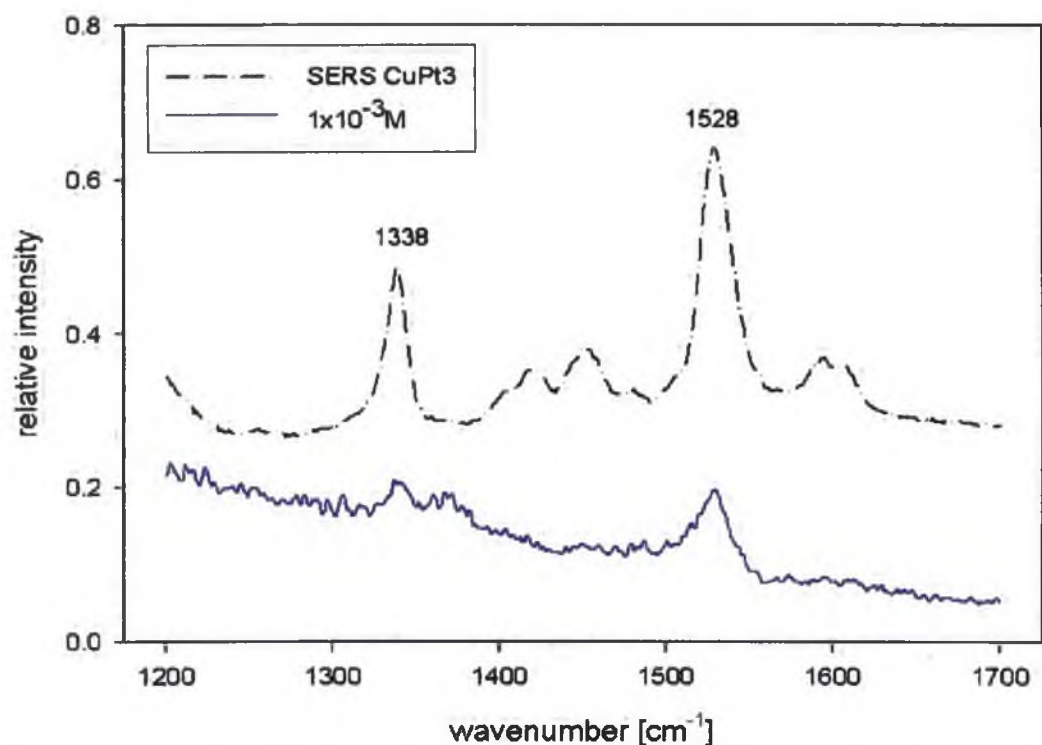
Figure 7.2. The Raman spectrum of CuPt3 for 1×10^{-3}M concentration. For comparison the SERS spectrum of CuPt3 (concentration 1×10^{-4}M for 75 min of soaking time) was added.
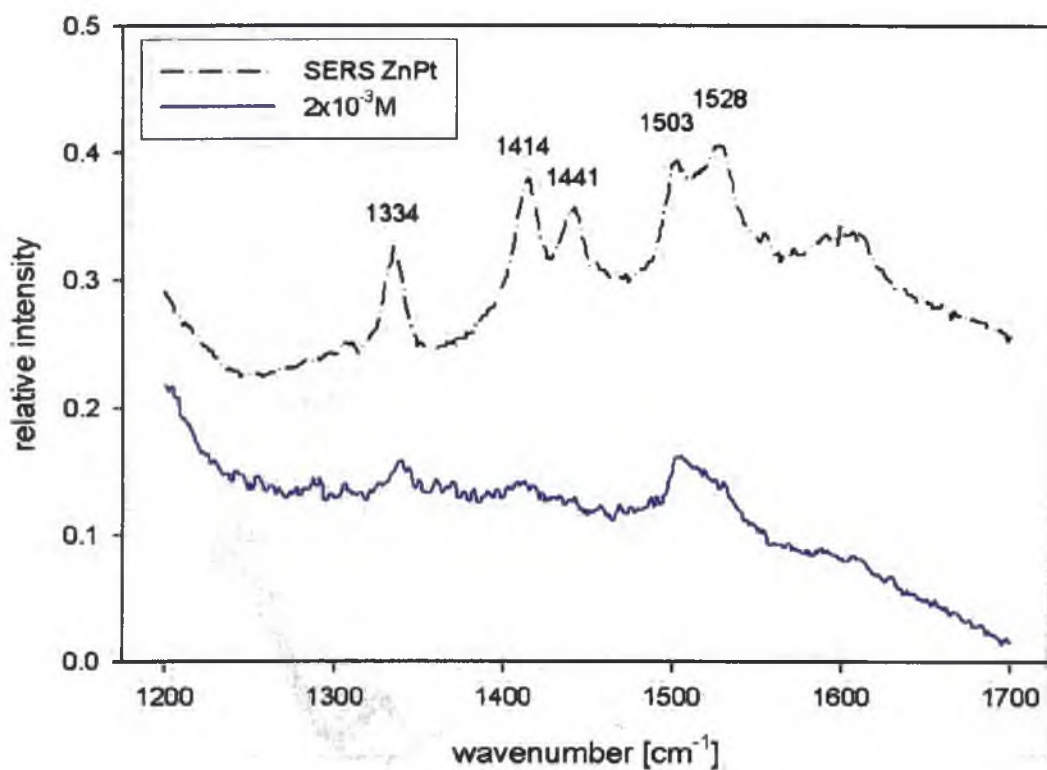

Figure 7.3. The Raman spectrum of ZnPt for 2×10^{-3}M concentration. For comparison the SERS spectrum of CuPt3 (concentration 1×10^{-4}M for 75 min of soaking time) was added.

Series of measurements for $1 \times 10^{-4} M$ concentration were carried out and no phthalocyanine signal was detected (not shown here). Raman signals of phthalocyanines are visible for higher concentration series. Obtained results are shown in Figures 7.1, 7.2 and 7.3 where at least the strongest two peaks at 1338 and 1528 cm^{-1} are observable. These results show that Raman scattering for $1 \times 10^{-4} M$ concentration does not affect measured SERS spectra, so our measurements are clearly SERS signals without Raman signals.

7.2   Zinc phthalocyanine

7.2.1   Time dependence of ZnPt

All of the time dependence studies with zinc phthalocyanine (ZnPt) were carried out using the "old" Raman spectrometer. For time dependence measurement a gold substrate was immersed in 1×10^{-4} M ZnPt aqueous solution. The first spectrum was measured after 5 minutes of soaking time, and further soaking times used were 10,15,20,25,30,45,60 and 75 minutes of soaking a substrate in the solution. The ZnPt time dependence was measured
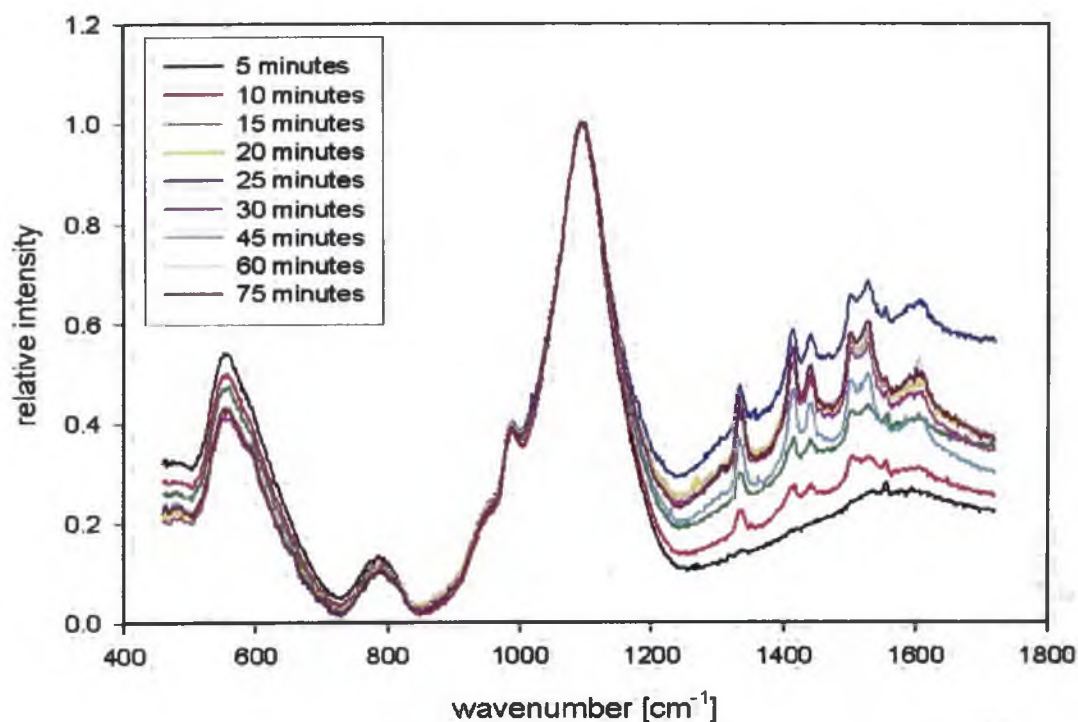

Figure 7.4: SERS spectra of zinc phthalocyanine adsorbed from $1 \times 10^{-4} M$ stock solutions on a gold substrate for different soaking times.
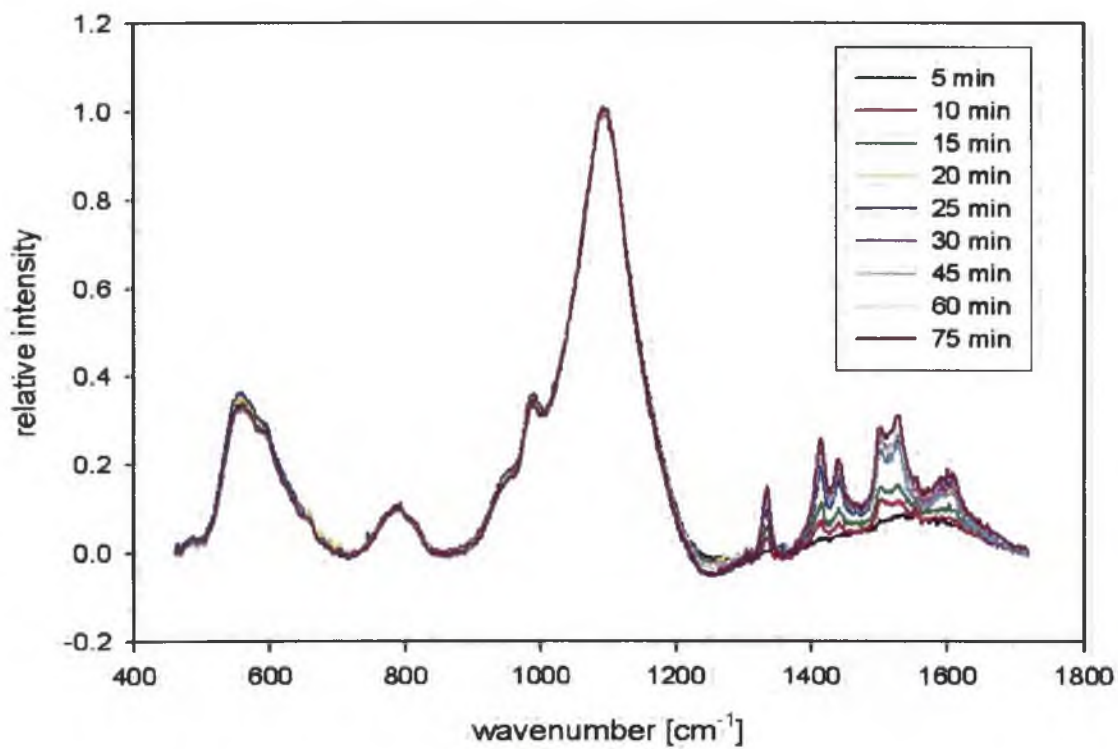
Figure 7.5: Same as in Figure 7.4. Normalized and linear baseline corrected SERS spectra.
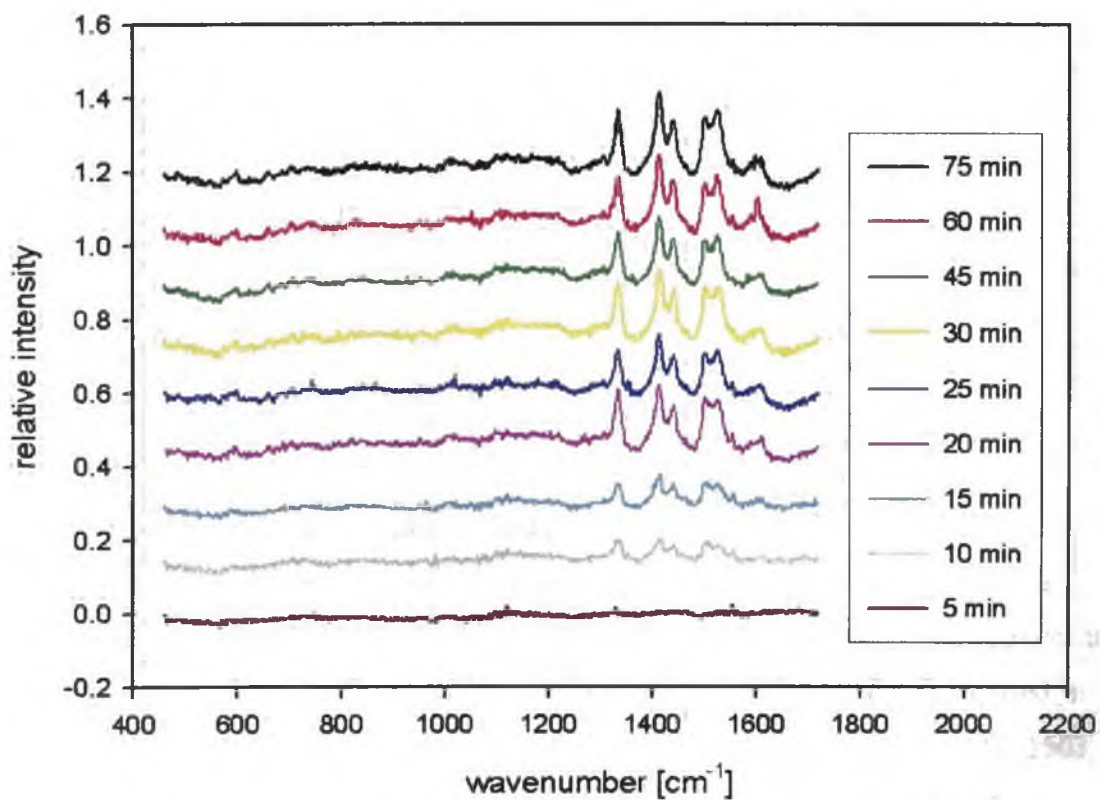

Figure 7.6: Same as in Figure 7.4. The Raman signal of glass is subtracted from the spectra.

separately on two gold substrates (sample A and B). Typical spectral series obtained from sample A are shown in Figure 7.4. The spectra are dominated by strong Raman bands of glass in region from 500 to 1200 cm^{-1} and the SERS signal of ZnPt varies with soaking time. Normalized (to the strong Raman band of glass) and baseline corrected SERS spectra are shown in Figure 7.5, spectra with the subtracted signal of glass are shown in Figure 7.6.
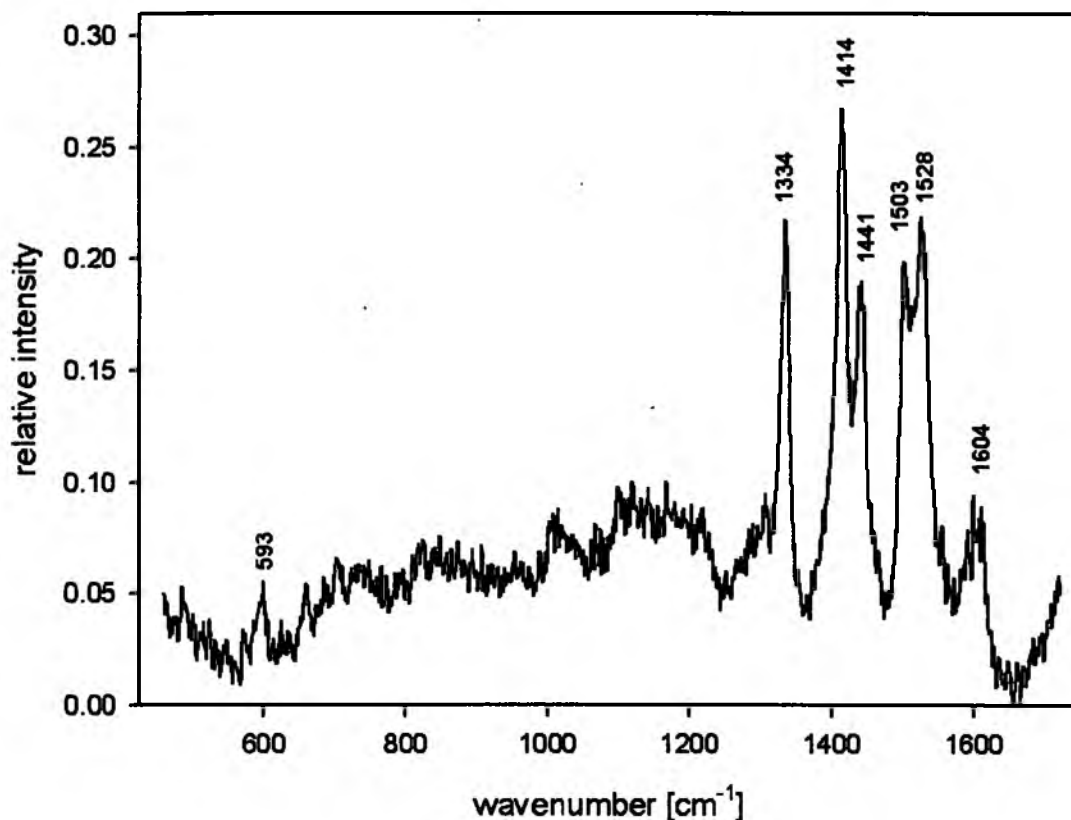

Figure 7.7: The subtracted SERS spectrum of ZnPt on gold substrates adsorbed in 1x10^{-4}M solution for 75minutes (magnified from Fig. 7.6).

Copper tetrasulphonated phthalocyanine tetrasodium salt electrodeposited on gold electrodes was studied by SERS and vibration spectra were calculated using the density functional theory (DFT) calculations by Karolien De Wael et al. [25]. Other studies of thin solid films of copper phthalocyanine were done by R. Aroca et al. in [26] showing a heating effect (shift of some bands with temperature) and R. Prabakaran et al. published a study of copper phthalocyanine thin films by SERS and absorption spectroscopy [27]. According to these three works, we assigned the spectral bands of ZnPt, the assignment is listed in Table 7.1. In the spectra the six strong peaks of zinc phthalocyanine (1334, 1414, 1441, 1503, 1528 and 1604 cm^{-1}) are seen. 593 cm^{-1} band is weak but clearly observable for longer soaking times.

Table 7.1. Raman active molecular vibrations of zinc phthalocyanine on a gold substrate.

Position (cm^{-1})	Interpretation
593 (w)	out-of-plane bending mode (a)
1334 (m)	C-N breathing (a)
1414 (m)	C-N stretching (c)
1441 (m)	pyrrole stretch (b)
1503 (m)	
1528 (m)	C=C pyrrole stretch (a)
1604 (m)	

Assignment (a) Karolien De Wael [a10]
        (b) R. Aroca [a11]
        (c) R. Prabakaran [a12]

In the time dependence, no changes of the character of the spectra except of a decrease of intensity ratio of 1503 versus 1528 cm^{-1} bands were observed. The possible origin of this change is discussed in the next chapter. The overall intensity of the SERS signal of zinc phthalocyanine is developes during measurements. To obtain the time dependence of SERS intensity of adsorbed ZnPt, the doublet formed by two intense peaks at 1503 and 1528 cm^{-1} was integrated. Results presented in Figure 7.8 clearly show that the SERS intensity of zinc phthalocyanine rapidly increases during first 20-30 minutes of soaking and then it reached the saturated value. Thus, 20-30 minutes of soaking time seems to be the optimal time to obtain the maximal SERS signal. Extinction spectra have not been measured for this series.
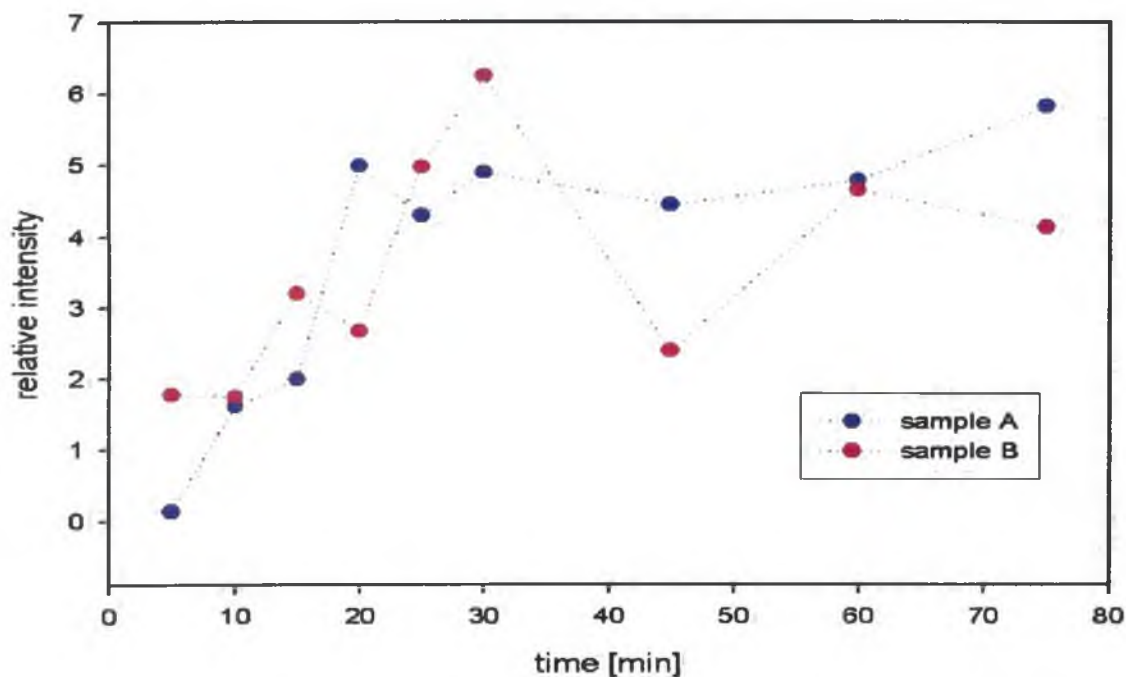

Figure 7.8. The total integrated intensity of Raman peaks at 1503 and 1528 cm^{-1} of zinc phthalocyanine peaks for two samples separately measured in the time dependence. (The lines directly connecting consecutive points are included as a guide for the eyes and do not represent real dependencies).

7.2.2 Concentration dependence of ZnPt

Four concentrations dependences of ZnPt were measured; two on the old Raman spectrometer and two on new one.

7.2.2.1 Measurement using the old Raman spectrometer

The concentration 5×10^{-7} M of ZnPt was chosen for the initial measurement where a substrate was immersed for 30 minutes and the SERS spectrum was measured. 30 minutes soaking time was estimated from time dependencies as the most optimal adsorption time. The following steps were repeated with higher concentration however for the same time. ZnPt concentrations were increased from 5×10^{-7}M to 1×10^{-4}M. Similarly to the time dependence, the concentration dependence was separately measured on two gold substrates (samples A and B).

Normalized and baseline corrected SERS spectra of ZnPt for different concentration of stock solution are shown in Figure 7.9 and 7.10.
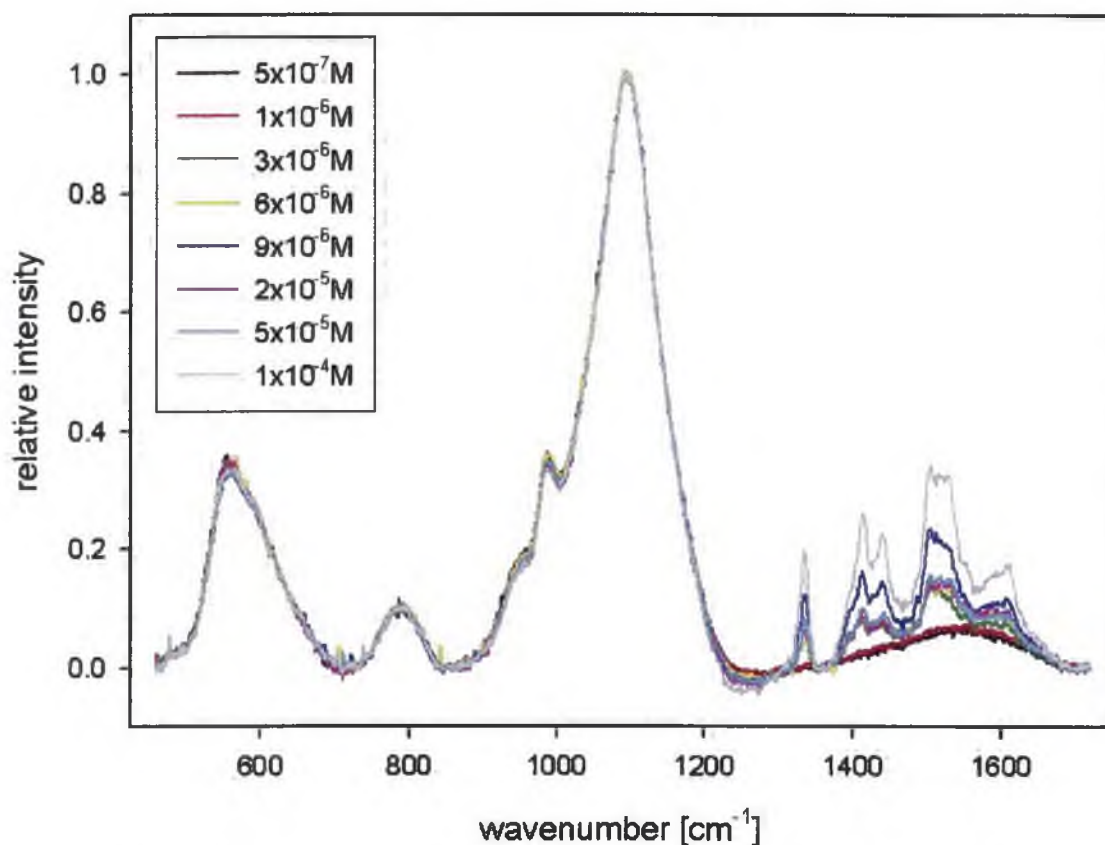

Figure 7.9: Normalized and baseline corrected SERS spectra of zinc phthalocyanine for different concentrations of stock solution
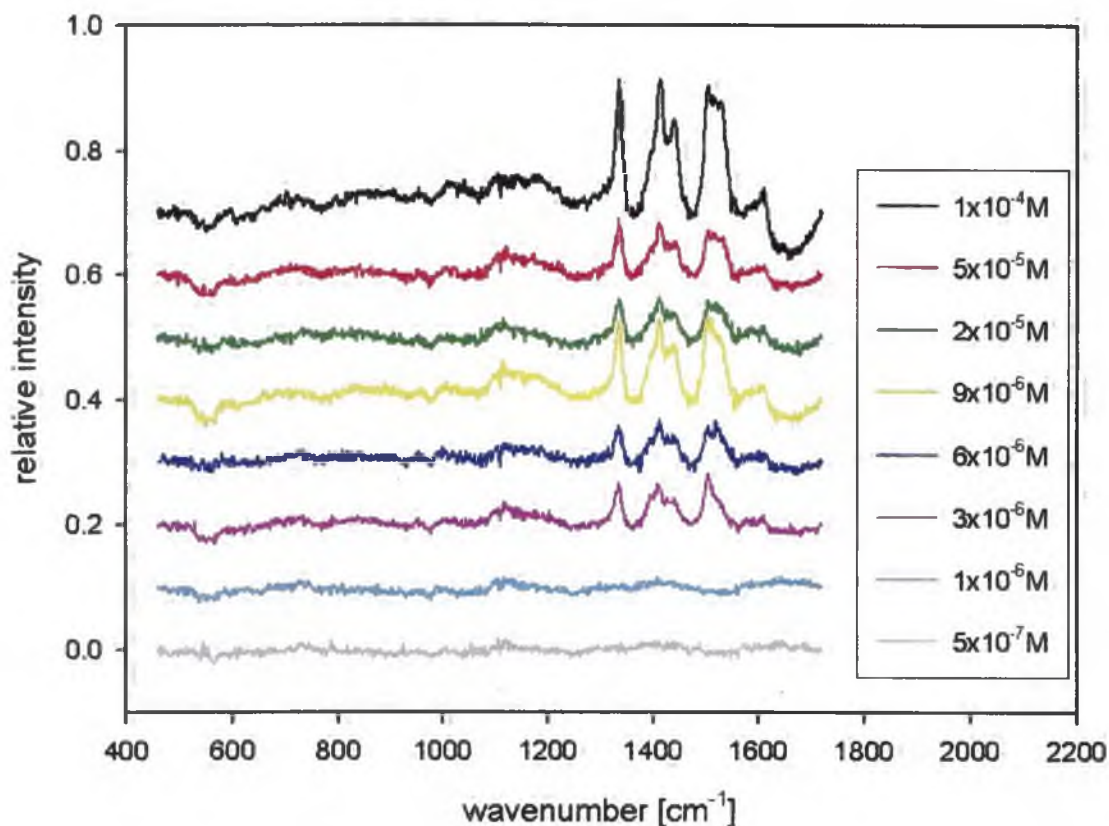
45

Figure 7.10: Same as in Figure 7.9. The Raman signal of glass is subtracted from the spectra.

The six peaks are presented in the spectrum and their assignment is mentioned in Tab 7.1 in the previous chapter. The peaks in concentration dependence are fixed in the same position as well as in time dependence, no position changes were observed. The relative intensities were also checked and no changes except two peaks 1503 and 1528 were found. Peak at 1528 cm^{-1} slightly grows with increasing concentration. The same effect appeared on the new spectrometer where peak 1528cm^{-1} is even more intensive than peak 1503cm^{-1} for higher concentrations (see Fig. 7.11). Since these spectral changes are observed in both time and concentration dependence and 1528cm^{-1} band was assigned to C=C or C=N pyrrole stretching vibration (see Table 7.1), we propose that these changes are connected to deformation of the central ring of a phthalocyanine molecule during adsorption.

Whole intensities were also determined where two peaks at 1503 and 1528 cm^{-1} were integrated. Results in Figure 7.12 showed very similar behavior for both samples. A signal increases during the whole measurement in both samples and a plateau is not reached even for the highest concentration 1x10^{-4}M. This experiment indicates that the saturation of signal for ZnPt is not reached for concentration 1x10^{-4}M at a given time of adsorption 30minutes.

We would like to mention that 1503 and 1528 cm^{-1} bands were chosen to determine the SERS intensity of ZnPts because 1528 cm^{-1} band was used also in the case of all CuPts. Since two peaks with varying relative intensity do not seem to be suitable for this purpose, we used also 1334 cm^{-1} in this case. In the Figure 7.12, the intensities of peak 1334 cm^{-1} and two peaks 1503 and 1528cm^{-1} are compared. Since the results are completely the same, we conclude that using the total intensity of both 1503 and 1528cm^{-1} peaks to determine SERS intensity is possible.

7.2.2.2   Measurements using the new Raman spectrometer

The conditions and the procedures of the measurement are nearly the same as in the case of the concentration dependence measured using the old Raman spectrometer. Two samples were investigated with the same initial and final concentrations in eight steps. A little difference was in the time of adsorption in order to compare the results with the measurement series of copper phthalocyanines. In this case the adsorption time was 15 minutes.
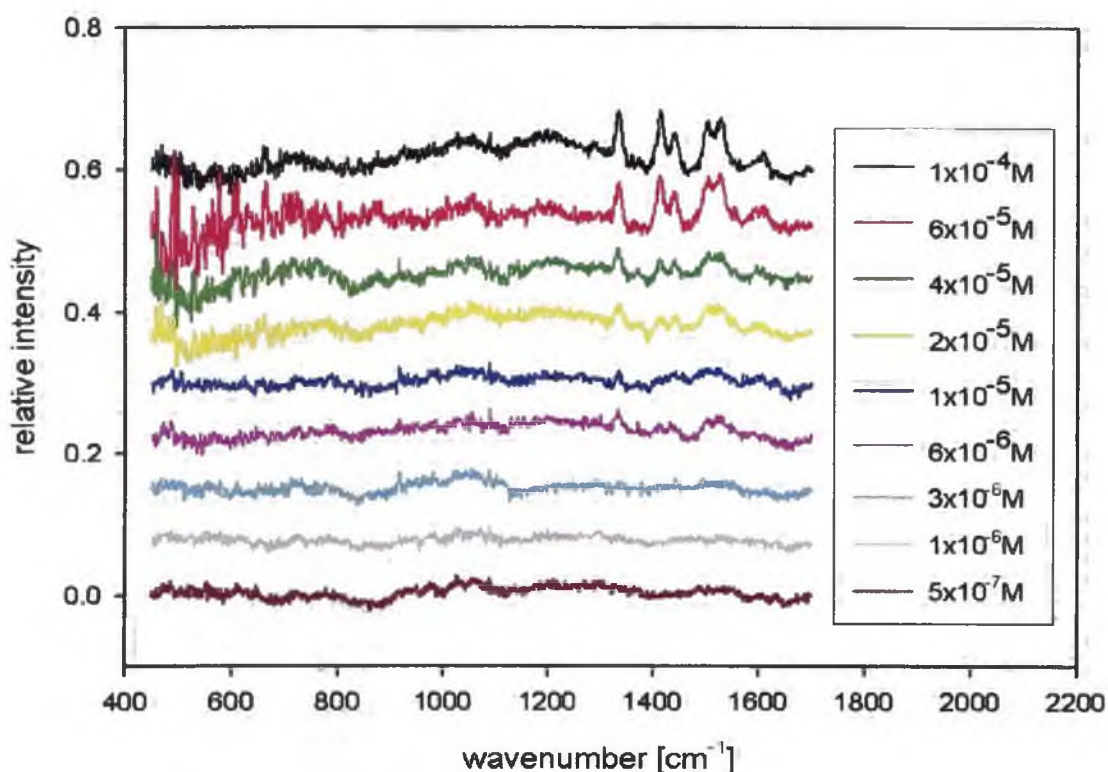

Figure 7.11: Subtracted spectra of zinc phthalocyanine in the concentration dependence.

The measured spectra were normalized, baseline corrected and Raman spectrum of glass subtracted. The spectra are presented in Figure 7.11. Five peaks are visible, centered at 1334, 1414, 1441, 1503 and 1528 cm^{-1}. Peaks at 593 and 1604 cm^{-1} are not clearly visible. No changes in spectrum shape except those mentioned in the previous part appeared. Although in this case, the intensity is lower that this one obtained by the old spectrometer, the tendency of the dependence is identical.

Two control measurements were done and are given also in Figure 7.12. Each substrate with adsorbed zinc phthalocyanine from the concentration dependencies was immersed into 10^{-4}M zinc phthalocyanine solution for another 30 minutes. Both samples show a weaker signal in comparison with the previous measurements at 10^{-4}M concentration for 15 minutes indicating a plateau is almost reached.
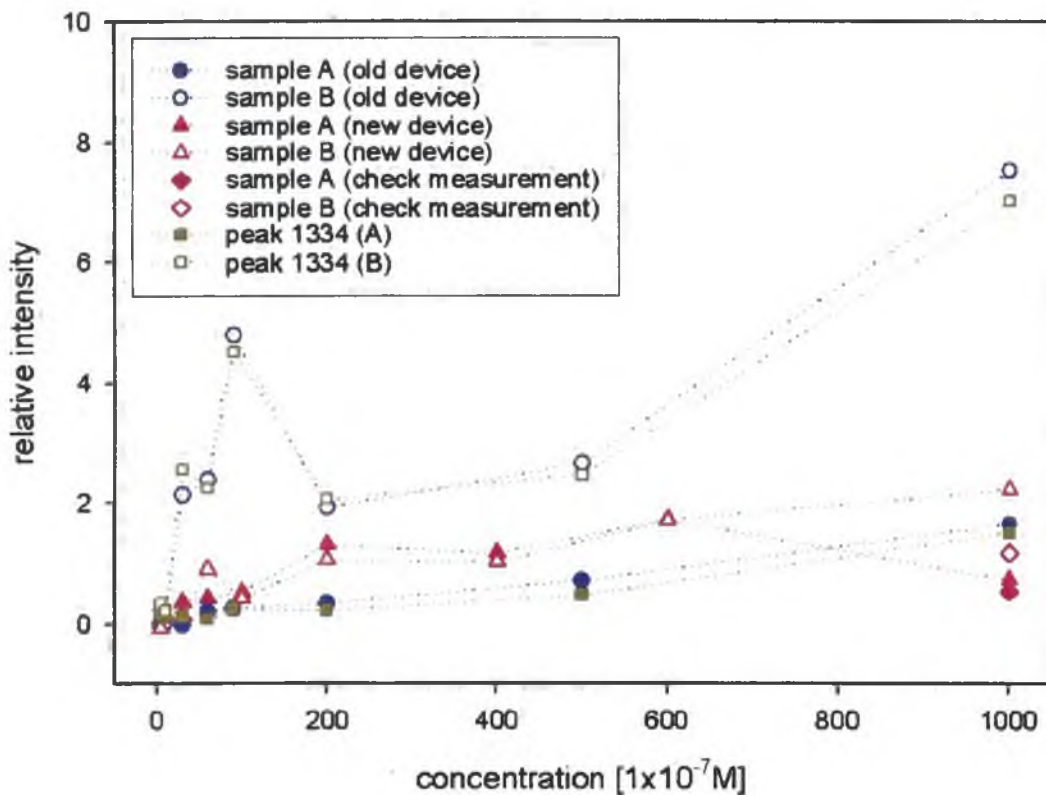

Figure 7.12: Intensities of zinc phthalocyanine peaks at 1503 and 1528 cm^{-1} for two samples concurrently measured on the old device (circles) and for two samples on the new device (triangles) in concentration dependency. Single diamonds at 1×10^4M present control measurements on the new spectrometer. Peak 1334cm^{-1} at the old spectrometer was also integrated. (The lines directly connecting consecutive points are included as a guide for the eyes and do not represent real dependences).

Extinction spectra of gold substrate and gold substrate/zinc phthalocyanine systems with different ZnPt stock solution concentrations are shown in Figure 7.13. The black solid

line shows the extinction spectrum of a clear substrate without adsorbed zinc phthalocyanine. The other spectra are obtained immediately after SERS detection. Extinction spectra show slow increasing of extinction of the gold substrate with concentration of adsorbed ZnPt. Although very weak, the shoulders corresponding to the Q band and Sorret band of ZnPt are clearly visible (compare with Figure 3.5).
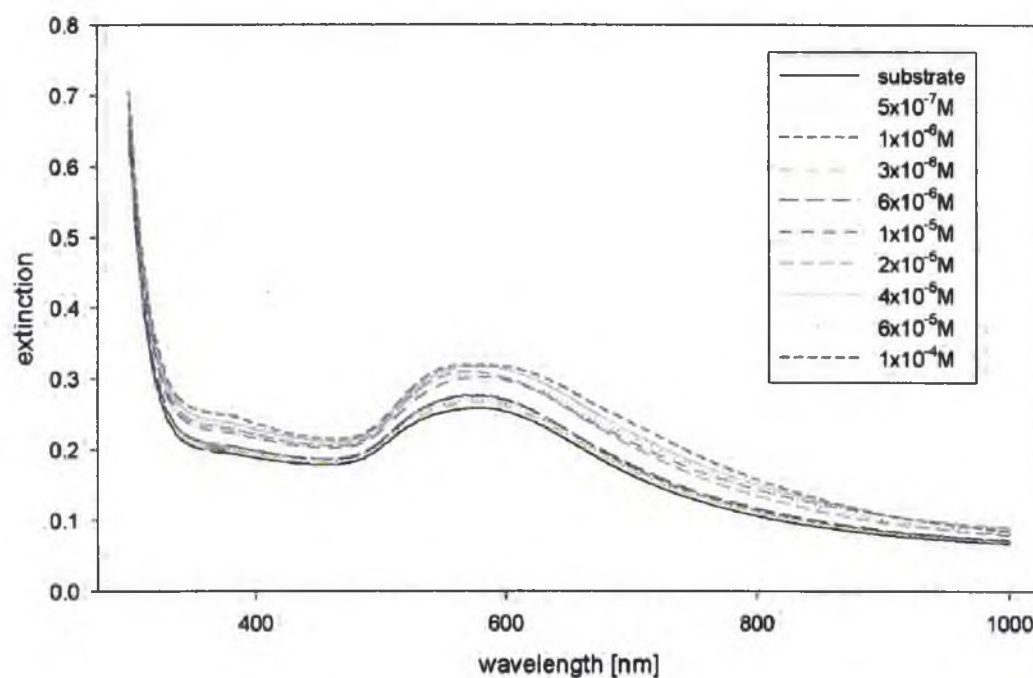

Figure 7.13: Extinction spectra of gold substrate and gold substrate/zinc phthalocyanine systems with different ZnPt stock solution concentrations.

7.2.3 Comparison of time and concentration dependencies of ZnPt

Results obtained from SERS spectra and extinction spectra show mostly slow and not very efficient adsorption of ZnPt onto gold surfaces. Tendency of time and concentration dependences of Raman signal intensity for ZnPt is slightly different. Although, in the case of time dependence, a maximum and, subsequently, a plateau is reached after 30 minutes of soaking time, the concentration dependence shows no saturation, instead a slight increase of the SERS signal even for higher concentrations was observed (see Figures 7.8 and 7.12). Observable relative changes of 1503 versus 1528 cm^{-1} bands in all spectra series indicate some deformation of the ZnPt macrocycle during the absorption process (Figures 7.6 and 7.11).

7.3 Copper Phthalocyanines

Phthalocyanines CuPt1, CuPt2 and CuPt3 dissolved in chloroform were investigated using the "new" Raman spectrometer.

7.3.1 Time dependence for CuPt1 and CuPt2

Time dependencies of adsorption of the phthalocyanines CuPt1 and CuPt2 onto the gold substrates were investigated first. Gold substrates were immersed into 1×10^{-4} M solution of copper phthalocyanine in chloroform. The procedure is the same as in the case of zinc phthalocyanine. The initial time was set on 5 minutes, next soaking times were 10, 15, 20, 30, 45 and 75 minutes. Concentration of CuPt remains the same during all measurements. The time dependences were separately measured on two gold substrates (sample A, B).

7.3.2 Time dependence of CuPt1

Normalized (to the strong Raman band of glass) and baseline corrected SERS spectra are shown in Figure 7.14. Strong phthalocyanine bands are well observed in 1300 to
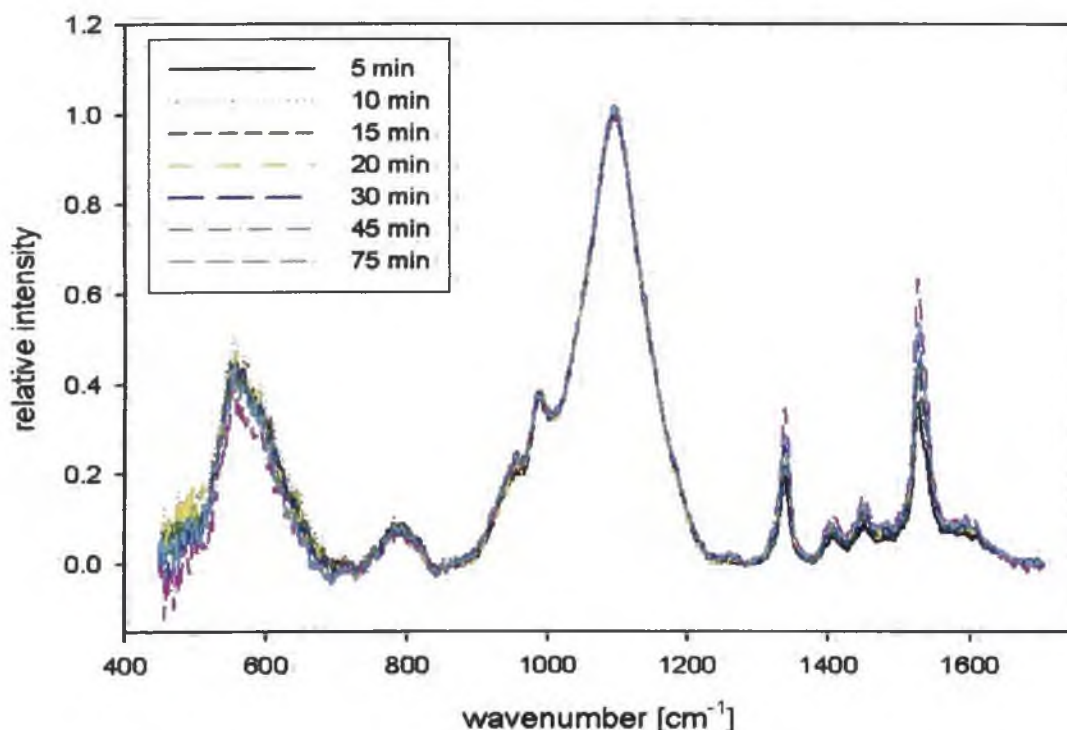

Figure 7.14: SERS spectra of CuPt1 adsorbed from 1×10^{-4}M stock solutions on a gold substrate for various soaking times. Normalized and linear baseline corrected spectra.

1600 cm⁻¹ region. The SERS spectra with subtracted glass spectrum are shown in Figure 7.15. The CuPt1 spectrum in the highest concentration (1x10⁻⁴ M) and for the longest time (75 minutes) is shown in Figure 7.16. The assignment of Raman lines is listed in the Table 7.2.
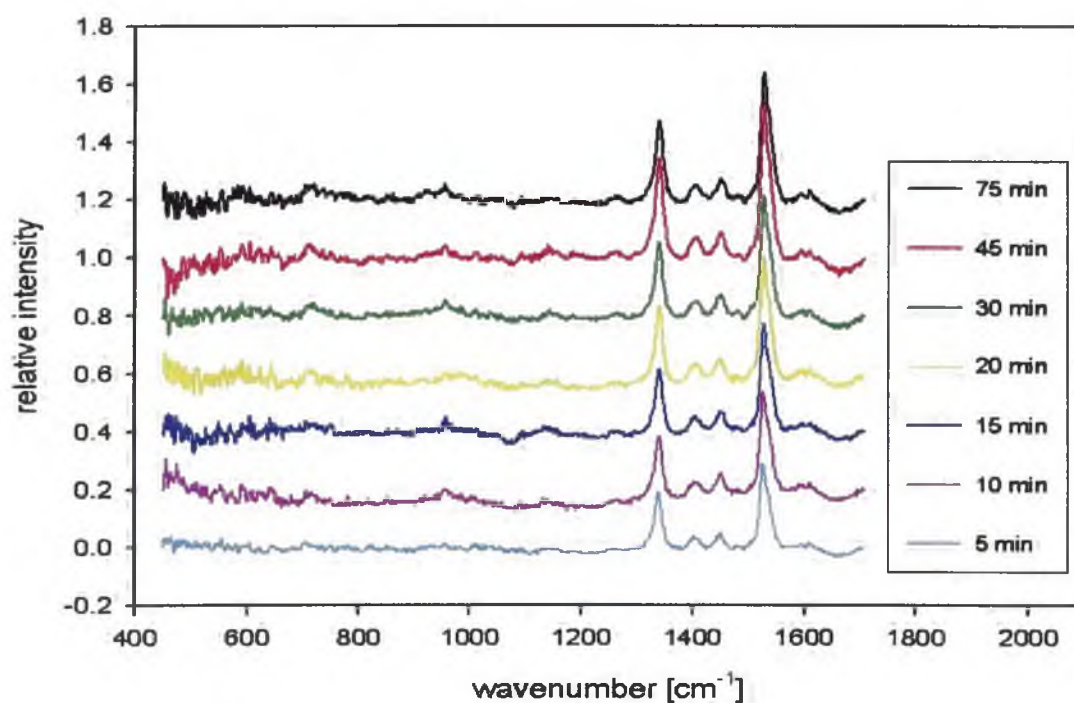

Figure 7.15: Same as in Figure 7.14. The Raman signal of glass is subtracted from the spectra.

Table 7.2: Raman active molecular vibrations of CuPt1 on a gold substrate

position	interpretation
710 (w)	
954 (w)	benzene breathing (a)
1011 (vw)	isoindole in-plane bending (c)
1033 (vw)	macrocycle deformation and C-H bending (a)
1091 (vw)	
1140 (vw)	C-H bending (a)
	Pyrrole stretch (b)
1262 (vw)	C-H bending (a)
1338 (s)	C-N breathing (a)
1404 (m)	
1450 (m)	C-N, isoindole ring stretch (a)
1480 (vw)	
1486 (vw)	
1527 (s)	C=C pyrrole stretch (a)
1593 (w)	
1609 (w)	

Assignment (a) Karolien De Wael [a10]
       (b) R. Aroca [a11]
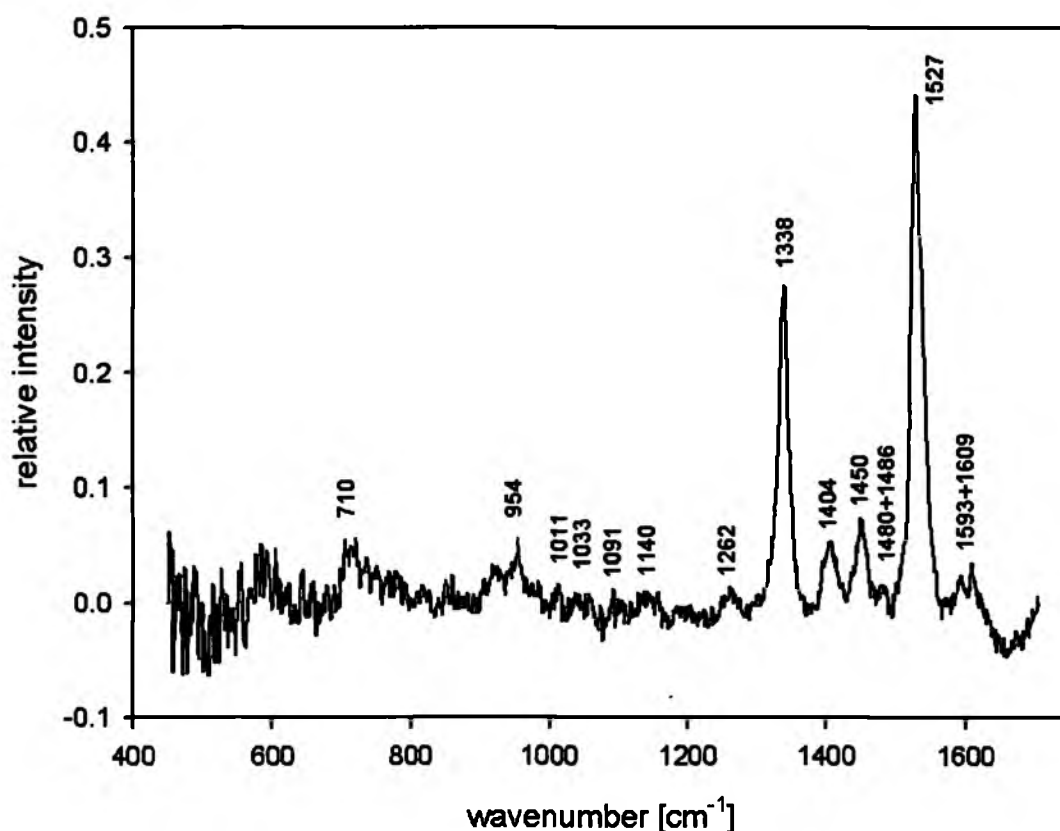   (c) R.Prabakaran [a12]

Figure 7.16: The SERS spectrum of CuPt1 on a gold substrate adsorbed from 1x10⁻⁴M CuPt1 solution for 75 minutes. The Raman signal of glass is subtracted from the spectrum.

The CuPt1 spectra measured at the same conditions are more intense that the spectra of ZnPt (see Figures 7.7 and 7.16). Two very strong vibrations of C=C pyrrole stretching and C-N breathing are evident and also some weaker vibrations, especially C-N stretching and C-N isoindole ring stretching are relatively strong. Other vibrations are weaker and for lower concentrations hardly observable. Only changes in overall intensity and no other spectral changes (in positions and relative intensities) are observed during the time dependence.

The obtained time dependence (where the band centered at 1527 cm⁻¹ was integrated) is shown in Figure 7.17. The most rapid intensity growth is observed during first 10 minutes and then the signal does not reach a constant value but slightly increases. This behavior is evident from the time dependence measured sample B. The similar tendency can be noticed from the dependence of sample A despite of some evidently incorrect points. Thus, adsorption of CuPt1 on a gold surface is very efficient and fast in the beginning and probably slower in longer times.

The extinction spectra are shown in Figure 7.18. The black solid line shows the extinction spectrum of a clean substrate without adsorbed phthalocyanine. The other spectra are obtained immediately after SERS detection. Extinction spectra show a considerable
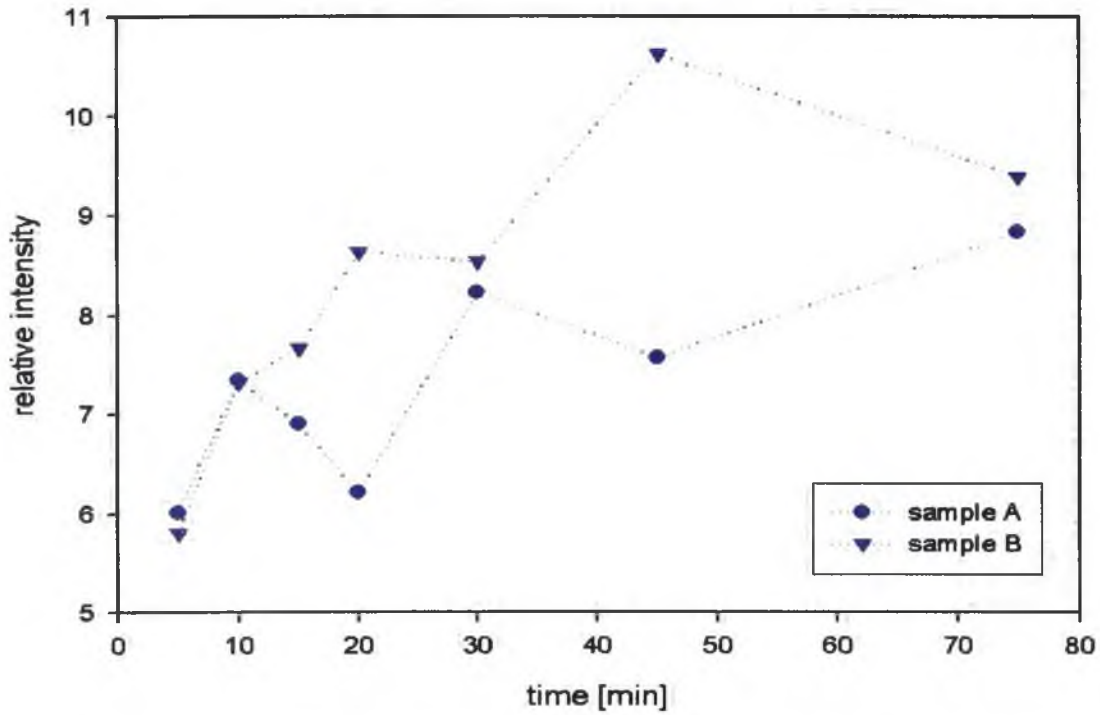
52

Figure 7.17: The intensities of CuPt1 peak at 1528 cm^{-1} for two samples separately measured in the time dependency (The lines directly connecting consecutive points are included as a guide for the eyes and do not represent real dependences).
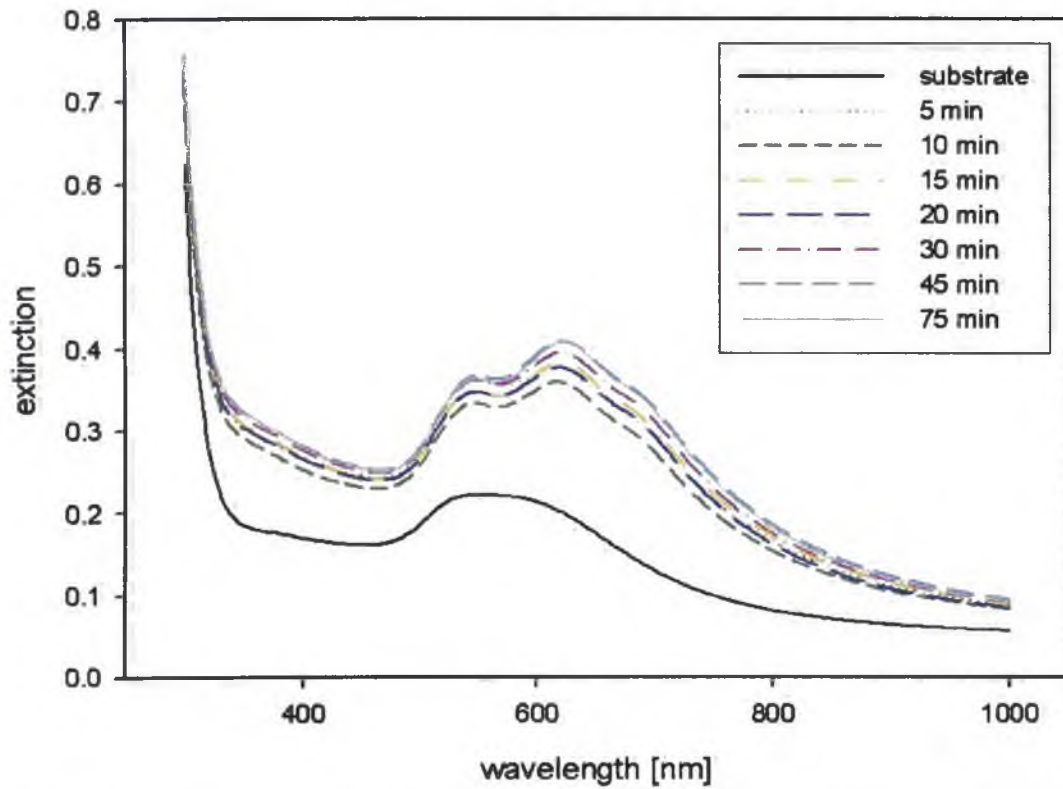

Figure 7.18: Extinction spectra of gold substrate and gold substrate/CuPt1 systems after various soaking times.

increase of extinction of the gold substrate even after 5 min of absorption of CuPt1 and than further a slight increase (more pronounced than in the case of ZnPt, see Figure 7.13). Extinction spectra of gold substrate/CuPt1 systems are dominated by extinction bands of CuPt1 itself indicating its efficient adsorption. The difference between position and shape of extinction bands of adsorbed CuPt1 and free CuPt1 measured in chloroform (see Figure 3.5 in chapter 3) can be explained by the fact that in the case of gold substrate/CuPt1, chloroform is evaporated from the surface. Thus, spectrum is closer to the spectrum of Ptc measured in water (ZnPt in Figure 3.5 in Chapter 3) and is dominated by the extinction bands of CuPt1 dimers. We note, that this behavior was also observed for all studied CuPts.

7.3.3 Time dependence of CuPt2

Normalized SERS spectra of CuPt2 measured for different soaking times are shown in Figure 7.19. Soaking time begins at 5 minutes and finishes after 75 minutes. Very strong CuPt2 peaks are evident in 1100-1700cm^{-1} region. The intensity of the adsorbed CuPt2 spectrum is very strong, it reaches nearly the intensity of glass spectrum for the longest times of adsorption.
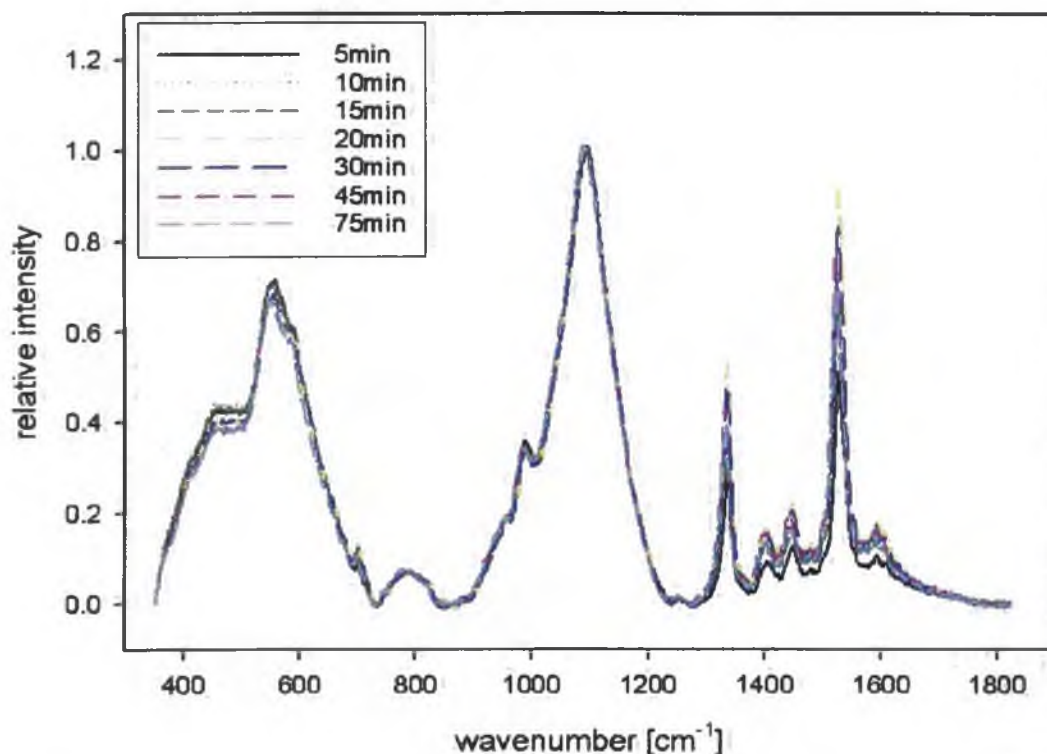

Figure 7.19: SERS spectra of CuPt2 adsorbed from 1x10^{-4}M stock solutions on a gold substrate for different soaking times. Normalized and linear baseline corrected spectra.
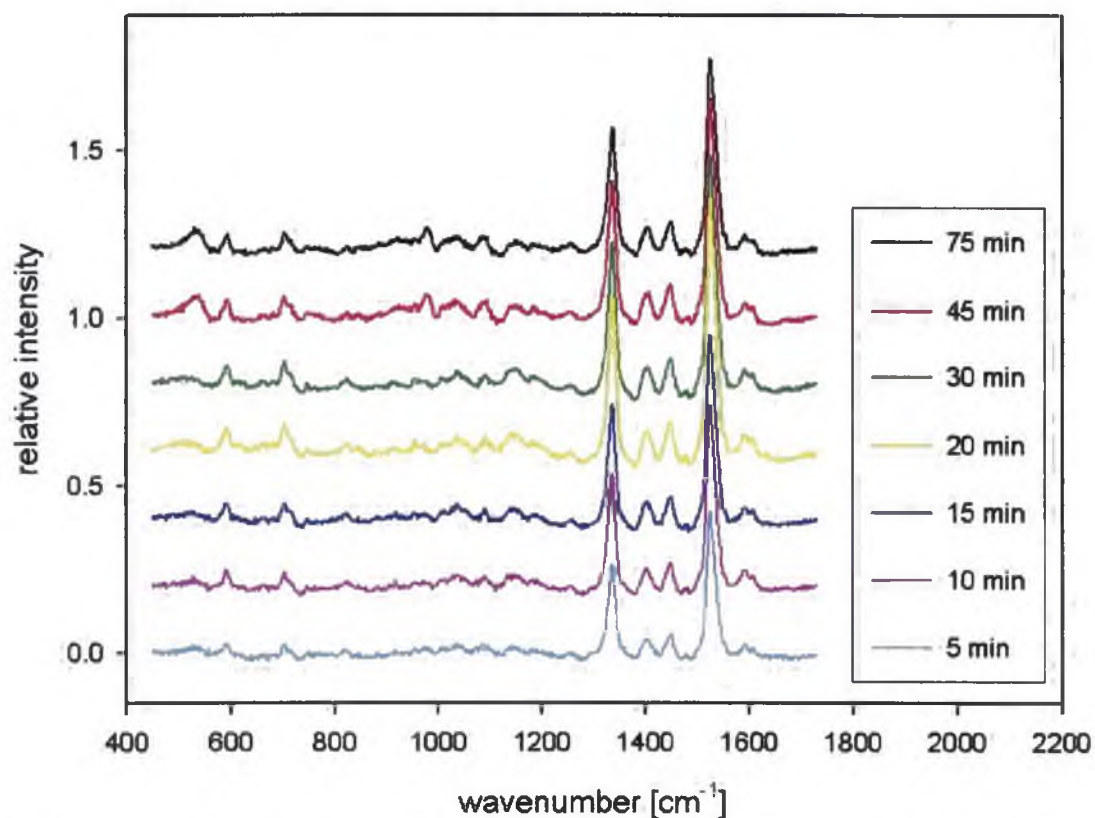
Figure 7.20: Same as in Figure 7.19. The Raman signal of glass is subtracted from the spectra.

CuPt2 spectra after all mathematical treatments are presented in Figure 7.20 and the spectrum of CuPt2 adsorbed for the longest (75 minutes) soaking time in Figure 7.21. The spectra are intense with many peaks in the whole observed region from 600 to 1600 cm^{-1}. The assignment is shown in Tab. 7.3. Two very strong bands of phthaloycanine at 1337 and 1527 cm^{-1} are clearly visible, however, many weaker vibrations are presented due to the highly intense signals. The spectra were investigated and no changes in peak positions and relative intensities were recognized. The obtained time dependences are shown in Figure 7.22. A very fast intensity increase is evident. The maximum is reached during about 20 minutes followed by a weak but significant intensity decrease for longer times. This decrease is probably caused by the depolarization effect that occurs when a maximal covering limit of absorbed molecules is reached and neighbor molecules start to interact. A depolarization effect is described by Murray [28] and observed in many studies, for example also in those ones using the same type of SERS substrates and similar molecules (porphyrins) [29].

The extinction spectra are shown in Figure 7.23 and the SPE spectrum of Au substrate/CuPt2 after subtraction of SPE spectra of a Au substrate is show in Figure 7.23a. Similarly to CuPt1, extinction spectra of gold substrate/CuPt2 systems show a considerable

increase of extinction even after 5 min of absorption of CuPt2 and are dominated by extinction bands of CuPt2 dimers. Comparison of the SPE spectra of a gold substrate with CuPt1 (Figure 7.18) and CuPt2 (after 75 minutes soaking time) show us that concentration of adsorbed CuPt2 is higher than that of CuPt1. Since an increase of adsorbed CuPt2 with soaking time is seen from the SPE spectra of gold substrate/CuPt2, we can assume that the decrease of the SERS signal for longer soaking times cannot be caused by some desorption and/or laser decomposition of CuPt2 and that our hypothesis of a depolarization effect between CuPt2 molecules explaining it is reasonable.
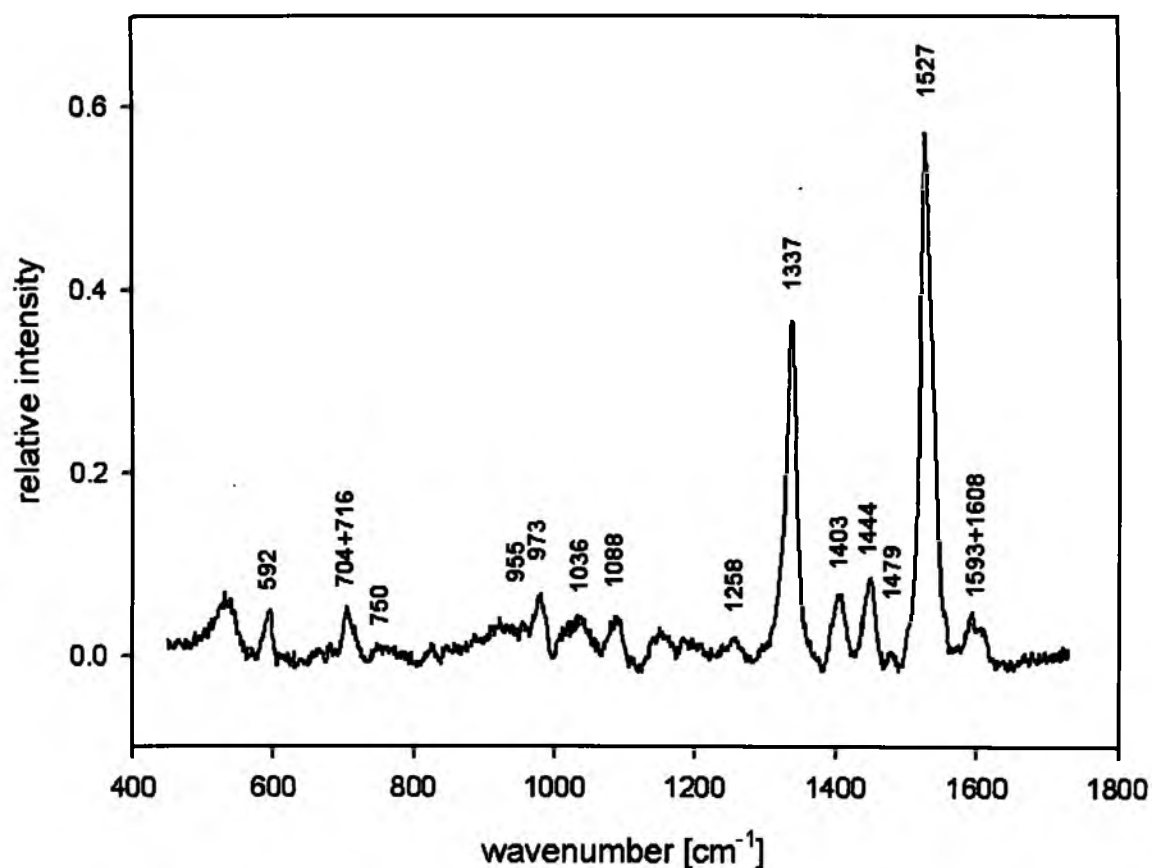

Figure 7.21: The subtracted SERS spectrum of CuPt2 on gold adsorbed in 10^{-4}M CuPt2 for 75 minutes.

Tab. 7.3: Raman active molecular vibrations of CuPt2 on a gold substrate

position	Interpretation
592 (m)	out-of-plane bending mode (a)
704 (m)	out-of-plane bending mode (a)
716 (vw)	
750 (w)	macrocycle deformation (a)
955 (w)	benzene breathing (a)
973 (w)	
1036 (w)	macrocycle deformation and C-H bending (a)
1088 (w)	
1258 (vw)	C-H bending (a)
1337 (vs)	C-N breathing (a)
1403 (m)	
1444 (m)	pyrrole stretch (b)
1479 (w)	
1527 (vs)	C=C pyrrole stretch (a)
1593 (w)	
1608 (w)	

Assignment (a) Karolien De Wael [a10]
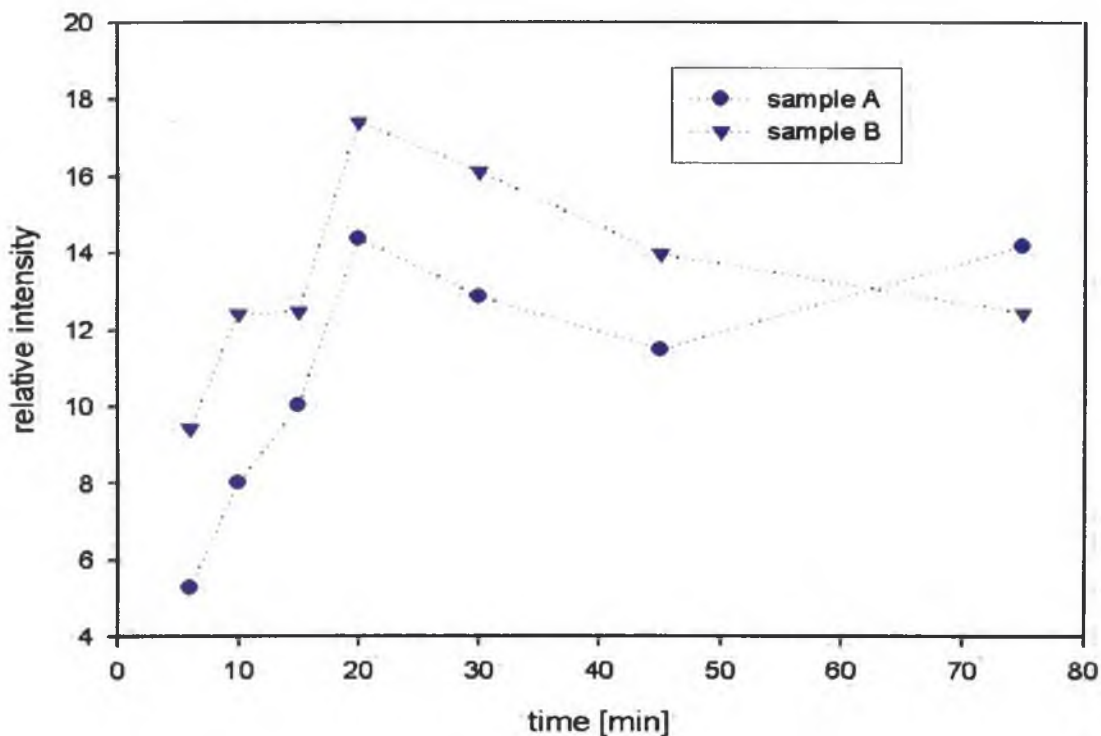   (b) R. Aroca [a11]
        (c) R. Prabakaran [a12]

Figure 7.22: The intensities of CuPt2 peak at 1527 cm^{-1} for two samples separately measured in the time dependency (The lines directly connecting consecutive points are included as a guide for the eyes and do not represent real dependences).
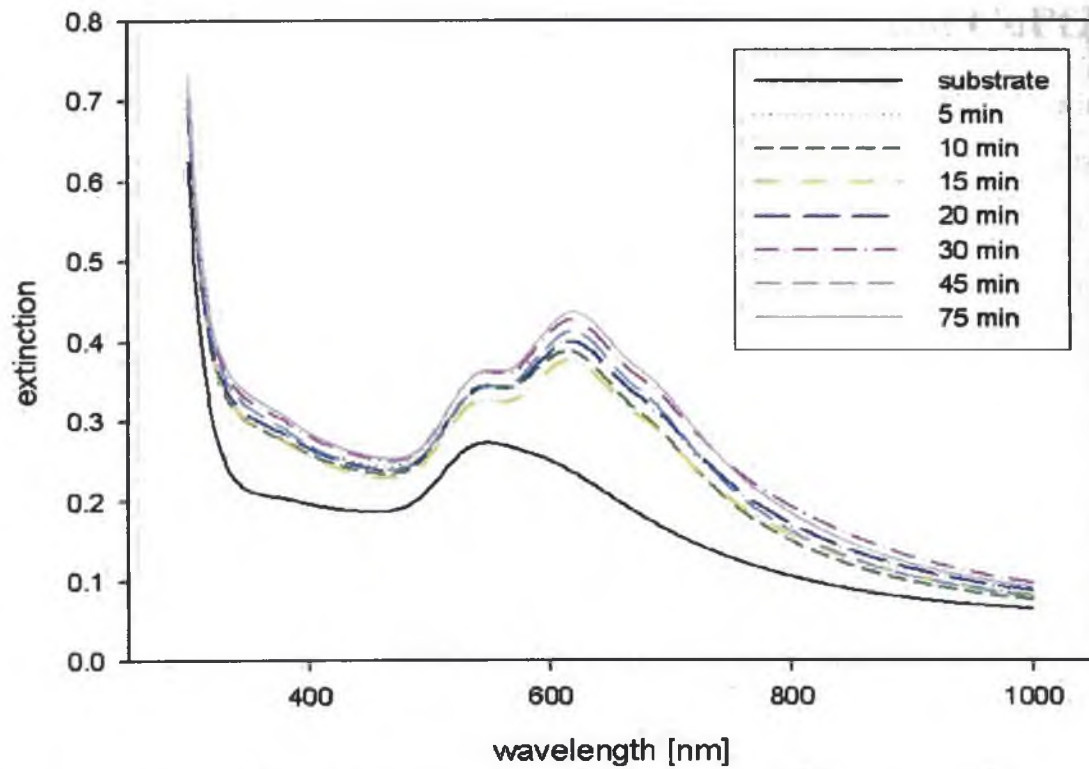
Figure 7.23: Extinction spectra of gold substrate and gold substrate/CuPt2 systems with different soaking times.
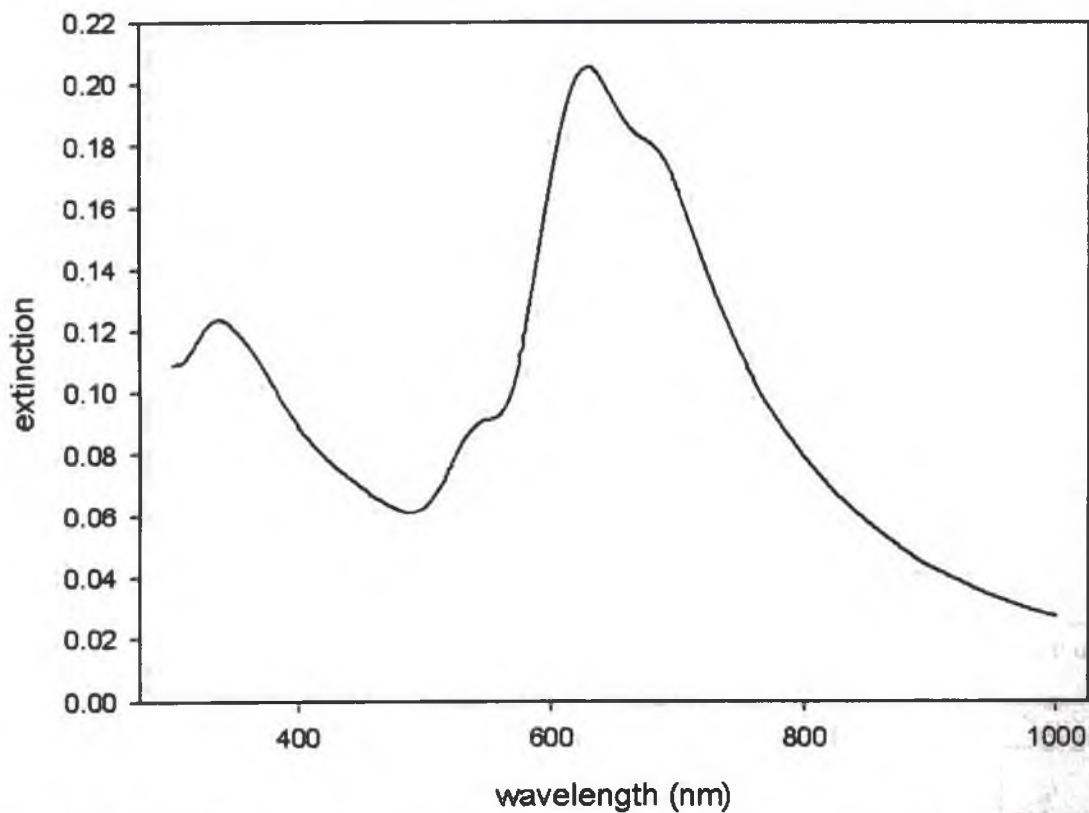

Figure 7.23a. The SPE spectrum of Au substrate/CuPt2 after subtraction of the SPE spectra of an Au substrate.

58

7.3.4 Concentration dependence for CuPt1 and CuPt2

The concentration dependencies of CuPt1 and CuPt2 were separately measured on two gold substrates in a broad concentration range (from 5×10^{-7}M to 1×10^{-4}M). Soaking time was fixed at 15 minutes for all concentrations.

7.3.5 Concentration dependence of CuPt1

The normalized (to the strong Raman band of glass) and baseline corrected SERS spectra are shown in Figure 7.24. The SERS spectra with subtracted glass spectrum are shown in Figure 7.25.
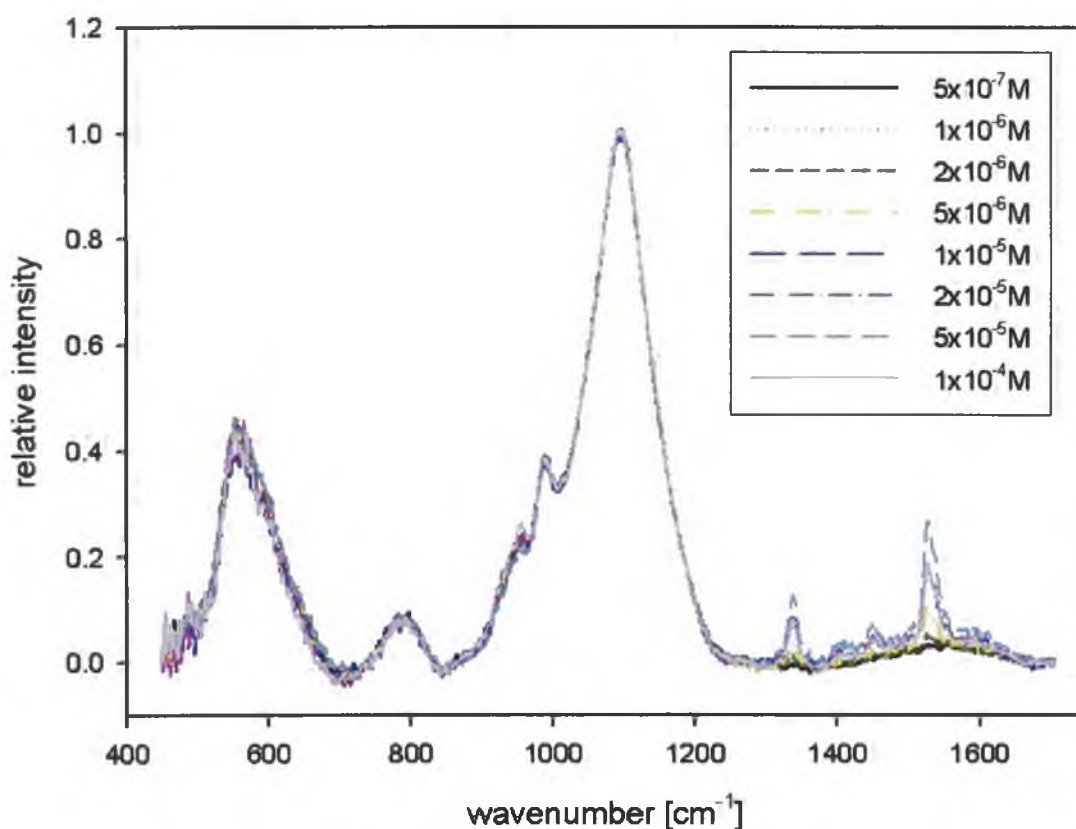

Figure 7.24: SERS spectra of CuPt1 adsorbed from different concentrations of stock solution on a gold substrate (15 min soaking times). Normalized and linear baseline corrected spectra.
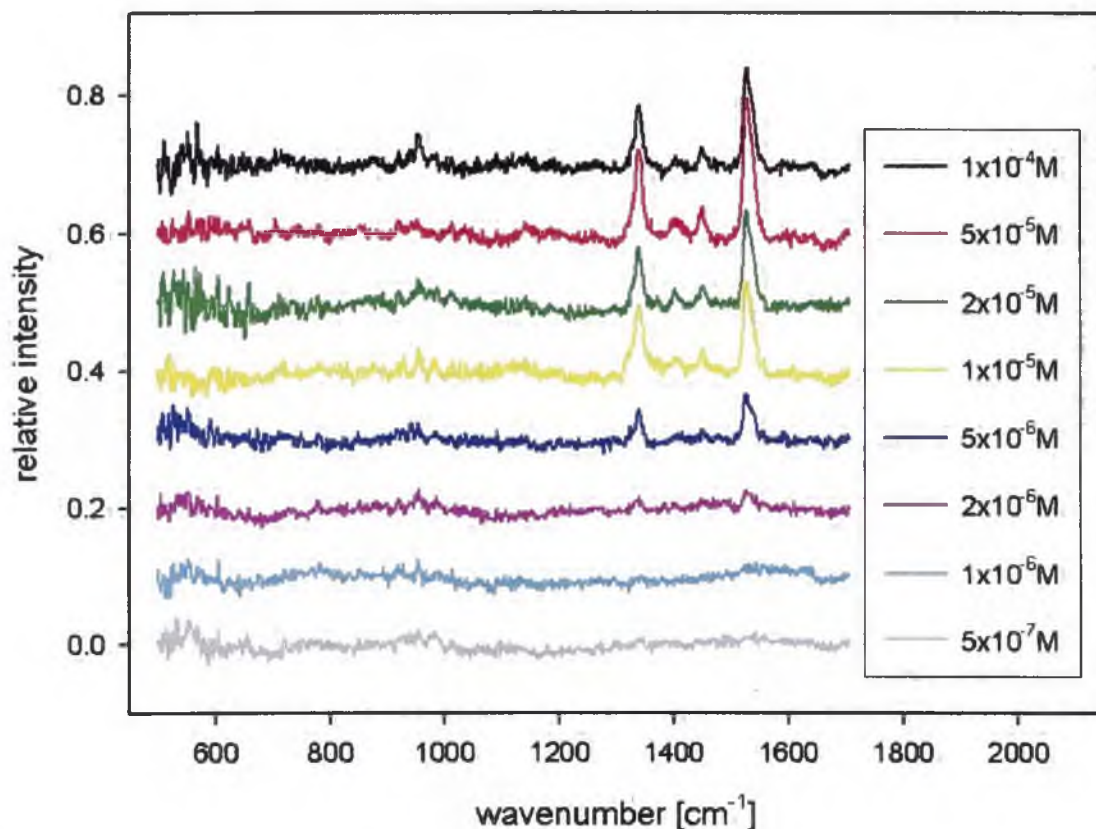
Figure 7.25: Same as in Figure 7.24. The Raman signal of glass is subtracted from the spectra.

The spectra contain bands in the same positions as mentioned in Tab. 7.2 in the previous chapter. The spectral bands are situated in the same positions during all concentration measurements, no changes in the relative intensities are observed, only the overall intensity increased. The peak 1527 cm^{-1} was integrated and results are presented in Figure 7.26. The intensity rapidly increases with concentration up to 5×10^{-5}M where the maximum and subsequently nearly a plateau is reached. These results are in accordance with the extinction spectra shown in Figure 7.27 that were also measured.

Similarly to the time dependence, extinction spectra of gold substrate/CuPt1 systems show a considerable increase of extinction even for the lowest adsorbed CuPt1 concentration and a further slight increase with concentration. Spectra for higher concentrations are dominated by extinction bands of CuPt1.
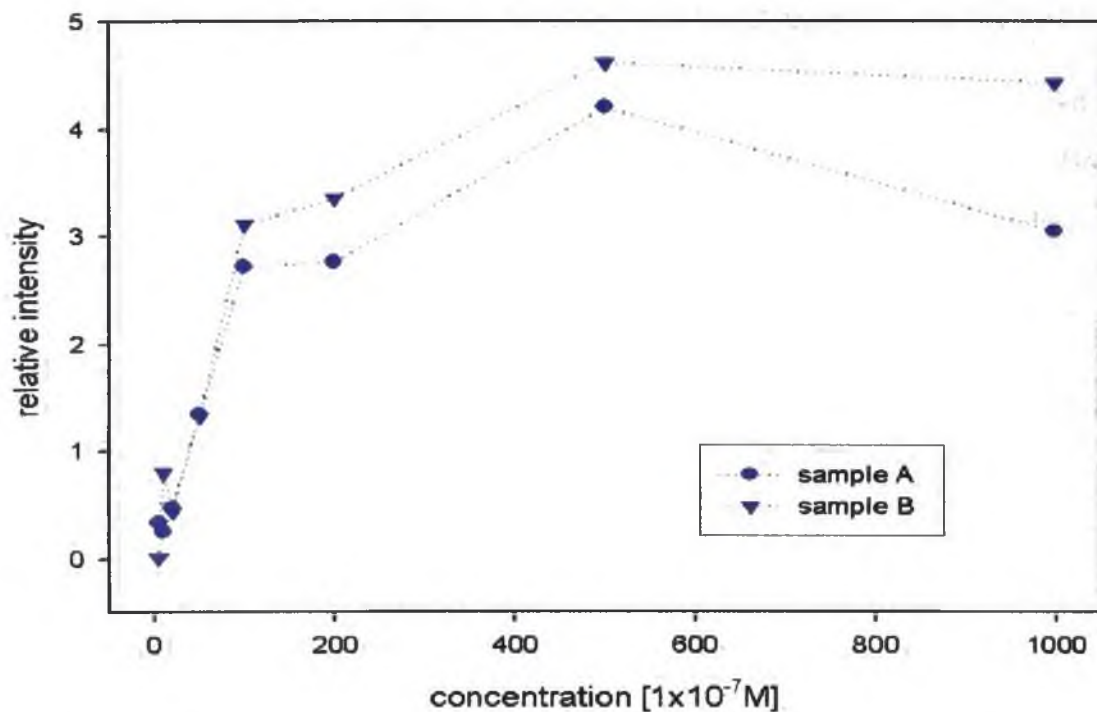
Figure 7.26: The intensities of CuPt1 peak at 1527 cm^{-1} for two samples. (The lines directly connecting consecutive points are included as a guide for the eyes and do not represent real dependencies).
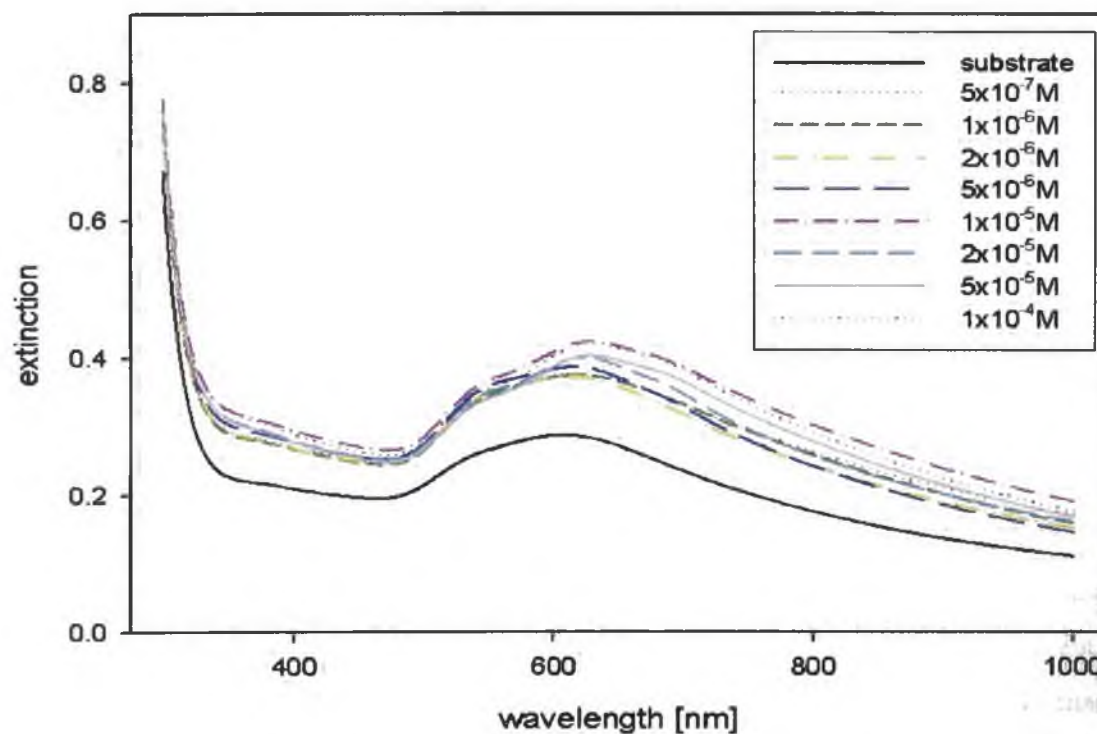

Figure 7.27: Extinction spectra of gold substrate and gold substrate/CuPt1 systems with different stock solution concentrations.

7.3.6 Concentration dependence of CuPt2

The normalized (to the strong Raman band of glass) and baseline corrected SERS spectra are shown in Figure 7.28. The relatively strong CuPt2 signal in 1300 to 1600cm^{-1} spectral region is observed. The spectra with subtracted glass spectrum are shown in Figure 7.29.
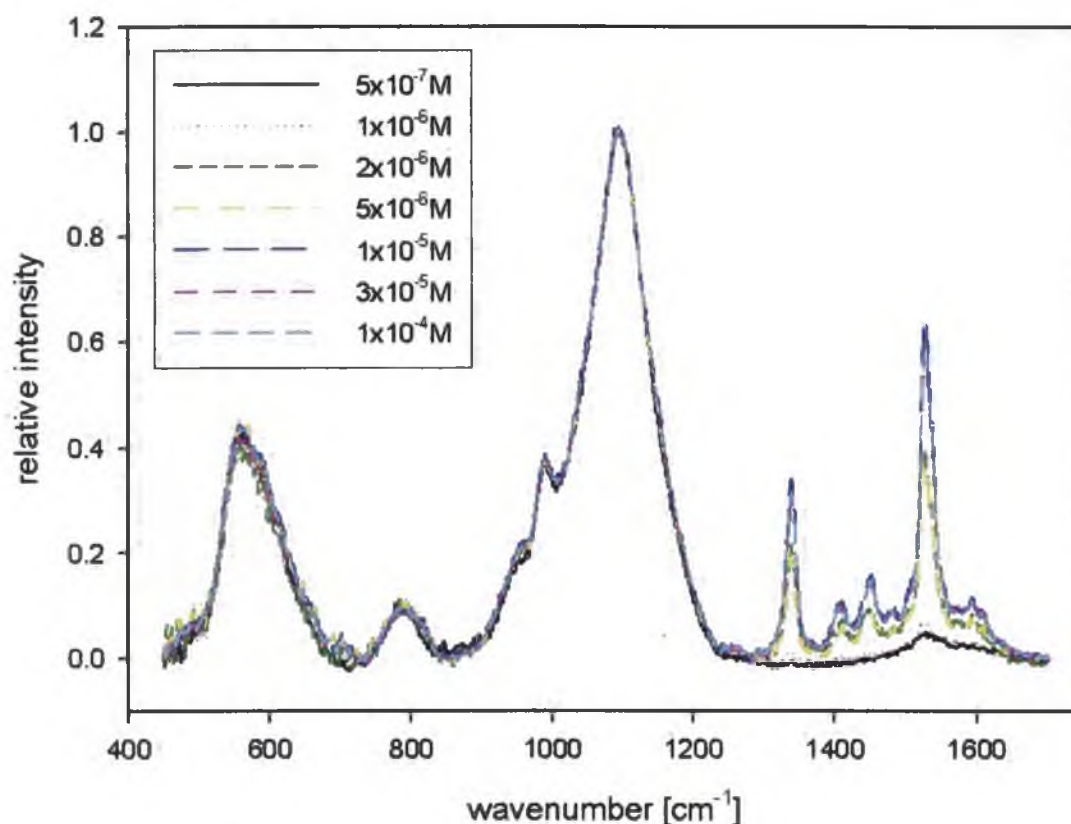

Figure 7.28: SERS spectra of CuPt2 adsorbed from different concentrations of stock solution on a gold substrate (15 min soaking times). Normalized and linear baseline corrected spectra.

The spectra contain of well-known CuPt2 bands, only an increase of the overall signal with concentration and no other changes were observed. The peak 1527 cm^{-1} was integrated and results are presented in Figure 7.30. The intensity maximum is reached about $1x10^{-5}$M concentration and a clear plateau is observed for higher concentrations.

The extinction spectra are shown in Figure 7.31. Similarly to CuPt1, the extinction spectra of gold substrate/CuPt2 systems show a considerable increase of extinction even for the lowest adsorbed CuPt2 concentration and a further slight increase with concentration. Spectra for higher concentrations are dominated by extinction bands of CuPt2. In that case, clear saturation concentration ($1x10^{-5}$M) can be detected confirming the results obtained from SERS spectra.
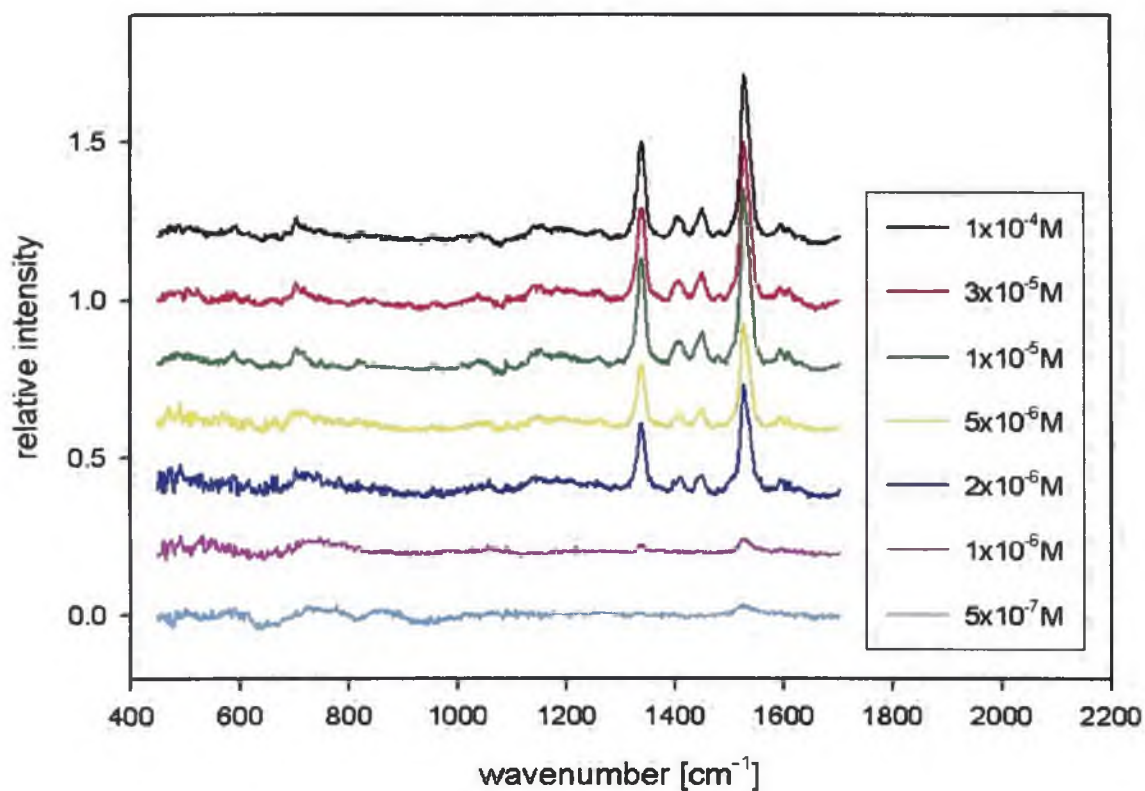
Figure 7.29: Same as in Figure 7.28. The Raman signal of glass is subtracted from the spectra.
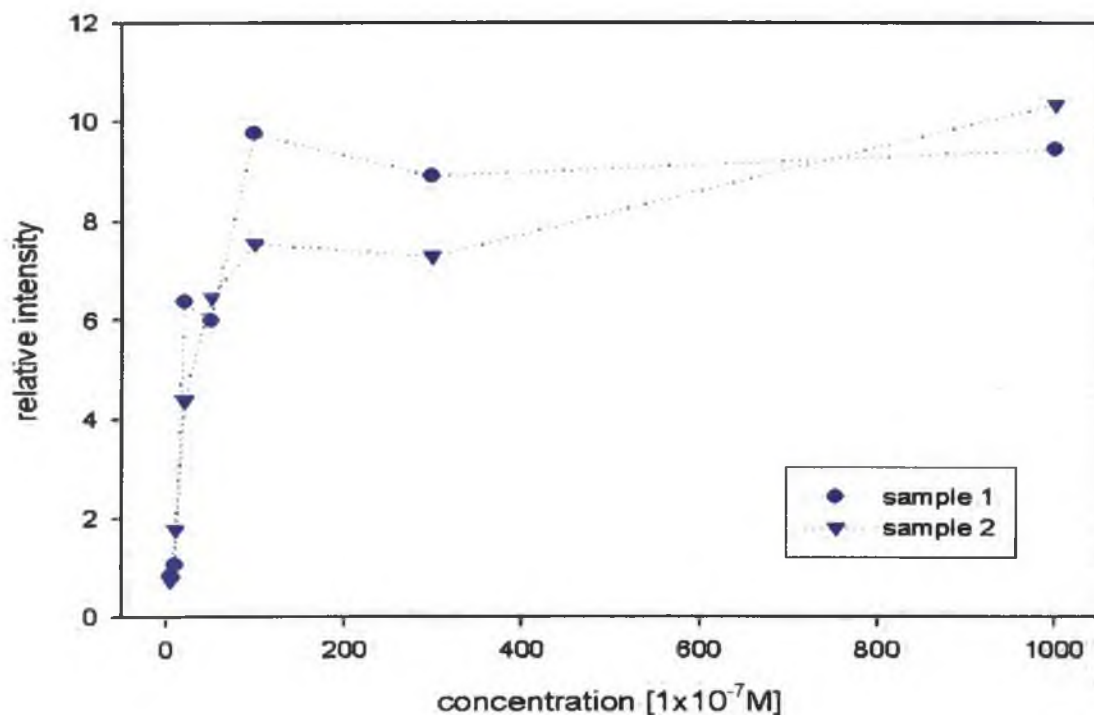

Figure 7.30: The intensities of CuPt2 peak at 1527 cm^{-1} for two samples separately (The lines directly connecting consecutive points are included as a guide for the eyes and do not represent real dependencies).
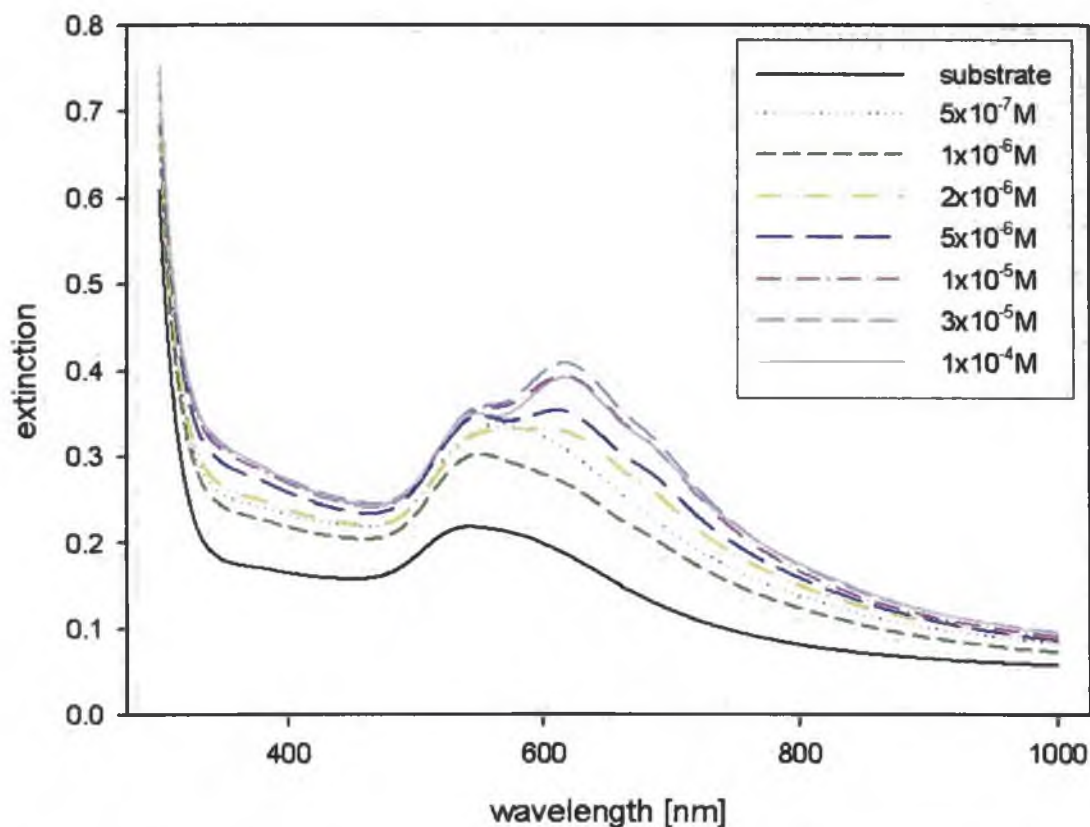
Figure 7.31: Extinction spectra of gold substrate and gold substrate/CuPt2 systems with different stock solution concentrations.

7.3.7 Comparison of time and concentration dependencies of CuPt1

Results obtained from SERS spectra and extinction spectra show mostly fast and very efficient adsorption of CuPt1 onto gold surfaces. In the time dependence the maximum was reached probably between 30 and 45 minutes and in the concentration dependence for 5×10^{-5}M (view Figure 7.17 and 7.26). This shows relatively good affinity of CuPt1 to a gold substrate. In all spectra shifts in positions of vibration were not observed, therefore probably no chemical or conformation changes happened during measurement.

7.3.8 Comparison of time and concentration dependencies of CuPt2

Similarly to CuPt1, the results obtained from SERS spectra and extinction spectra show mostly fast and very efficient adsorption of CuPt2 onto gold surfaces. The maximum in the concentration dependence occurred after 20 minutes of adsorption and in the concentration dependence a signal plateau was reached for about 1×10^{-5}M. The very fast growth and the very high SERS signal in both dependencies show high affinity to a gold surface (view Figure 7.22 and 7.30). These results are confirmed by extinction spectra in Figures 7.23 and 7.31. Peak positions and relative intensities at various soaking time and concentrations were compared, however, no changes were observed predicating conformational and chemical stability during the adsorption process.

7.3.9 Time dependence of CuPt3

Phthalocyanine CuPt3 was measured under the same conditions as phthalocyanines CuPt1 and CuPt2 in the previous parts. The spectra were acquired after 5,10,15,20,30,45 and 75 minutes of soaking in 1×10^{-4}M solution of CuPt3 phthalocyanine in chloroform. Two samples were measured separately.

The normalized (to the strong Raman band of glass) and baseline corrected SERS spectra are shown in Figure 7.32. Very strong CuPt2 signal in 1300 to 1600cm^{-1} spectral region is observed. The spectra with subtracted glass spectrum are shown in Figure 7.33. The CuPt3 spectrum for the longest soaking time (75 min) is presented in Figure 7.34.
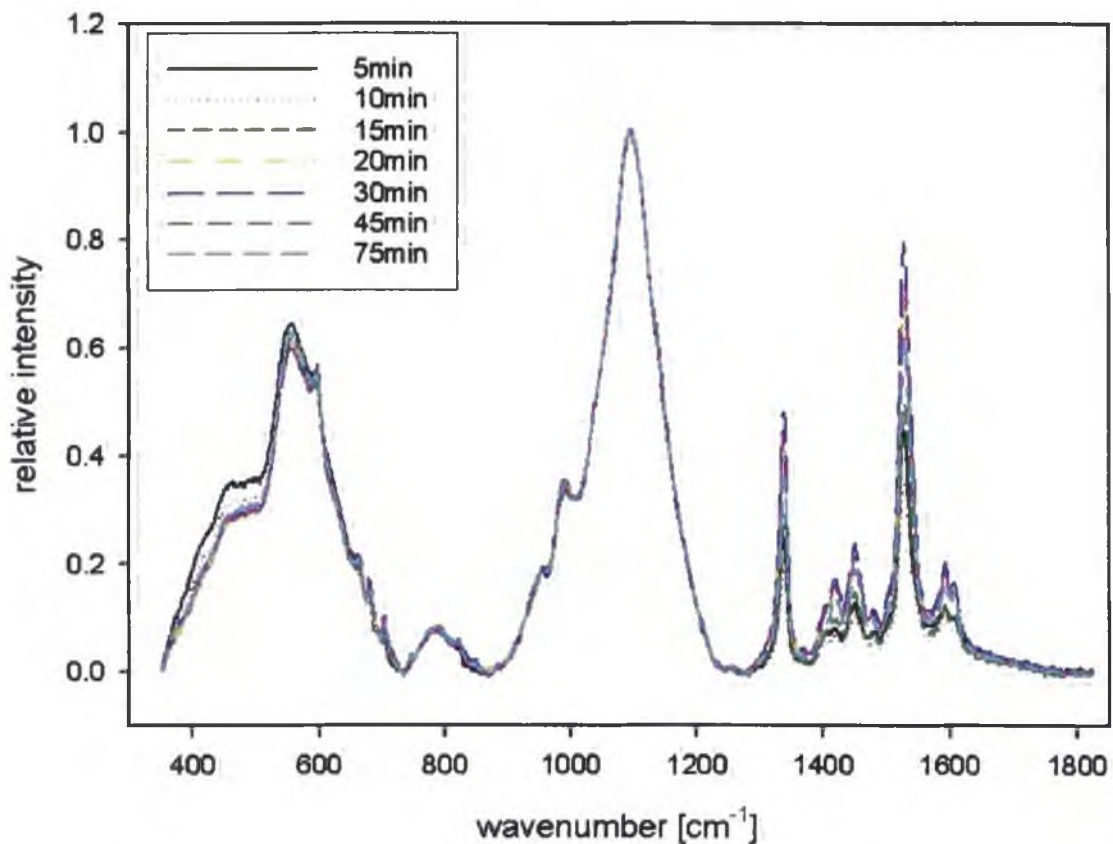
Figure 7.32: SERS spectra of CuPt3 adsorbed from 1×10^{-4}M stock solutions on a gold substrate for different soaking times. Normalized and linear baseline corrected spectra.
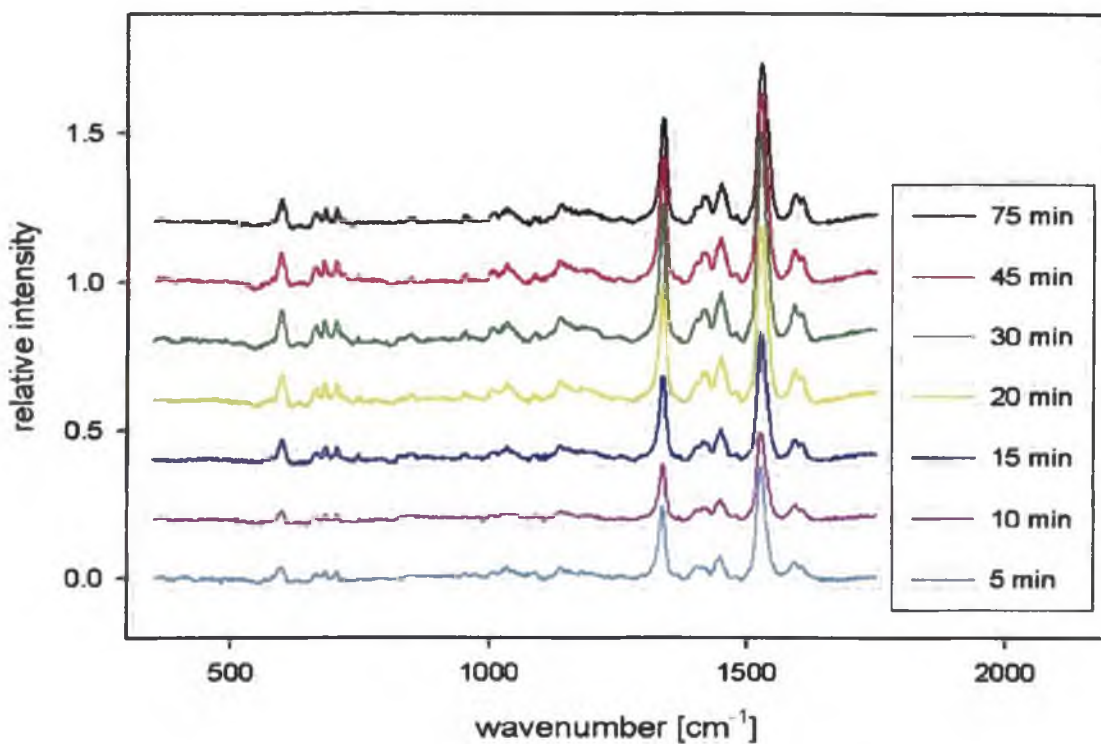

Figure 7.33: Same as in Figure 7.32. The Raman signal of glass is subtracted from the spectra.
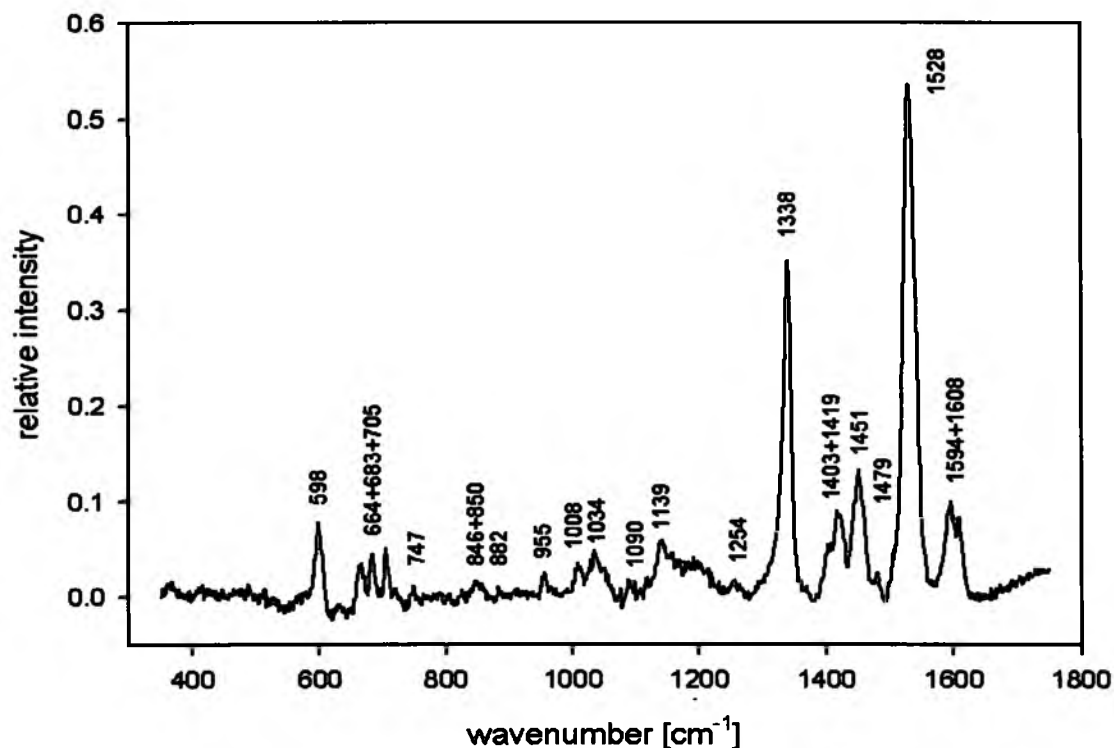
Figure 7.34. The subtracted SERS spectrum of CuPt3 on gold adsorbed from 1×10^{-4}M for 75 minutes.

The spectrum of CuPt3 phthalocyanine is very rich. Except of well-known vibrations in the region from 1300 to 1650cm^{-1}, many other vibrations are visible in the spectra (view Figure 7.33 or 7.44). The assignment is done in Tab 7.4. Four vibrations with a relatively high intensity are observable in the region from 600cm^{-1} to 750cm^{-1}. The peaks remain at the same positions during all time measurements, no significant changes in relative intensities are observed except two peaks 1403 and 1419cm^{-1}. The intensity of 1419cm^{-1} band increases in time whereas second one very slightly decreases. This tendency is presented in Figure 7.36 where spectra were normalized to peak 1338cm^{-1}. This can indicate some deformation in the phthalocyanine central ring of CuPt2 (see the assignment in Tab 7.4) during adsorption. Figure 7.35 where peak 1528cm^{-1} was integrated shows dependence of overall intensity. The intensity of CuPt3 rapidly increases, reaches the maximum during about 30 minutes, however, a significant intensity decrease is observed for longer times. The reason of a signal decreasing can be also depolarization effects among CuPt3 molecules as mentioned in the case of CuPt2. Unfortunately, extinction spectra have been not measured for this series.

Tab 7.4. Raman active molecular vibrations of CuPt3 on a gold substrate.

position	interpretation	position	interpretation
598 (m)	out-of-plane bending mode (a)	1090 (w)	
664 (m)		1139 (w)	C-H bending (a)
683 (m)	macrocycle deformation (a)		Pyrrole stretch (b)
705 (m)	out of plane bending mode (a)	1254 (vw)	C-H bending (a)
747 (w)	macrocycle deformation (a)	1338 (s)	C-N breathing (a)
825 (w)		1403 (w)	
846 (vw)		1419 (m)	C-N stretching (c)
850 (vw)		1451 (m)	C-N, isoindole ring stretch (a)
882 (w)		1479 (w)	
955 (w)	benzene breathing (a)	1528 (s)	C=C pyrrole stretch (a)
1008 (w)	isoindoline in-plane bending (c)	1594 (m)	
1034 (w)	Macrocycle deformation and C-H bending (a)	1608 (m)	

Assignment (a) Karolien De Wael [a10]
  (b) R. Aroca [a11]
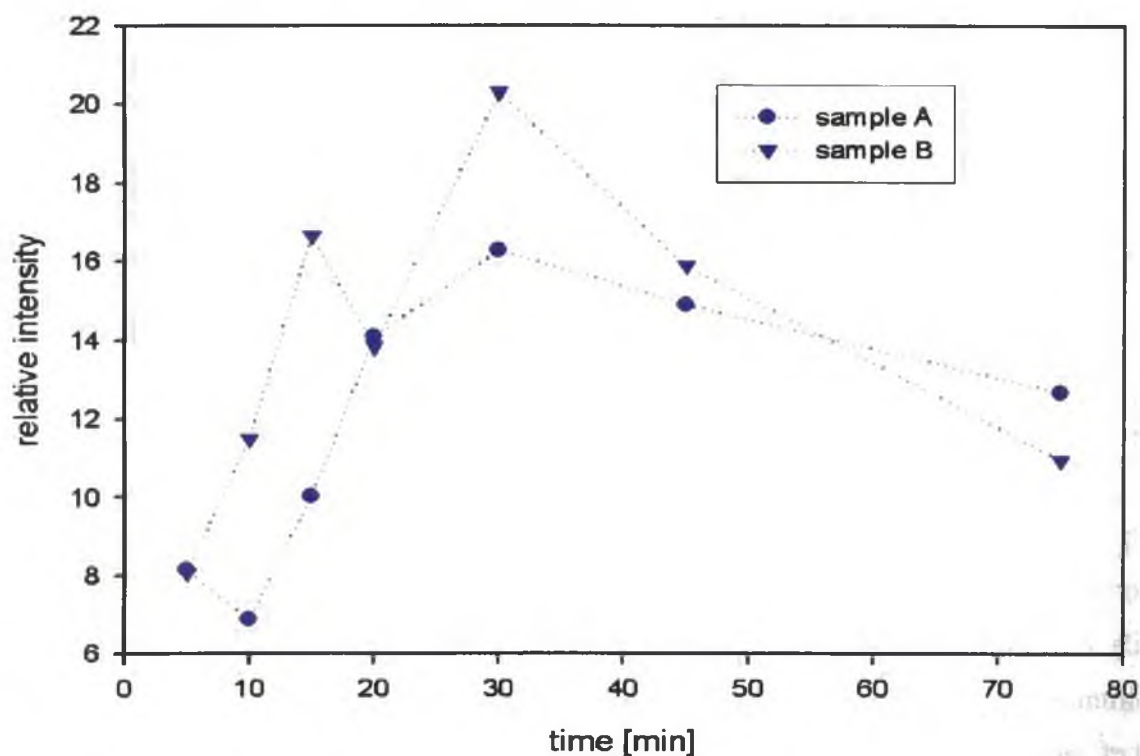 (c) R. Prabakaran [a12]

Figure 7.35: The intensities of CuPt3 peak at 1527 cm^{-1} for two samples separately measured in the time dependency (The lines directly connecting consecutive points are included as a guide for the eyes and do not represent real dependences).
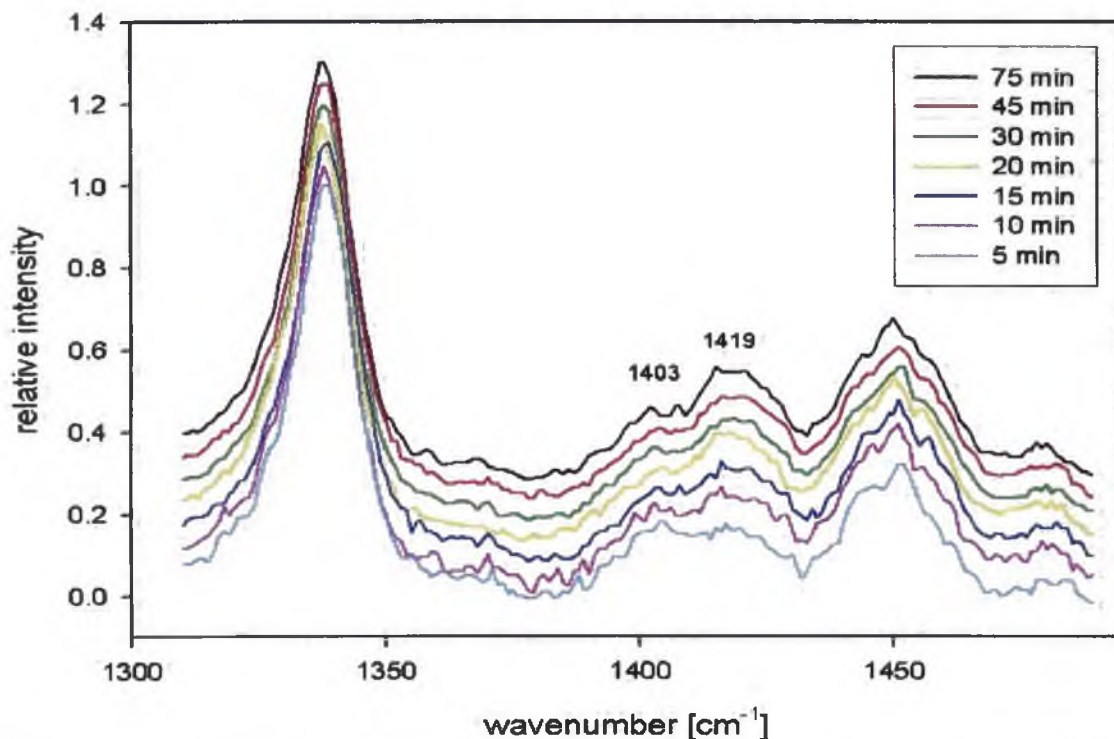
Figure 7.36: Spectral changes of 1403 and 1419cm⁻¹ peaks during the time dependency of CuPt3.

7.3.10 Concentration dependence of CuPt3

Concentration dependence of CuPt3 phthalocyanine was measured in the $5x10^{-7}$M to $1x10^{-4}$M concentration range, soaking time was fixed to 15 minutes.

Normalized (to the strong Raman band of glass) and baseline corrected SERS spectra are shown in Figure 7.37. Spectra with the subtracted glass spectrum are shown in Figure 7.38.

No spectral changes except of the overall intensity were observed. The strongest peak at 1528 cm⁻¹ were integrated and results are presented in Figure 7.39. In both samples, intensities grow very fast to $3x10^{-5}$ M where sample A reaches maximum and a slight decrease was observed in contrast to continuously increasing sample B. The maximum of sample B seems to occur around $1x10^{-4}$ M. Regarding to other phthalocyanines results, in this case behavior of sample A is probably more real then that of sample B.
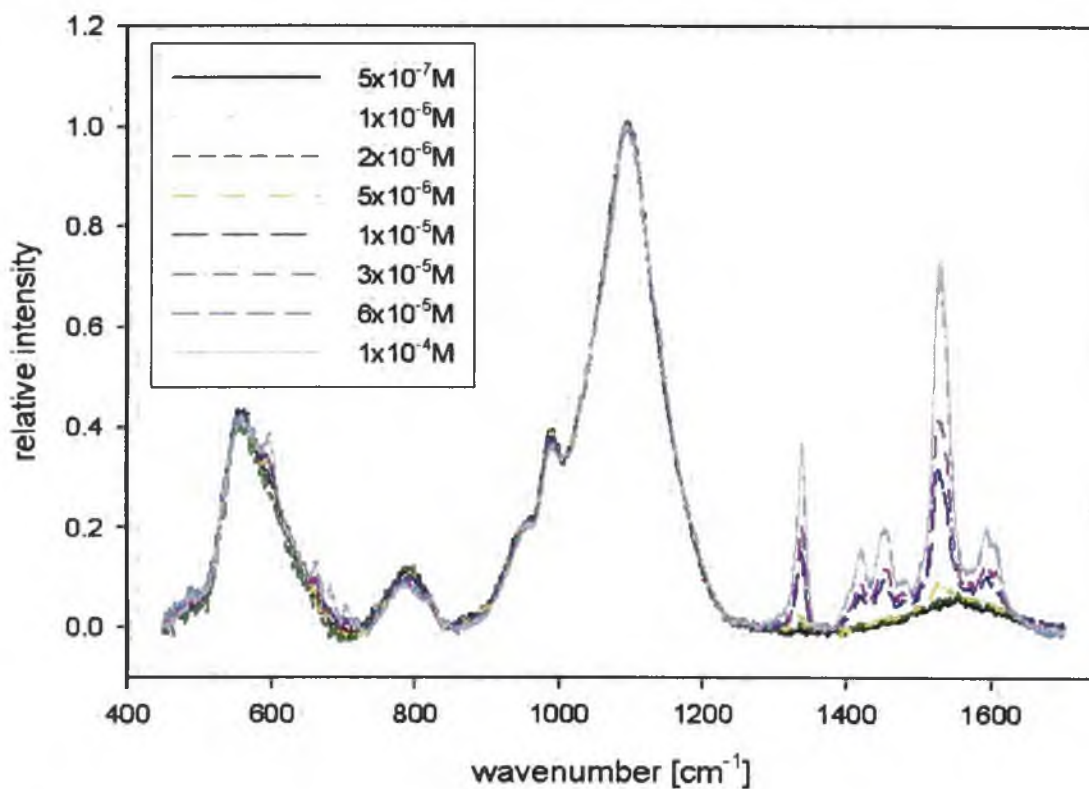
Figure 7.37. SERS spectra of CuPt3 adsorbed from different concentrations of stock solution on gold substrate (15 min soaking times). Normalized and linear baseline corrected spectra.
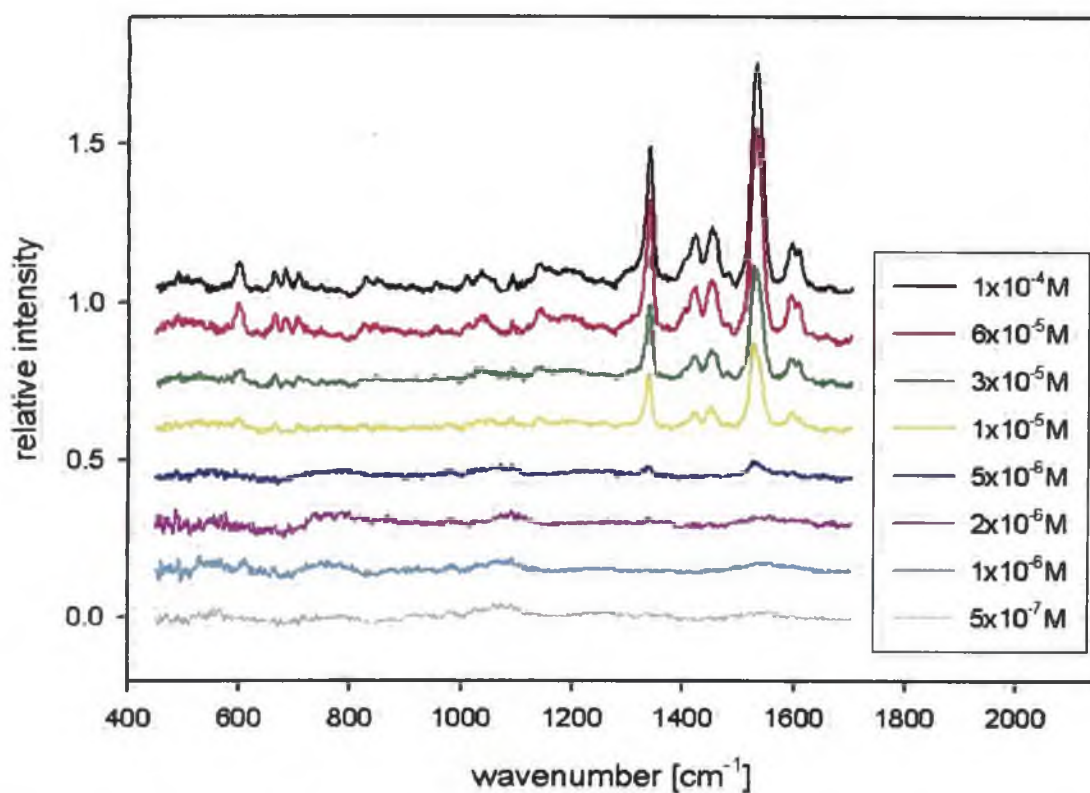

Figure 7.38: Same as in Figure 7.37. The Raman signal of glass is subtracted from the spectra.

Extinction spectra measured from sample A are shown in Figure 7.40. Similarly to the CuPt1 and CuPt2, extinction spectra of gold substrate/CuPt3 systems show a considerable increase of extinction even for the lowest adsorbed CuPt3 concentration and further high increasing with concentration. The spectra for higher concentrations are dominated by extinction bands of CuPt3 dimers and do not show any decrease of amount of adsorbed CuPt3, explanation of the SERS signal decrease for higher concentration by depolarization effects seems to be reasonable.

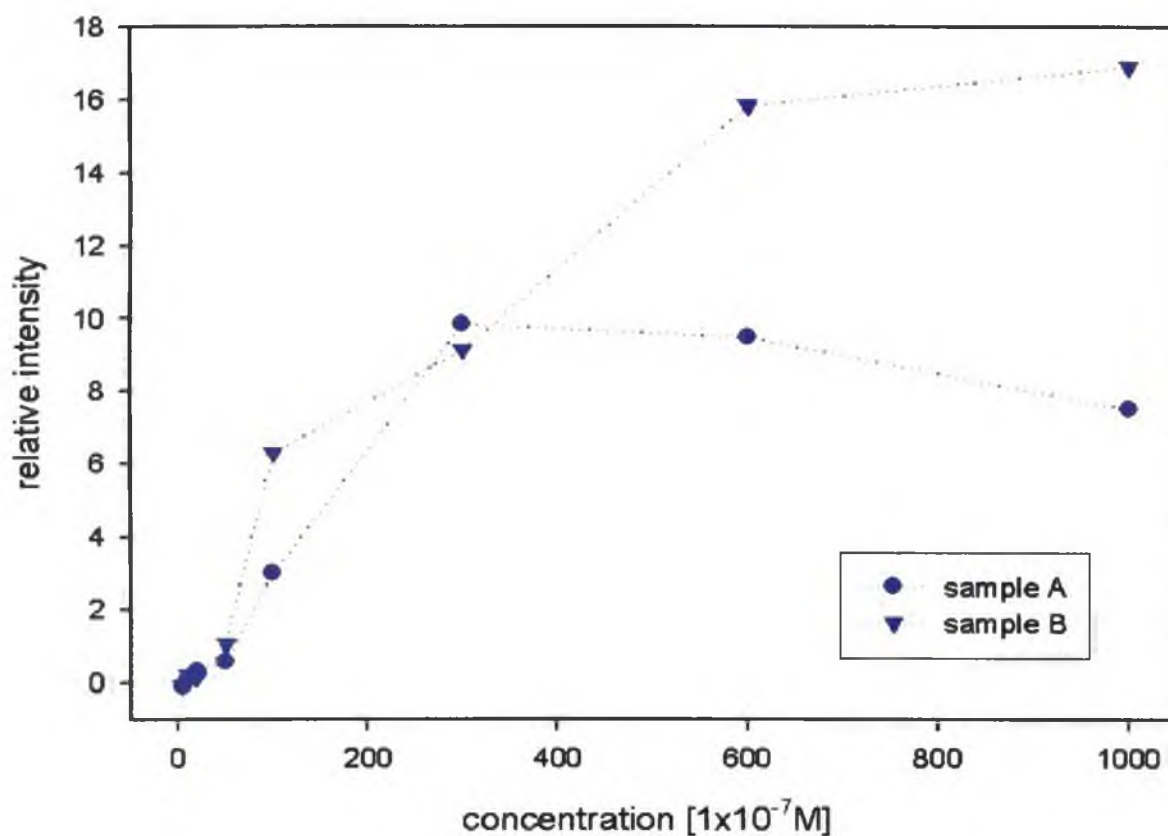
Figure 7.39: The intensities of CuPt3 peak at 1527 cm^{-1} for two samples separately measured in the time dependence (The lines directly connecting consecutive points are included as a guide for the eyes and do not represent real dependences).
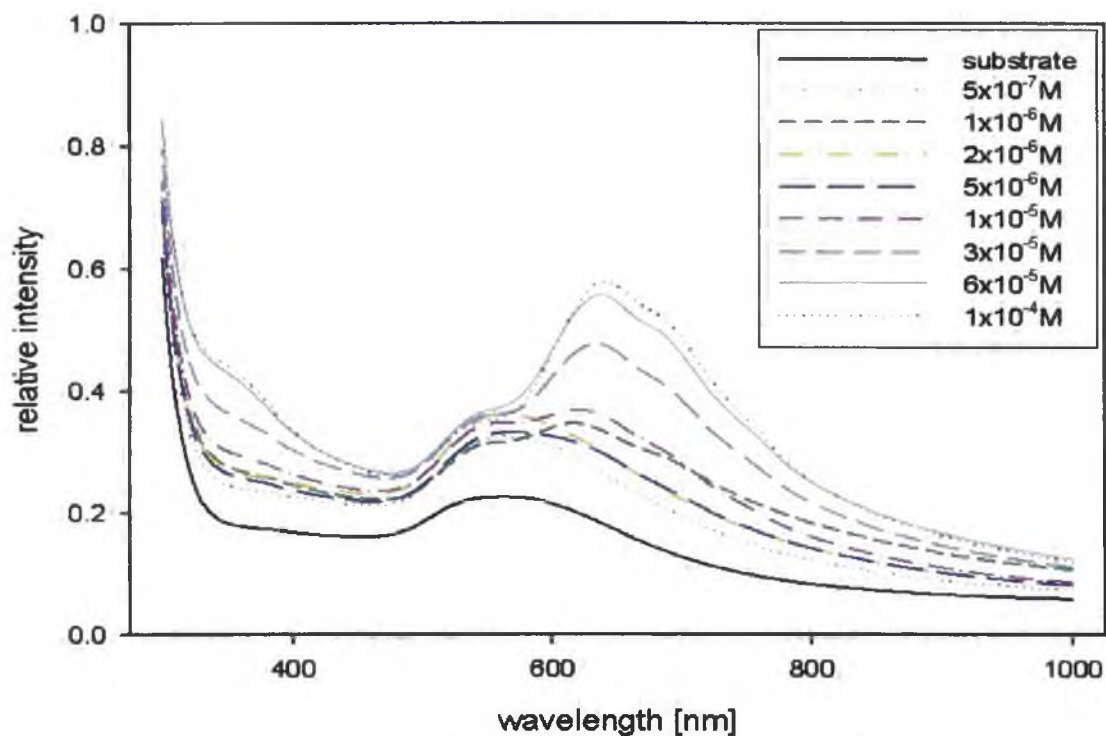
Figure 7.40: Extinction spectra of gold substrate and gold substrate/CuPt3 systems with different stock solution concentrations.

7.3.11 Comparison of time and concentration dependencies of CuPt3

Similarly to both CuPt1 and CuPt2, results obtained from SERS spectra and the extinction spectra show mostly fast and very efficient adsorption of CuPt3 onto gold surfaces. Tendency of CuPt3 is very similar in both dependencies (view Figures 7.35 and 7.39). In the time dependence the maximum was reached in 30 minutes and in the concentration dependence for 5×10^{-6} M. In the time measurement a significant decrease of intensity is observed probably caused by depolarization effects of absorbed CuPt3 at high concentration. The high SERS signal with significant changes in extinction spectra after adsorption confirms very good CuPt3 affinity to a gold substrate. Intensity ratio of two peaks 1403 and 1419 cm^{-1} changes (1419 cm^{-1} band increases) in the time dependence and thus, probably some deformation of the CuPt3 macrocycle occurs during adsorption. (see Figure 7.36).

7.4 Comparison of phthalocyanine SERS spectra

The typical SERS spectra of all studied phthalocyanines adsorbed from 1×10^{-4}M stock solutions and for 75 minutes soaking time are compared in Figure 7.41. Upper spectra of three copper phthalocyanines (CuPts: CuPt1, CuPt2 and CuPt3) have nearly identical spectra except of relative intensities of tree peaks at 664, 683 and 705 cm^{-1} on the left side and some small changing of 1419cm^{-1} peak in the case of CuPt3. On the other hand, the SERS spectrum of ZnPt differ from that of CuPts. Positions of four more intense SERS bands are significantly shifted, 1528 cm^{-1} band is split on two bands (1503 and 1528 cm^{-1}). These changes can be clearly explained by influence of different metal in the phtalocyanine macrocycle on its vibrations.
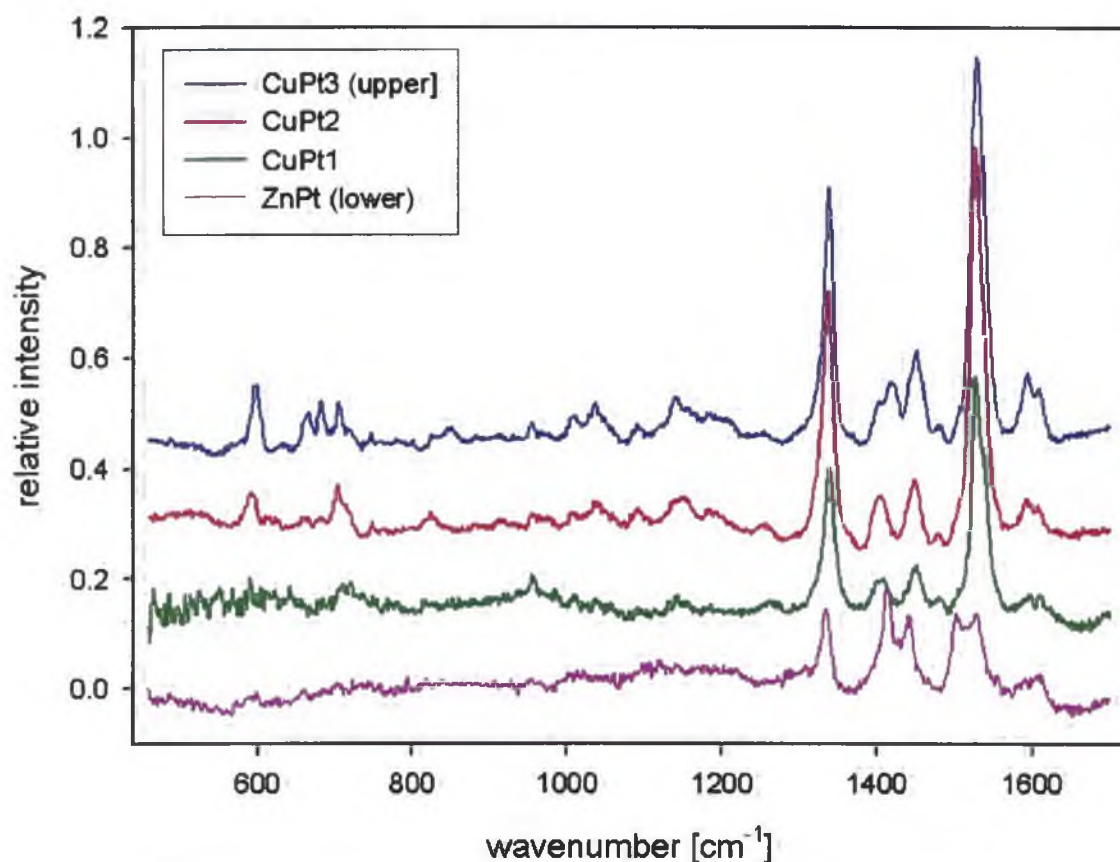

Figure 7.41. SERS spectra of all phthalocyanines adsorbed from 1×10^{-4}M solution for 75 minutes on gold surfaces.

7.5 Comparison of time and concentration dependencies of all studied phthalocyanines

All studied phthalocyanines were successfully adsorbed on gold substrates and their SERS spectra were obtained. No significant changes appeared in positions and relative intensities of spectral bands during all measurements except of intensity ratio of two peaks 1503 and 1528cm^{-1} of ZnPt and of two peaks 1403 and 1419cm^{-1} observed only in the time dependence of CuPt3. According to the assignment (Tables 7.1 and 7.4), all these changes are connected with deformations of the central ring of phthalocyanines during adsorption of phthalocyanine onto a gold substrate. Effect of interaction between dimers of phtalocyanines on their SERS spectra cannot also be excluded.

Comparison of SERS intensities from time and concentration measurements for all phthalocyanines where peak 1528 cm^{-1} (or two peaks 1503 and 1528cm^{-1} for ZnPt) was integrated is shown in Figures 7.42 and 7.43, respectively.
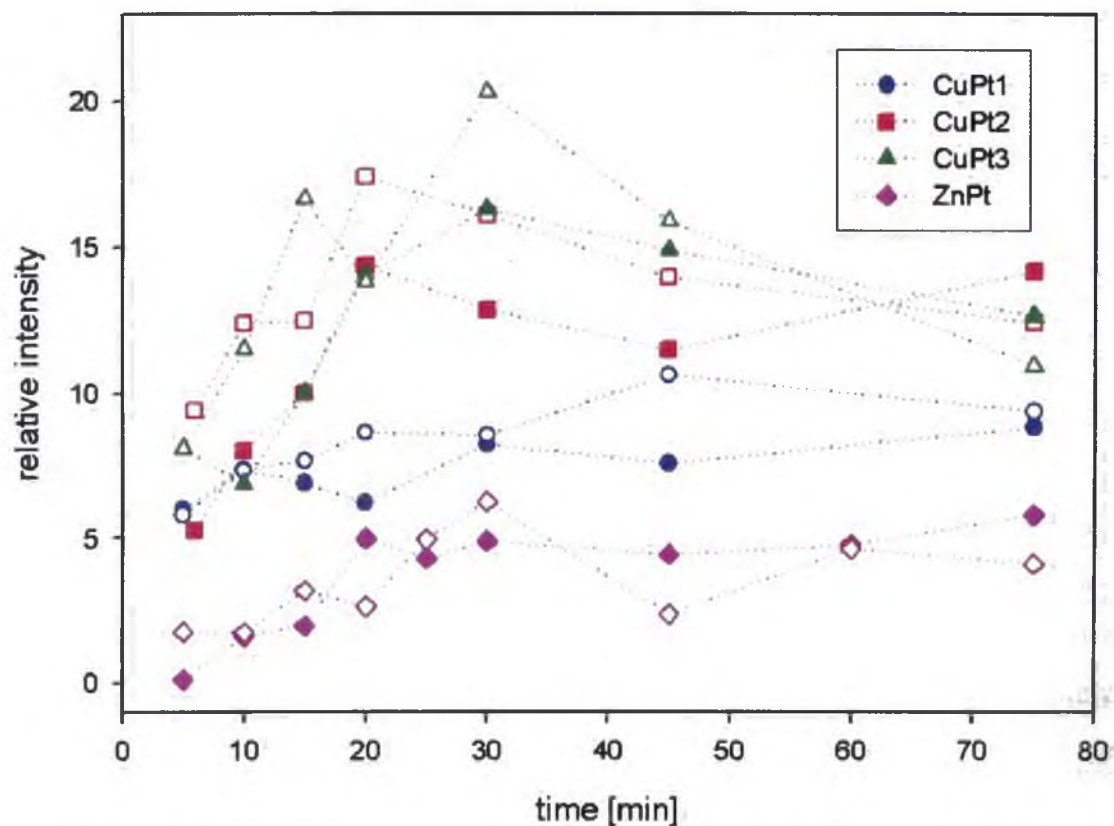

Figure 7.42: Time dependencies of CuPt1, CuPt2, CuPt3 and ZnPt adsorption on gold substrates. Filled and empty symbols represent samples A and B, respectively. (The lines directly connecting consecutive points are included as a guide for the eyes and do not represent real dependences).

Figures 7.42 and 7.43 clearly show that both samples for each phthalocyanine have very similar behaviors in time and concentration dependence and thus, SERS on the gold substrates seems to be a suitable method for phthalocyanine studies with relatively good reproducibility.

The process of adsorption for different soaking times is very similar for all phthalocyanines but small differences were observed depending on the central atom and the substituent. After 20 - 30 minutes of fast increasing of a SERS signal a maximum is reached. For longer soaking times, SERS signal is constant or very slightly increasing (ZnPt and CuPt1) or a slight decreasing in some cases (CuPt2 and CuPt3). The assumption that the decrease of CuPt2 and CuPt3 is caused by depolarization effects seems to be convenient because the highest decrease is observed for CuPt3 with partial charges and consequently, the more efficient depolarization effect. SPE spectra (showing increase of adsorbed amount of CuPts) also support this hypothesis. Moreover, the presence of phtalocyanines dimers on Au surfaces (proved by SPE spectra) also promotes depolarization effects. It is logical that the depolarization effects strongly differ from a molecule to a molecule as was observed in the case of two different porphyrins adsorbed on gold substrates [29]. If we compare absolute intensity values at maximum, the results are following: The lowest signal was observed for ZnPt, two times higher one for CuPt1 and the highest one for both CuPt2 and CuPt3 (approximately three times higher than ZnPt). Thus, our results shows that CuPt2 and CuPt3 have the highest and ZnPt the lowest efficiency of adsorption onto the gold substrates.

Results obtained from the time dependence are confirmed in concentration dependence (see Figure 7.43). Results show again that both samples for each phthalocyanine have very similar behavior with high reproducibility (expect of CuPt3 for higher concentrations). The SERS intensity for all samples rapidly increases to approximately 1×10^{-5}M – 5×10^{-5}M concentration and then a clear plateau is reached expect of ZnPt when the intensity slightly increases. Thus, 1×10^{-5}M – 5×10^{-5}M phthalocyanine concentration seems to be a covering concentration limit, i.e. phthalocyanine concentration necessary to cover all accessible gold nanoparticles. The lowest signal was observed for ZnPt, two times higher one for CuPt1 and the highest ones for both CuPt2 and CuPt3 (approximately five times higher than ZnPt).

The time and concentration comparisons show the same results. The highest signal on gold substrates provides CuPt2 and CuPt3 following by CuPt1. The lowest signal is observed for ZnPt. These tendencies are supported by SPE spectra of gold substrate/phtalocyanine systems (although unfortunately not measured for all series) where extinction bands of

adsorbed phtalocyanines can be seen. The intensity of SPE maximum of adsorbed CuPt3 is about 75% higher than in the case of adsorbed ZnPt. Thus, the concentration of adsorbed CuPt3 is substantially higher than that of ZnPt. We suggest that a reason of this behavior arises from different charge of studied phthalocyanines. Negatively charged ZnPt is repelled from negative ion shell covering metal particle and thus adsorption is slower and less efficient. On the other hand, positive and/or partially positive charge on CuPt3 increases efficiency of its adsorption on gold surfaces. Very interesting is also not the same adsorption for CuPt1 and CuPt2 although they differ each other only in the substituent on the aminogroup (dimethyl- or diethyl-, respectively). We suppose that higher adsorption of CuPt2 is caused by methyl in adjacent chains instead of ethyl group, so smaller CuPt2 can easily reached metal surface through an ion shell. It would mean that the adsorption on Au surface proceeds via dialkyl substituted amino groups at the end of the alifatic chain.

Differences between efficiency of adsorption can be also deduced from concentration dependences (compare samples CuPt2 and CuPt3 in Figure 7.43). Faster increase and subsequently constant signal of CuPt2 with comparison to CuPt3 was observed. The charge differences of these two molecules probably play again the main role in this effect. A non-polar molecule seems to have easier and thus faster adsorption on gold surfaces compared to a molecule with partial charges.

In these comparisons two factors are important to underline. ZnPt was measured on the old spectrometer in contrast to the others phthalocyanines measured on new one. However, differences between the spectrometers should be insignificant because the intensity is normalized to the strong Raman band of glass and thus the signals of all phthalocyanines are absolutely comparable. Secondly, the strongest peak at 1528 cm^{-1} is integrated for all copper phthalocyanines whereas two peaks at 1503 and 1528 cm^{-1} were used in the case of ZnPt. As mentioned in the zinc part, the relative intensities of these two peaks change in the spectral series, but whole intensity of these two peaks very well corresponds to the overall intensity.
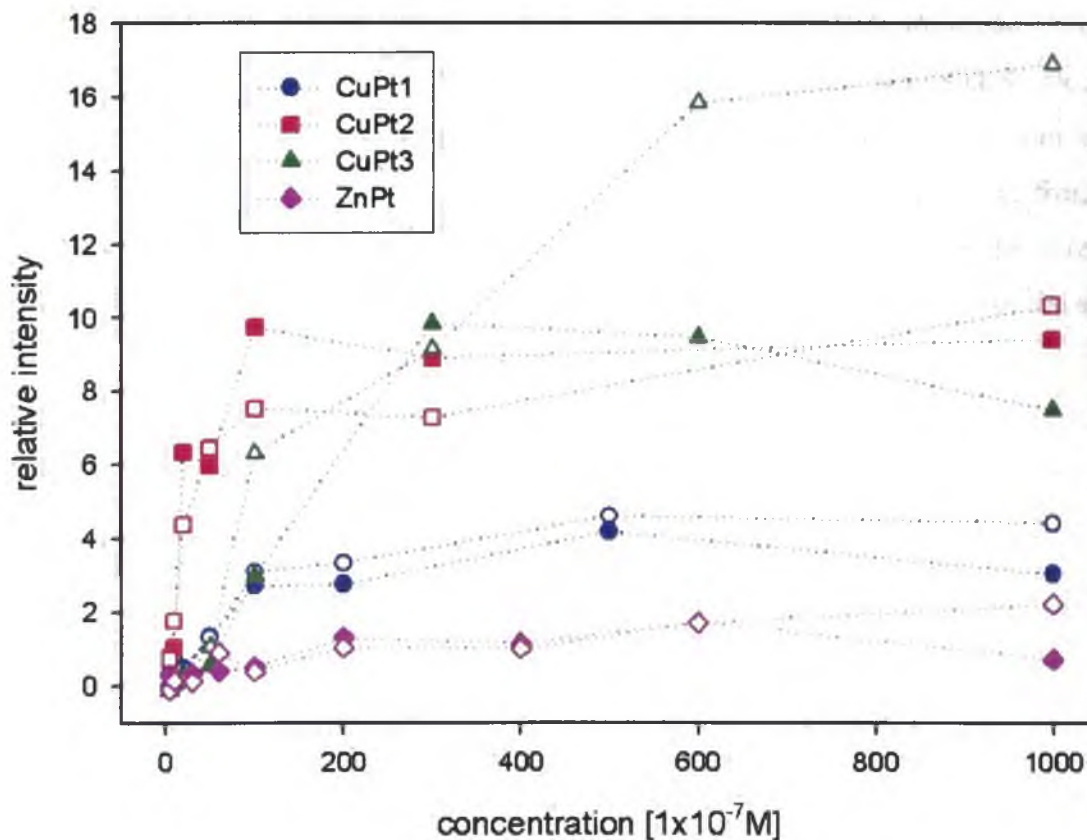
Figure 7.43: Concentration dependencies of CuPt1, CuPt2, CuPt3 and ZnPt adsorption on gold substrates. Filled and empty symbols represent samples A and B, respectively. (The lines directly connecting consecutive points are included as a guide for the eyes and do not represent real dependences).

7.6 Measurement on Raman confocal microscope

Installation of a Raman confocal microscope, LABRAM HR-800 (Horiba Jobin-Yvon), finished at the beginning of 2006, in laboratory of Division of Biomolecular Physics. Using this experimental device, detection of solid samples together with a lower laser power and high sensitivity enables obtaining very good spectra of observed molecules with high signal/noise ratio and without undesired background (e.g. a Raman signal of glass).

We tested possibility to use Raman confocal microscope to measure Raman and SERS spectra of studied phtalocyanines. Experimental conditions was following: excitation wavelength 632.8 nm of He-Cd laser, laser power (0.02-20mW), entrance slit 100 μm,

confocal hole 400 μm, accumulation time 60s. Raman spectra of phtalocyanines measured from dried drop (from 1×10^{-4} M solutions) onto glass slides and SERS spectra of phthalocyanines (adsorbed on gold/substrates from 1×10^{-4} M solutions for 75 min soaking time) are compared in Figures 7.44-7.47. In the case of Raman measurement from dried drops maximal laser power (20 mW) was used while in the case of SERS measurements, laser power was diminished to 0.02 mW to avoid possible photodecomposition of the sample.
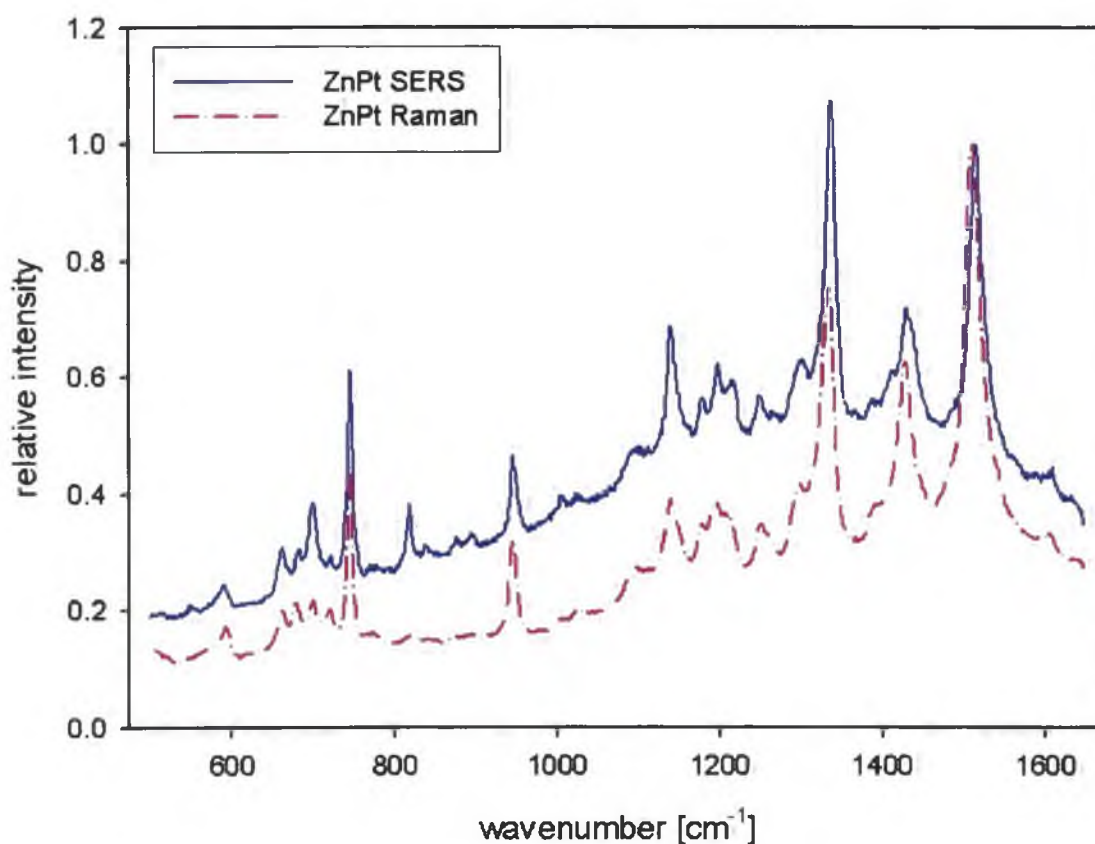

Figure 7.44. SERS and Raman spectra of ZnPt using the new Raman confocal microscope.
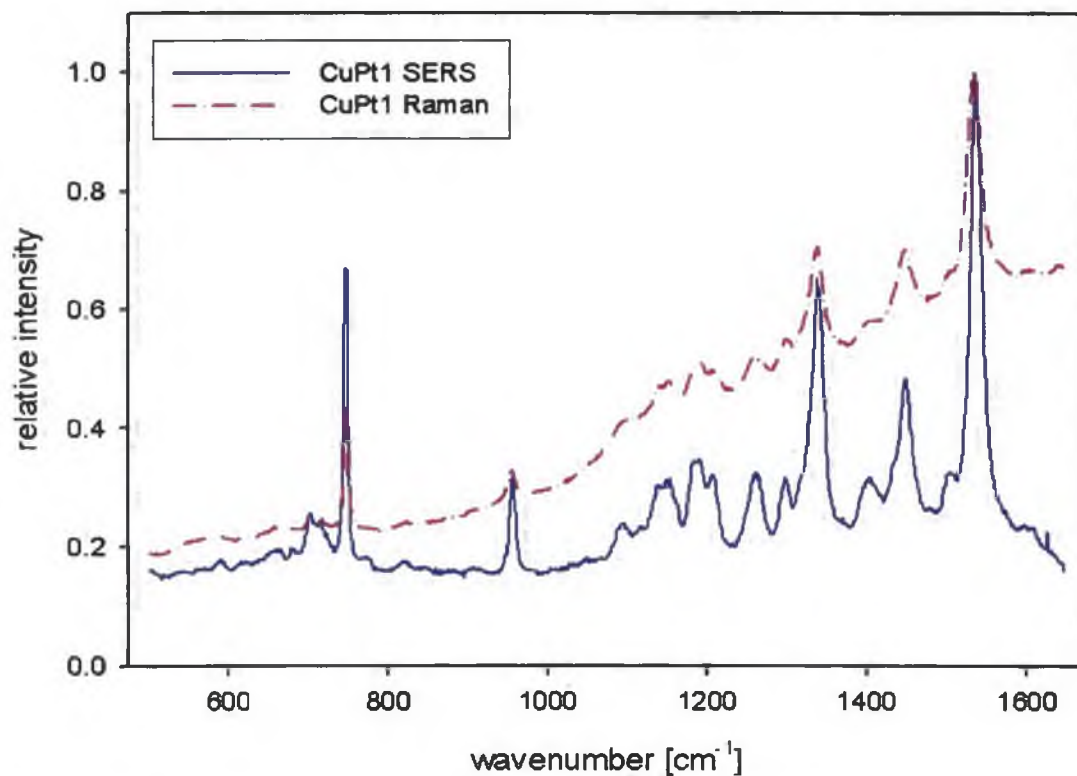
Figure 7.45. SERS and Raman spectra of CuPt1 using the new Raman confocal microscope.
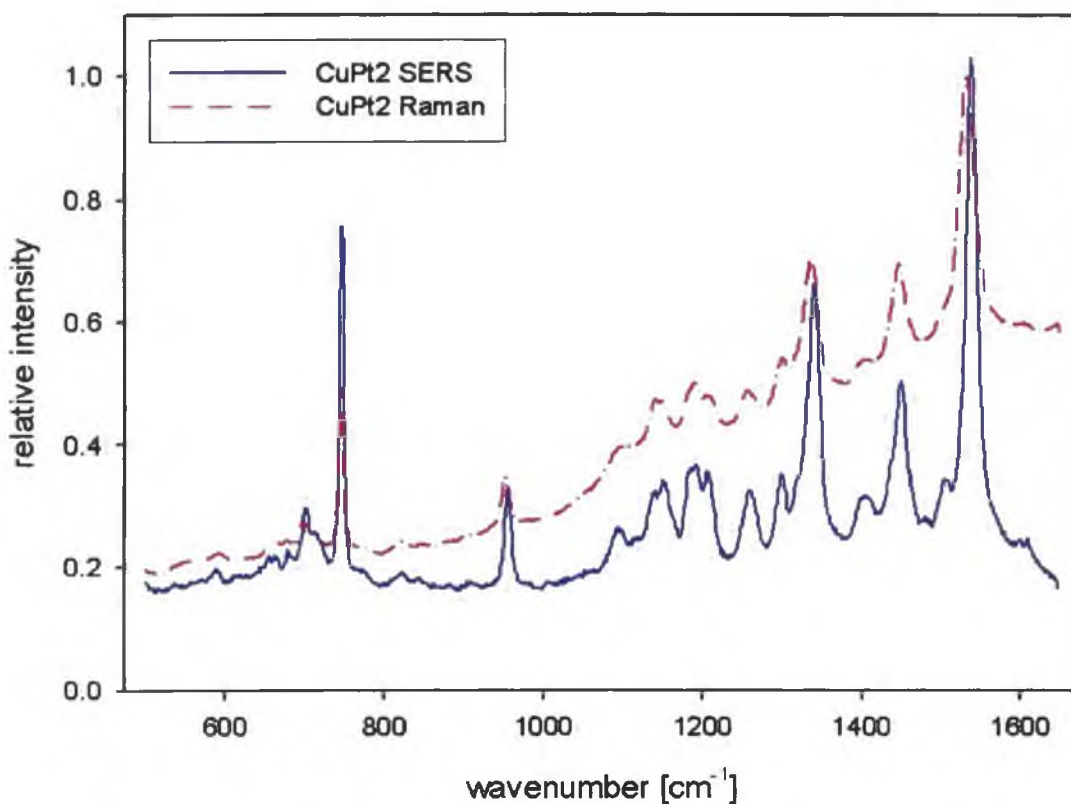

Figure 7.46. SERS and Raman spectra of CuPt2 using the new Raman confocal microscope.
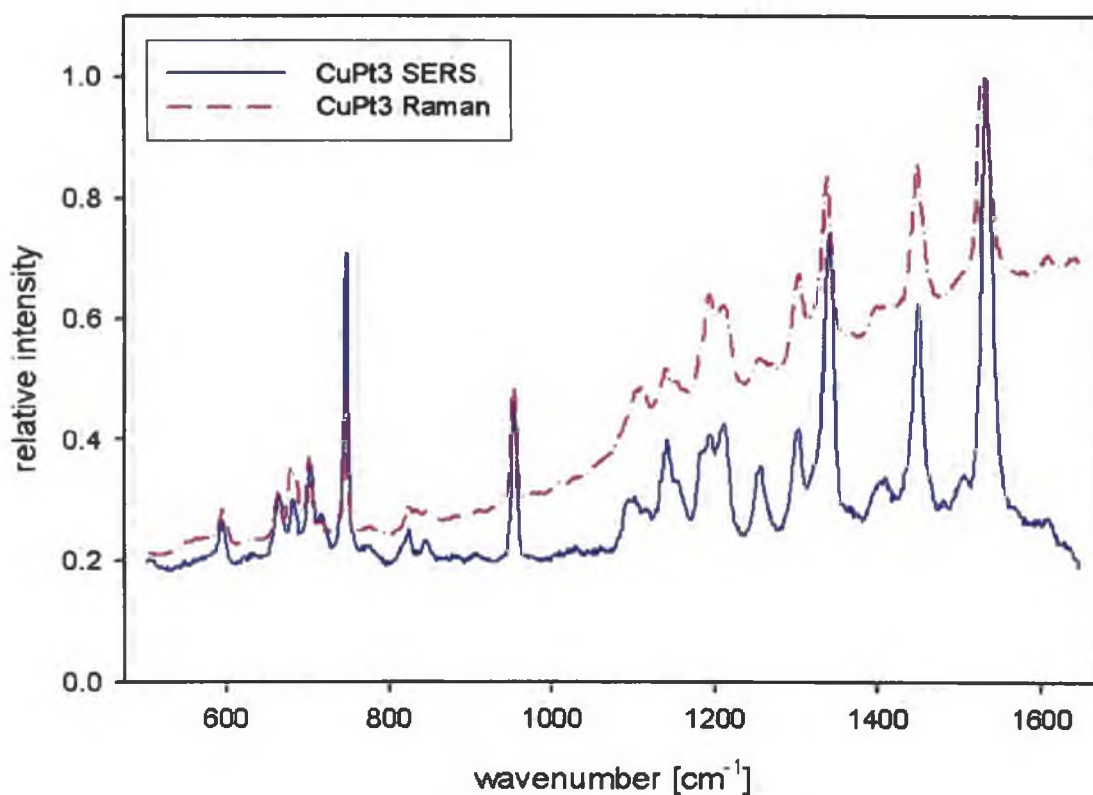
Figure 7.47. SERS and Raman spectra of CuPt3 using the new Raman confocal microscope.
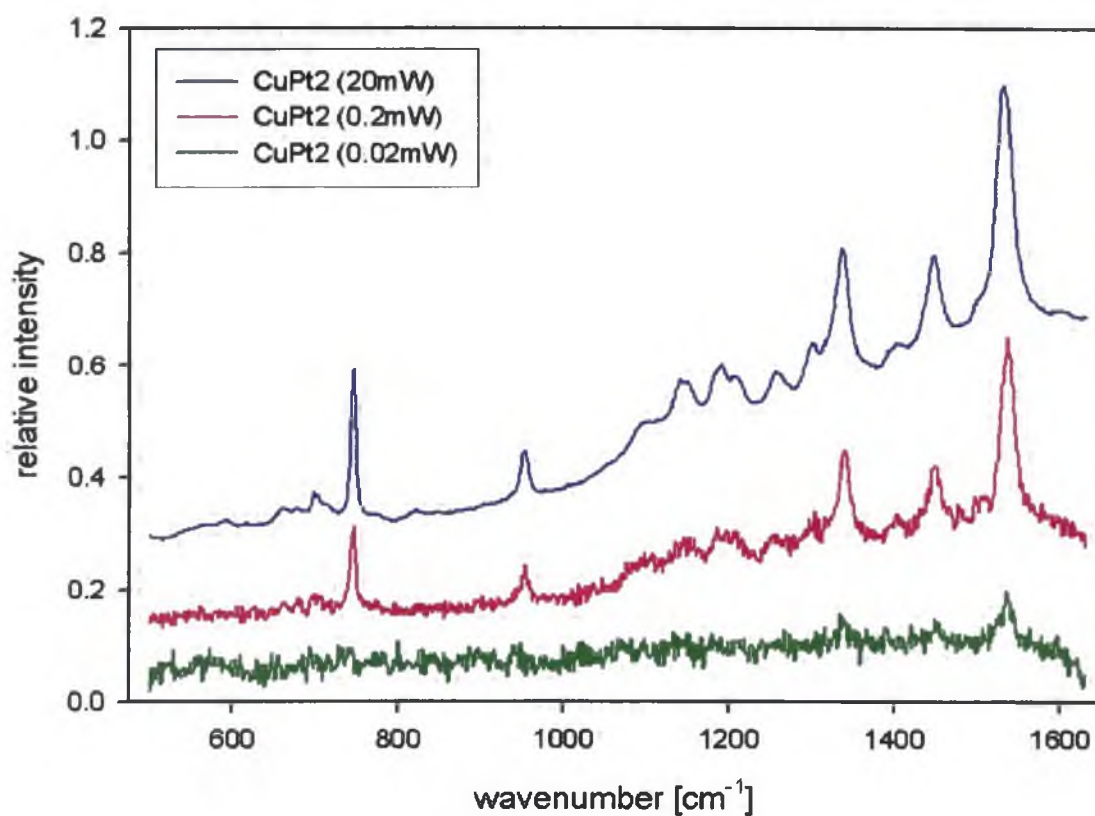

Figure 7.48. Raman spectra of CuPt2 comparing different laser power.

Very nice spectra without Raman signal of glass were obtained from all studied samples. Both Raman and SERS spectra are very rich and positions of the spectral bands are the same for each particular sample. There are some small differences in relative intensities of bands in the spectra probably due to adsorption of Pts onto gold substrate. In the case of the Raman spectra, significant fluorescence backgrounds were observed. It is logical because 632.8 nm excitation line falls into molecular absorption of phtalocyanines (see Figure 3.5). Thus, Raman spectra measured for dried drops are the resonance Raman (RR) spectra of phtalocyanines, and with an overlapped fluorescence signal observed.

Figure 7.48 compares the RR spectra of CuPt2 measured using different laser power. Results clearly shows that using 0.02 mW laser power only negligible spectrum of CuPt2 is detected and thus, our spectra of Ptcs measured from gold substrates using 0.02 mW laser power are the SERS (or mostly SERRS in this case) spectra of phthalocyanines.

Comparison of SERS spectra obtained using 514.5 nm (macro) and 632.8 nm (micro) shows that SERS spectra obtained using 632.8 nm are substantially richer mostly in low wavenumber region probably due to resonance excitation (see Figures 7.49-7.52).
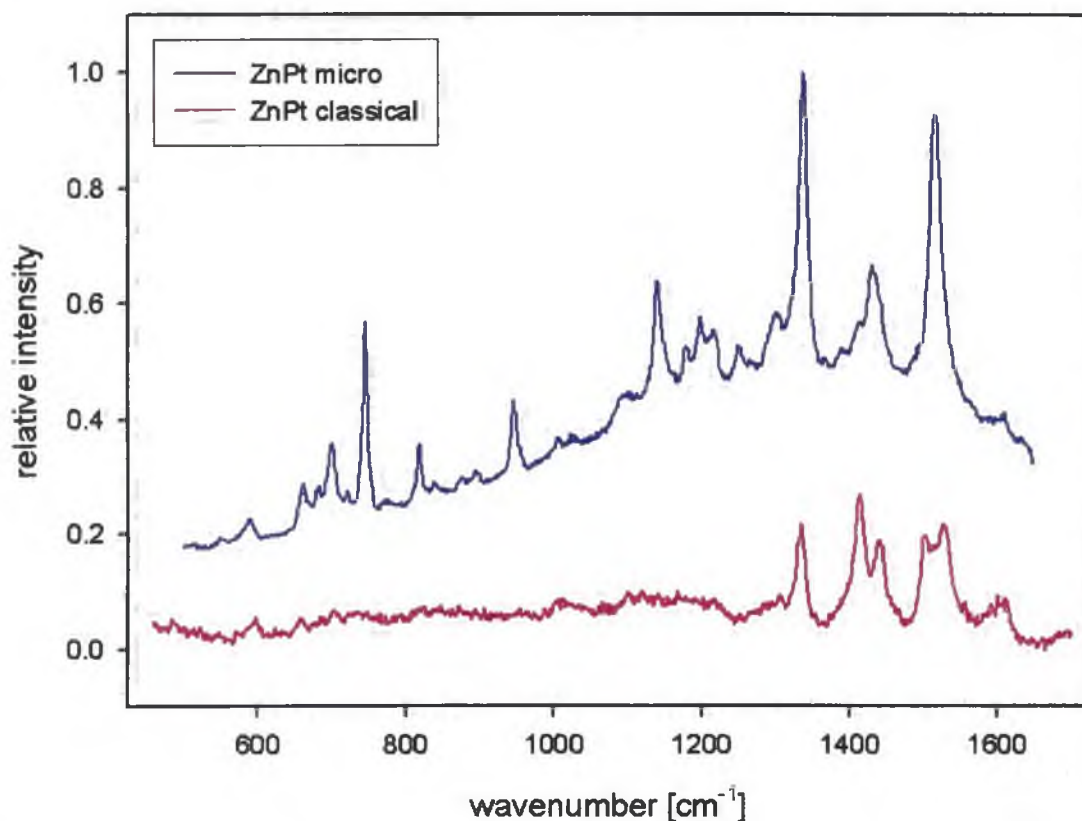

Figure 7.49. Comparison of ZnPt spectra obtained by the Raman confocal microscope (freshly measured without correction) and the "classical" Raman spectroscope.

Figure 7.50. Comparison of CuPt1 spectra obtained by the Raman confocal microscope (freshly measured without correction) and the "classical" Raman spectroscope.

Figure 7.51. Comparison of CuPt2 spectra obtained by the Raman confocal microscope (freshly measured without correction) and the "classical" Raman spectroscope.
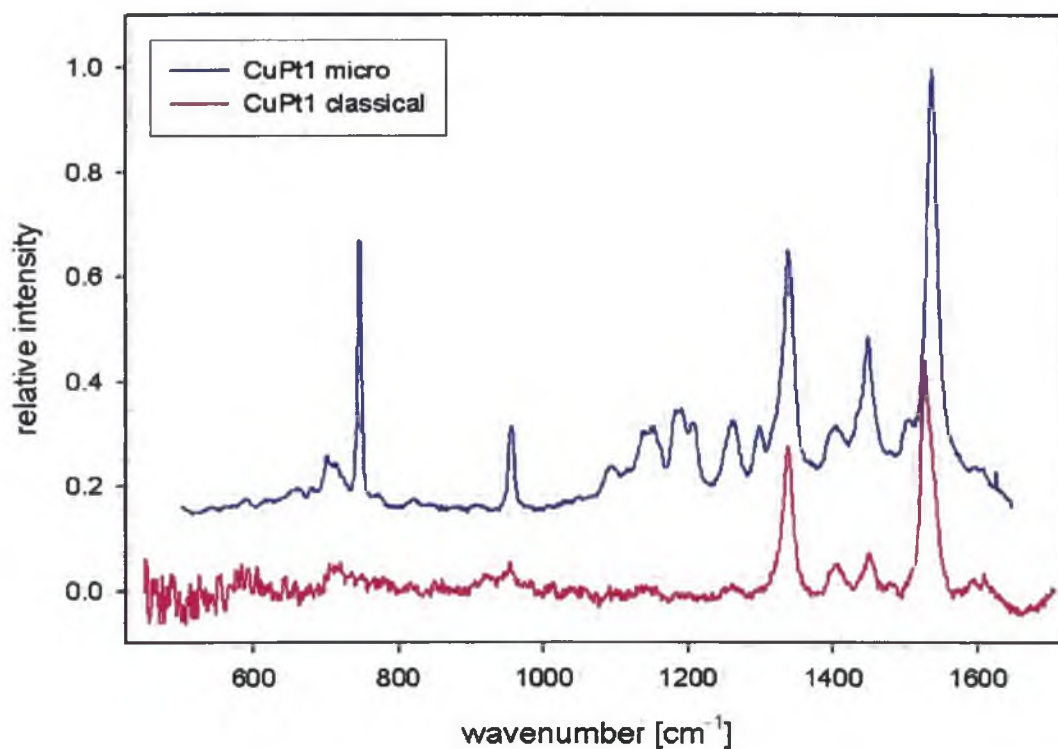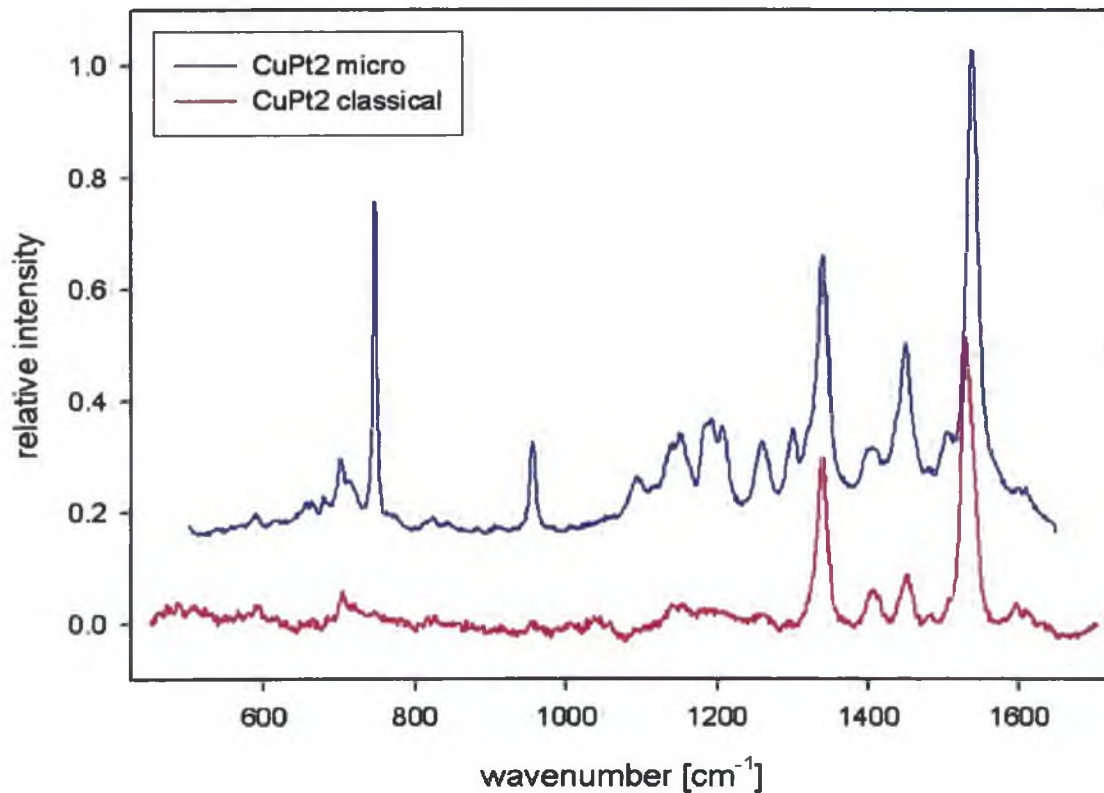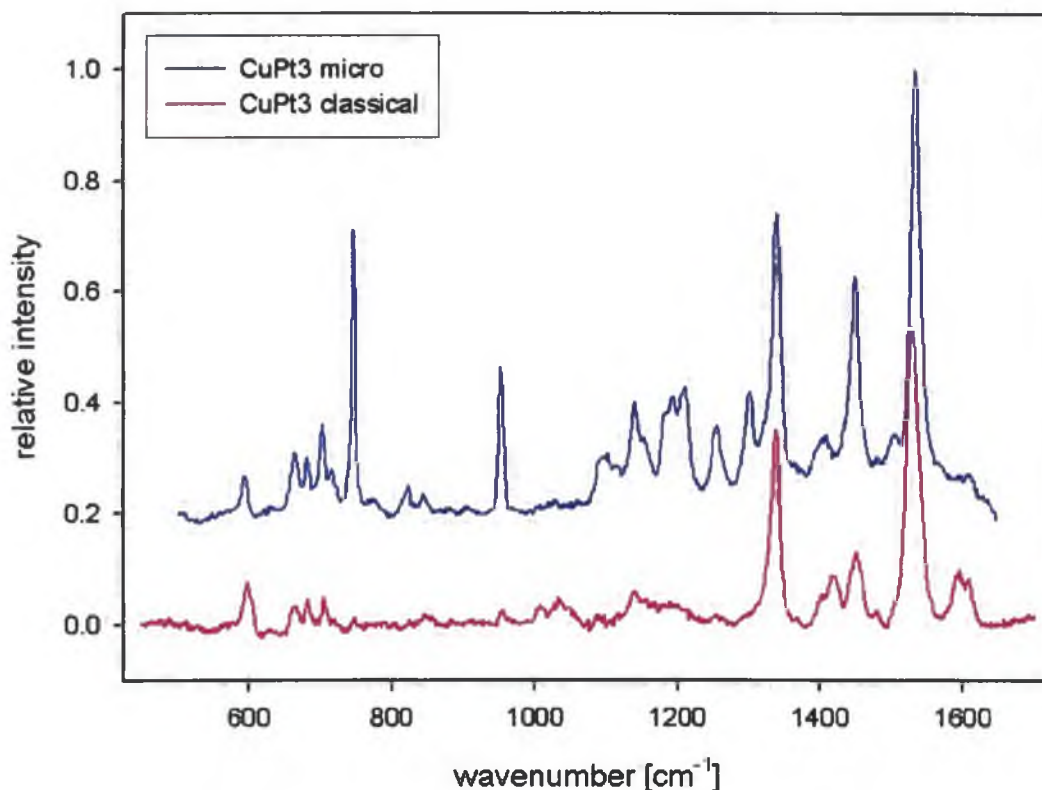
Figure 7.52. Comparison of CuPt3 spectra obtained by the Raman confocal microscope (freshly measured without correction) and the "classical" Raman spectroscope.

The confocal Raman microspectrometer offers a more intensive, richer and nearly noiseless signal of samples measured from glass slides. The main advantage is easer manipulation and substantially shorter acquisition times (5 times shorter than in the case of measurement using classical Raman spectrometer). Moreover, confocal system allows us to simply avoid problems with strong Raman signal of glass. We propose that using Raman microspectrometer more detail Raman xy-mapping of our gold substrate will be also possible.

8 AZO dye molecule

Time and concentration dependencies of "Azo molecule" (dissolved in chloroform) adsorbed on gold surfaces were measured using the "old" Raman spectrometer.

8.1 Time dependence of Azo dye

For time dependence $1\times10^{-4}M$ azo concentration was used. A gold substrate was immersed into the solution for 1, 5, 10, 15, 30, 60, 90 and 120 minutes soaking times. The experiment was carried out only on one gold substrate. Obtained normalized spectra are shown in Figure 8.1 where a clear signal of azo is observable from the shortest times over the glass background. Subtracted and baseline corrected spectra are presented in Figure 8.2. In Figure 8.3 the spectrum of $1\times10^{-4}M$ azo for 120 minutes soaking time is shown in detail.
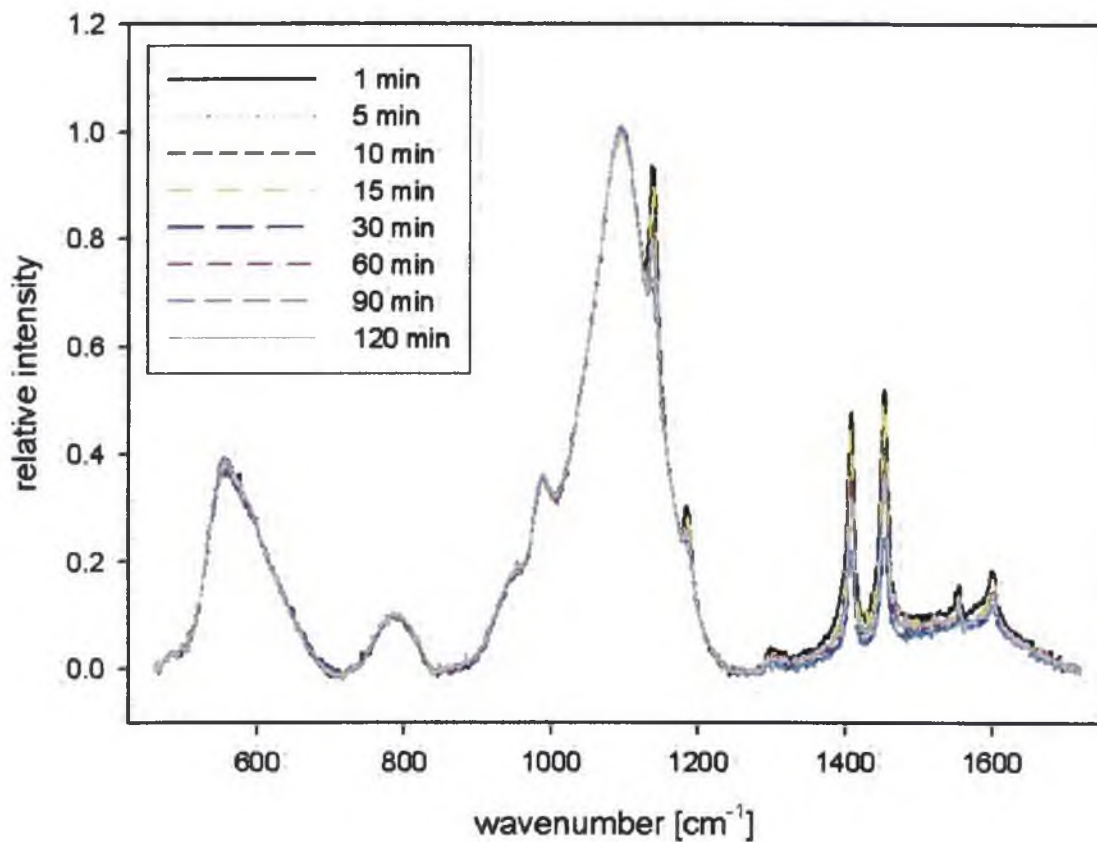
Figure 8.1. Normalized and baseline-corrected SERS spectra of azo dye on gold substrate absorbed from 1x10⁻⁴M stock solution for different soaking times.
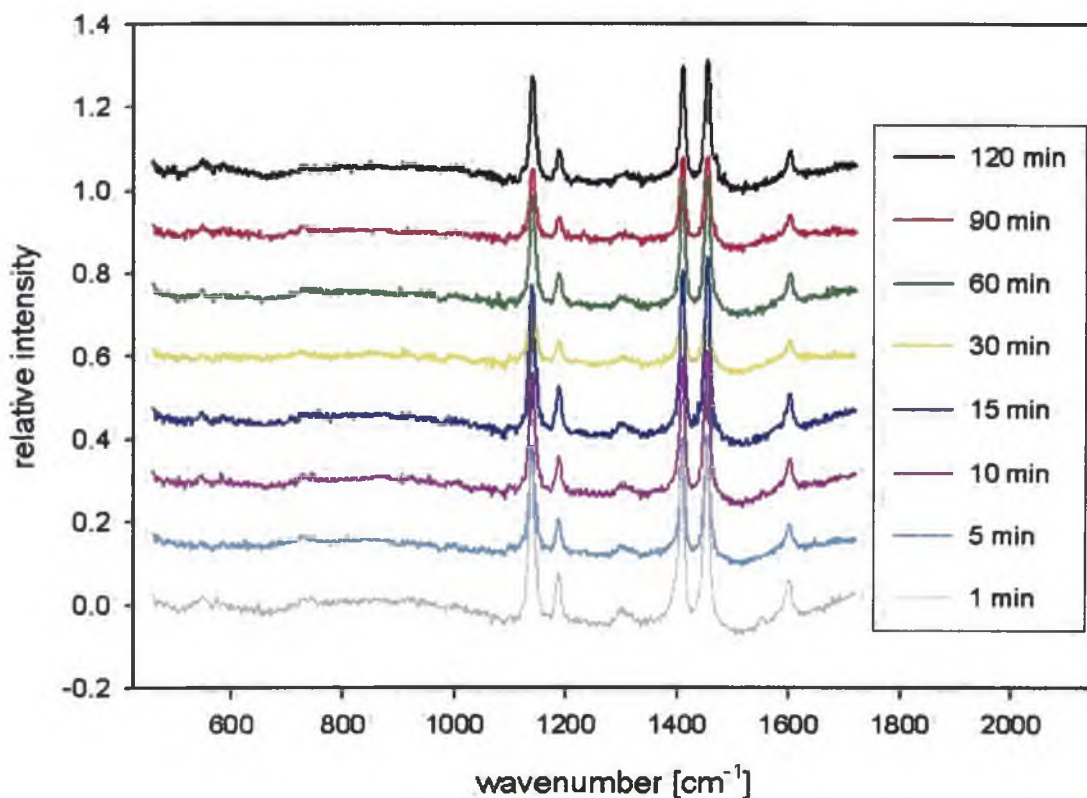

Figure 8.2. Same as in Figure 8.1. The Raman signal of glass is subtracted from the spectra.
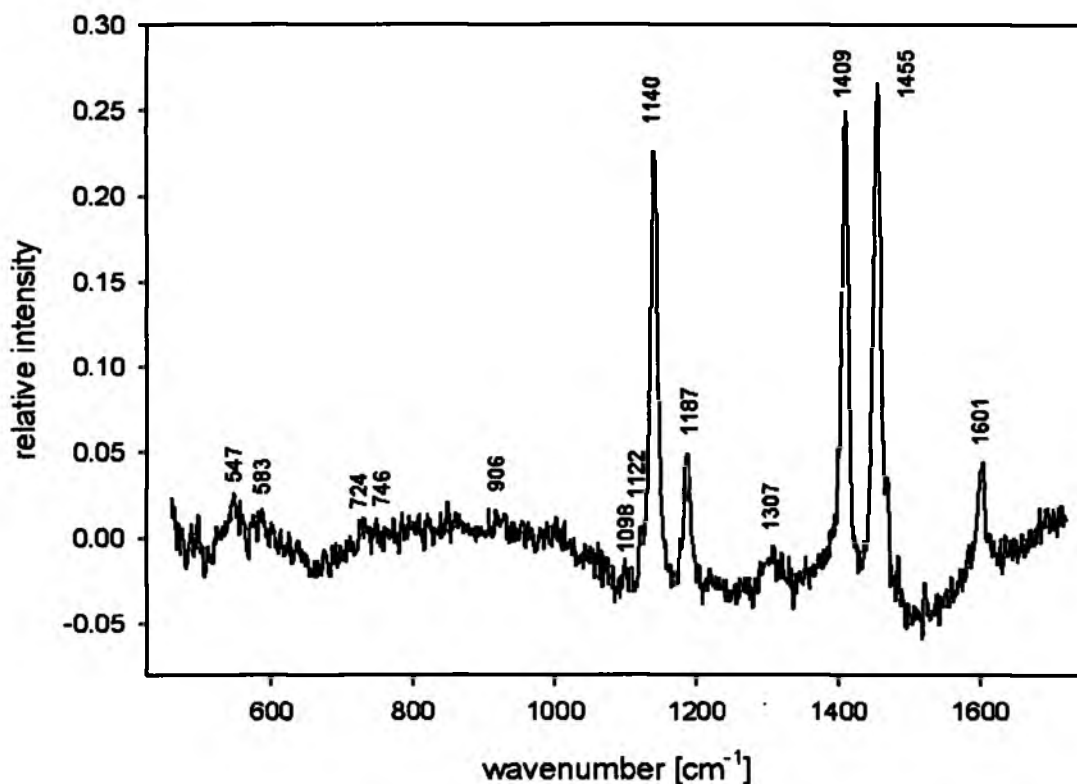
Figure 8.3. The SERS spectrum of 1×10^{-4}M azo dye on gold adsorbed for 120 minutes.

Five peaks (at 1140, 1187, 1409, 1455 and 1601 cm^{-1}) are clearly visible in all spectra (view Figures 8.2 and 8.3). Some other weaker bands (view Fig. 8.3) are also observable in low wavenumber region. No changes in position and relative intensity happened in the time dependence, only overall intensity changes. The intensity of signal is relatively high from the shortest times, even for 1 minutes the signal is the most intensive. This dependence shows that adsorption-desorption balance is reached very rapidly. This behavior can arise from linearity of an azo molecule, absence of charges and, mainly, the presence of –SH group on azo dye molecule with its high affinity to the gold surface. Although dependence for longer soaking times is not clear from our experimental points, a slight intensity decrease is evident (see Fig. 8.4) probably caused by some depolarization effects for high concentration density of adsorbed molecules.
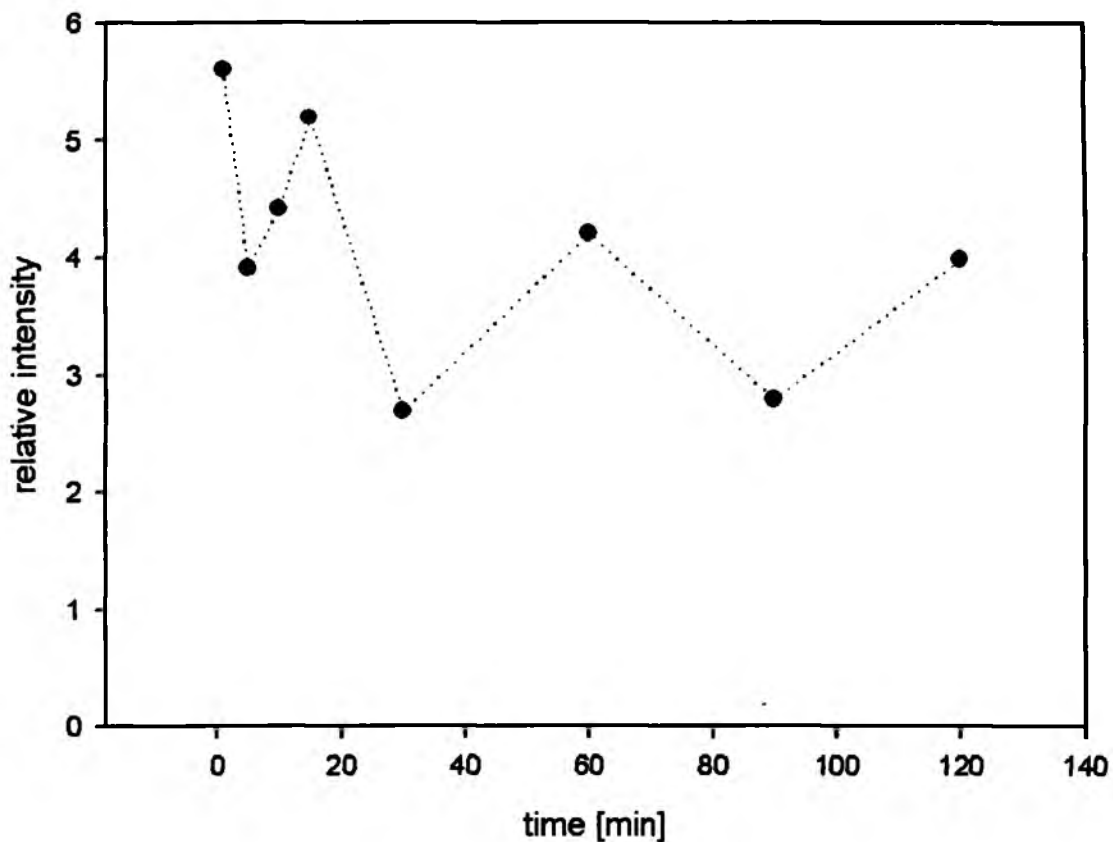
Figure 8.4. The intensity of the azo peak at 1409 cm^{-1} measured in the time dependency (The lines directly connecting consecutive points are included as a guide for the eyes and do not represent real dependences).

8.2 Concentration dependence of azo dye

Concentration measurements of azo molecule were also carried out. Seven concentrations from 5x10^{-7}M to 1x10^{-4}M region were chosen. Soaking time was fixed to 10 minutes for all samples. The time dependence was measured only on one gold substrate.

Figure 8.5 shows normalized and baseline corrected spectra. Subtracted spectra are presented in Figure 8.6.
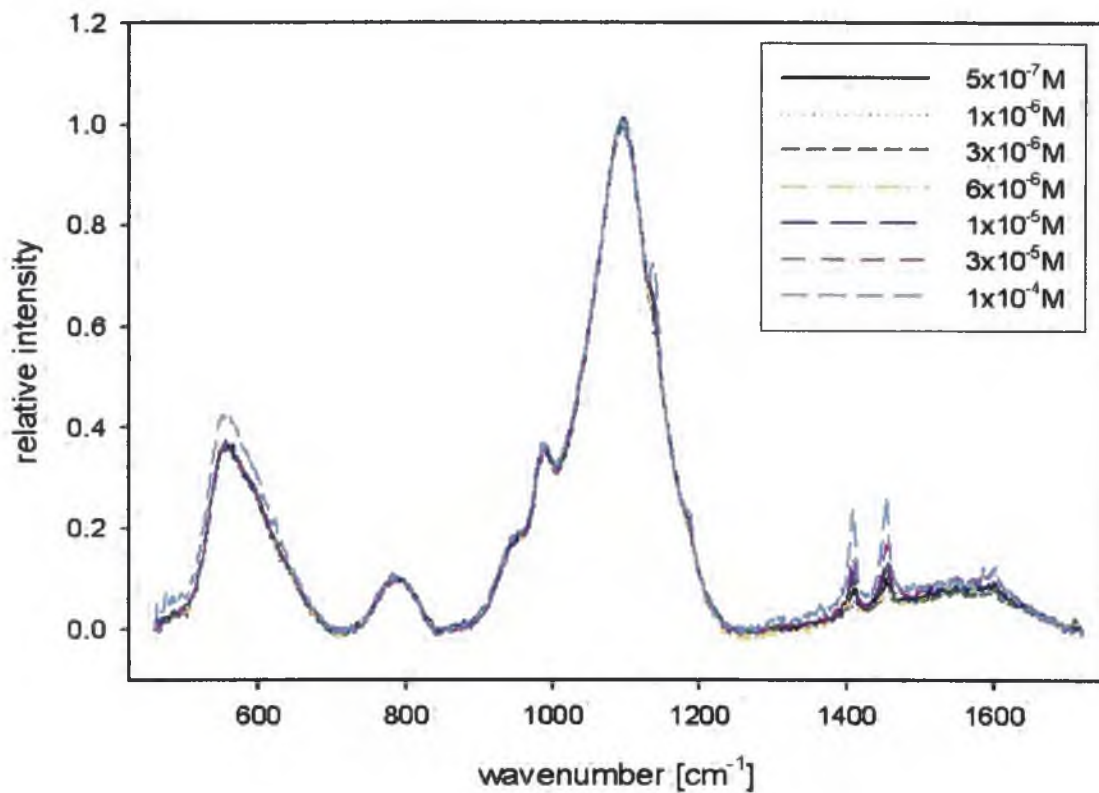
Figure 8.5. Normalized and baseline corrected SERS spectra of azo dye for different concentration of stock solution.
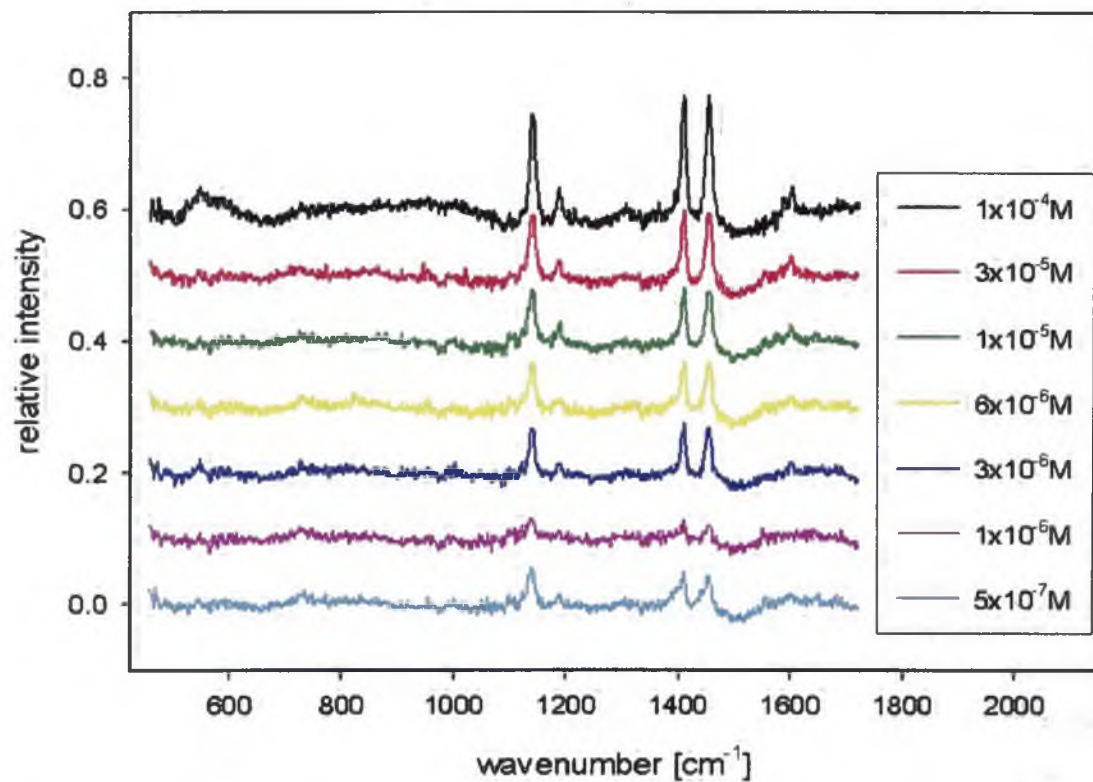
Figure 8.6. Same as in Figure 8.5. The Raman signal of glass is subtracted from the spectra.

The same peaks appeared in azo spectra as at the time dependence. No changes were found in positions and relative intensities in azo spectra bands measured in the concentration dependence. The concentration dependence is presented in Figure 8.7 where a signal increases rapidly to 3×10^{-6} M concentration and slower but a continuous increase is observed for higher concentrations. A slight decrease for 1×10^{-6}M caused probably by irreproducibility of measurement was observed.
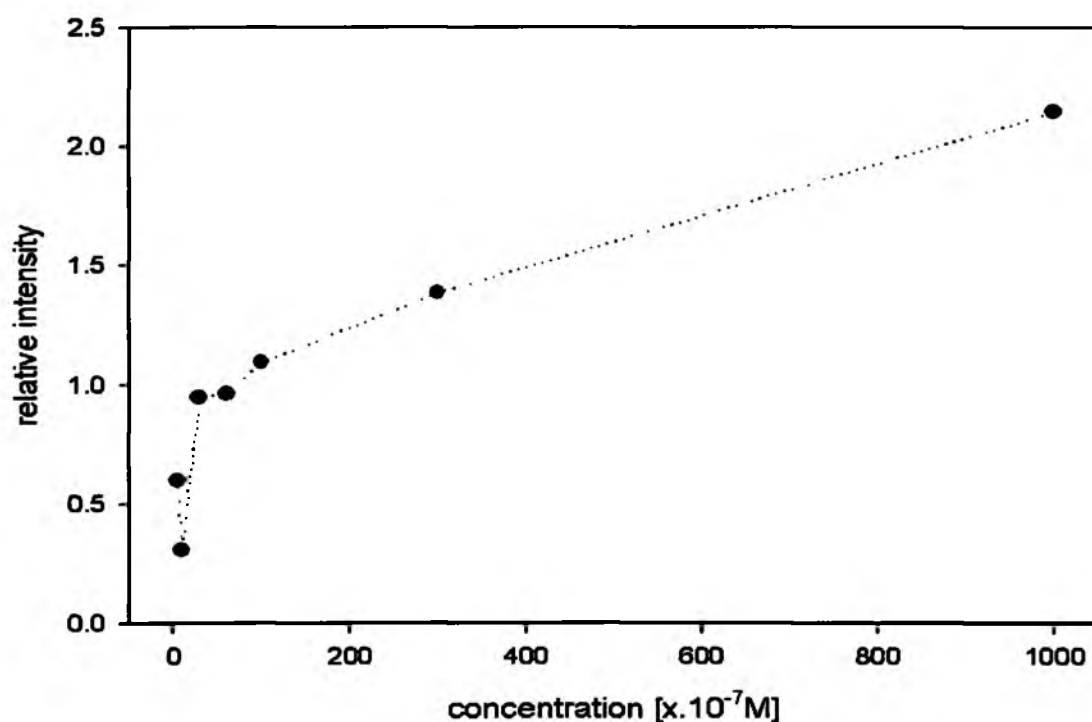

Figure 8.7. The intensity of azo peak at 1409 cm^{-1} measured on the old device in the concentration dependency (The lines directly connecting consecutive points are included as a guide for the eyes and do not represent real dependences).

8.3 Comparison of time and concentration dependencies of azo dye

No changes in positions and relative intensities of bands were observed in both dependencies; only intensities were changed. In the time dependency the signal grows extremely fast, the first measurement (1 minute) was the strongest and subsequently a slight signal increasing is observed, indicating very fast adsorption. We propose that azo molecule is adsorbed via –SH group onto a gold surface. A signal increase during the whole measurement in the concentration dependence predicts that the limit for surface density of adsorbed azo molecules is not reached even for 1×10^{-4}M. The linearity of the molecule can cause that the high surface density is possible.

Chapter V

Conclusion

8 Conclusion

SERS-active surfaces, citrate-reduced gold colloidal nanoparticles immobilized on silane-modified glass slides, were routinely prepared with high stability and reproducibility. These gold surfaces have been successfully employed to study newly synthesized photoactive molecules, zinc and copper phthalocyanines. SERS spectra even from phtalocyanines non-soluble in water have been obtained using these gold surfaces without interference of solvents.

Results obtained from phthalocyanine studies, can be summarized as followed:

1) All studied phthalocyanines were successfully adsorbed on gold substrates and their SERS spectra were obtained. SERS spectra of copper phthalocyanines are very similar, so different substituents do not have great influence on their spectra. Zinc phthalocyanine spectra show slight changes in comparison to copper phthalocyanine ones caused by different metal in phthalocyanine macrocycle. Some changes in relative intensities at CuPt3 and ZnPt spectra were observed in time and concentration dependent series indicating some deformations of the phthalocyanine macrocycle during its adsorption onto a gold substrate.

2) Results obtained from time and concentration dependences allow us to compare adsorption process of studied phthalocyanines onto gold surfaces. In first 20-30 minutes a signal reached a maximum followed in some cases of an increase (ZnPt and CuPt1) or a slight decrease (CuPt2 and CuPt3). This decrease is probably caused by a depolarization effect that occurs for higher concentrations when neighbor molecules interact. Maximal signal in the

concentration dependencies (except of a slightly but continuously increasing signal in the case of ZnPt) was reached approximately at 1×10^{-5}M $-$ 5×10^{-5}M concentration showing probably a covering concentration limit of studied molecules. A detection limit was estimated approximately from 1×10^{-6}M to 6×10^{-6}M (concentration of stock solutions) for all phthalocyanines.

3) On the other hand, obtained dependencies showed different efficiency of adsorption of studied molecules onto gold surfaces. The lowest signal provides ZnPt, two times higher CuPt1 and three (in time dependencies) or five times (in concentration dependences) CuPt2 and CuPt3. We propose that negative charged molecules are repealed from gold citrate SERS-active surfaces. On the other side, positive and/or partially positive charges on molecules facilitate adsorption. Size of studied molecules also seems to affect the efficiency of adsorption. Smaller molecules can easily reach metal surfaces.

Results of the Azo dye molecule study are following:

1) Azo dye molecule successfully adsorbed on gold substrates provides intensive SERS signal for all soaking times. A slight decrease occurred for longer times is caused probably by depolarization effects. A covering concentration limit was not reached even for 1×10^{-4}M concentration.

We also tested possibility to use a new experimental device, Raman confocal microscope, to measure Raman and SERS spectra of studied phtalocyanines. We conclude that the confocal Raman microspectrometer provides a more intensive, richer and nearly noiseless signal (without interference of the Raman spectrum of glass) for substantially shorter acquisition times than the classical macro Raman spectrometer.

Chapter VI

References

[1]   Fleischmann M, Hendra P. J., McQuillan A. J. (1974): Raman spectra of pyridine adsorbed at a silver electrode. *Chem. Phys. Lett.* **26**, 163-166.

[2]   Jeanmaire D. J., Van Duyne R. P. (1977): Heterocyclic, aromatic, and aliphatic amines adsorbed on the anodized silver electrode. *J. Electroanal. Chem* **84**, 1-20.

[3]   Albrecht M. G., Creighton J. A. (1977): Anomalously intense Raman spectra of pyridine at a silver surface. *J. Am. Chem. Soc* **99**, 5215-5217.

[4]   Moskovits M. (1978): Surface roughness and the enhanced intensity of Raman scattering by molecules adsorbed on metals. *J. Chem. Phys.* **69**, 4159-4161.

[5]   Creighton J. A., Blatchford C. G., Albrecht M. G. (1979): Plasma resonance enhancement of Raman scattering by pyridine adsorbed on silver or gold sol particles of size comparable to the excitation wavelength. *J. Chem. Soc. Faraday Trans.* **75**, 790-798.

[6]   Kneipp H., Itzkan I., Ramachandra R. D., Feld M.S. (1999): Ultrasensitive Chemical Analysis by Raman Spectroscopy. *Chem. Rev.* **99**, 2957-2975.

[7]   Kambhampati P., Child C. M., Foster M. C., Campion A. (1998): On the chemical mechanism of surface enhanced Raman scattering: Experiment and theory. *J. Chem. Phys.* **108**, 5013-5026.

[8]   Lee P. C., Meisel D. (1982): Adsorption and Surface-Enhanced Raman of Dyes on Silver and Gold Sols. *J. Phys. Chem.* **86**, 3391-3395.

[9]   Fojtík A., Henglein A. (1993): Laser ablation of films and suspended particles in a solvent: formation of cluster and colloid solutions. *Ber. Bunseges Phys. Chem.* **97**, 252-254.

[10]   Neddersen J., Chumanov G., Cotton T. M. (1993): Laser Ablation of Metals: A New Method for Preparing SERS Active Colloids. *Appl. Spectrosc.* **47**, 1959-1964.

[11]   Prosser V. et al. (1989): Experimentální metody biofyziky. Academia, Praha.

[12]   Brolo A.G, Irish D. E., Smith B.D. (1997): Applications of Surface Enhanced Raman Scattering to the Study of Metal-Adsorbate Interactions. *Journal of molecular structure* **405**, 29-44.

[13]   Keating C. D. Musick M. D., Keefe M.H., Natan M. J., *J. Chem. Educ.* **76** (1999), 949-955.

[14]   Kneipp K., Kneipp H., Itzkan I., Dasari R. R., Feld M. S. (2002): Surface-enhanced Raman scattering and biophysics. *J. Phys.: Condens. Matter* **14**, 597-624.

[15]   Aroca R. F., Alvarez-Puebla R. A., Pieczonka N., Sanchez-Cortez S., Garcia-Ramos J. V. (2005): Surface-enhanced Raman scattering on colloidal nanostructures. *Advances in Colloid and Interface Science* **116**, 45-61.

[16] Karageorgiev P., Stiller B., Prescher D., Dietzel B., Schulz B., Brehmer L. (2000): Modification of the Surface Potential of Azobenzene-Containing Langmuir-Blodgett Films in the Near Field of a Scanning Kelvin Microscope Tip by Irradiation. *Langmuir* **16**(13), 5515-5518.

[17] Geue T., Schultz M., Grenzer J., Pietsch U., Natansohn A., Rochon P. (2000): X-ray investigations of the molecular mobility within polymer surface gratings. *J. Appl. Phys.* **87**(11), 7712-7719.

[18] Stiller B., Karageorgiev P., Luengling T., Prescher D., Zetzsche T., Dietzel R., Knochenhauer G., Brehmer L., *Mol. Cryst. Liq. Cryst.* **355**, 401 (2001).

[19] Rand P. B., Peumans P., Forrest S. R. (2004): Long-range absorption enhancement in organic tandem thin-film solar cells containing silver nanoclusters. *Journal of Applied physics* **96**, No 12, 7519-7526.

[20] Procházka M., Mojzeš P., Štěpánek J., Vlčková B., Turpin P. Y. (1997): Probing applications of laser ablated ag colloids in sers spectroscopy: improvement of ablation procedure and sers spectral testing, *Anal. Chem.* **69**, 5103.

[21] Freeman R. G., Grabar K. C., Allison K. J., Bright R. M., Davis J. A., Jackson M. A., Smith P. C., Walter D. G., Natan M. J. (1995): Metal Nanoparticle Deposition for TOF-SIMS Signal Enhancement of Polymers. *Science* **267**, 1629-1632.

[22] Keating C. D., Musick M. D., Keefe M. H., Natan M. J. (1999): Kinetics and Thermodynamics of Au Colloid Monolayer Self-Assembly: Undergraduate Experiments in Surface and Nanomaterials Chemistry. *J. Chem. Educ.* **76**, 949-955.

[23] Hajduková N. (2005): Kovové částice imobilizované na skleněné podložky a jejich využití jako SERS-aktivních povrchů při studiu biomolekul (Msc. Thesis). MFF UK, Prague.

[24] Němeček D. (2004): Doctoral Thesis, MFF UK, Praha

[25] Karolien de Wael, Westbroek P., Bultinck P., Depla D., Vandenabeele P., Adriaens A., Temmerman E. (2005): Study of the deposition and Raman and XPS characterization of a metal ion tetrasulphonated phthalocyanine layer at gold surfaces: density function theory calculations to model the vibration spectra. *Electrochemistry* **7**, 87-96.

[26] Aroca R, Pieczonka N., Kam A.P. (2001): Surface-enhanced Ramna scattering and SERRS imaging of phthalocyanine mixed films. *J. Porphzrins Phthalocyanines* **5**, 25-32.

[27] Prabakaran R., Kesavamoorthz R., Reddy G. L. N., Xavier F.P (2002): Structural Investigation of Copper Phthalocyanine Thin Films Using X-Ray diffraction, Raman Scattering and optical Absorption Measurements. *Phys. Stat. Sol.* **229**, No 3, 1175-1186.

[28]   Murray C. A, Bodoff S. (1984): Depolarization Effects in Raman Scattering from Monolayers on Surfaces: The Classical Microscopic Local Field. *Phys. Rev. Lett.* **52**, 2273-2276.

[29]   Procházka M., Hajduková N., Štěpánek J. SERRS of Porphyrins on Gold Nanoparticles Attached to Silanized Glass Plates. *Biopolymers, in press.*